DLR-IB-SL-HF-2022-66

Development of a Vertical Take-Off and Landing Aircraft Design Tool for the Application in a System of Systems Simulation Framework

Masterarbeit

Patrick Ratei

Deutsches Zentrum
DLR für Luft- und Raumfahrt

Dokumenteigenschaften

Titel	Development of a Vertical Take-Off and Landing Aircraft Design Tool for the Application in a System of Systems Simulation Framework
Betreff	Masterarbeit
Institut	Institut für Systemarchitekturen in der Luftfahrt (SL)
Erstellt von	Patrick Ratei
Beteiligte	
Geprüft von	Prof. Dr.-Ing. Martin Wagner (HAW Hamburg), Prajwal Shiva Praskasha, M.Sc. (DLR-SL)
Freigabe von	
Datum	Juni 2022
Version	1.0
Dateipfad	

Titel: Development of a VTOL Aircraft Design Tool for the Application in a System of Systems Simulation Framework
Version: 1.0

Seite: 2

Master Thesis

Patrick Ratei

Development of a Vertical Take-Off and Landing Aircraft Design Tool for the Application in a System of Systems Simulation Framework

Fakultät Technik und Informatik
Department Fahrzeugtechnik und Flugzeugbau

Faculty of Engineering and Computer Science
Department of Automotive and
Aeronautical Engineering

Patrick Ratei

Development of a Vertical Take-Off and Landing Aircraft Design Tool for the Application in a System of Systems Simulation Framework

Abstract

Patrick Ratei

Thema der Abschlussarbeit
Entwicklung eines Tools zum Entwurf von senkrechtstart und -landefähigen Flugzeugen für die Anwendung in einem System of Systems Simulationsumgebung

Stichworte
Flugzeugentwurf, Dimensionierung, Entwurfstool, Senkrechtstart und -landung, Urban Air Mobility, System of Systems

Kurzfassung

Systemarchitekturen und Anwendungsfälle in der Luftfahrt zeichnen sich durch ein komplexes Zusammenspiel mehrerer Teilsysteme, Systeme und Betriebskonzepte oder -taktiken aus. Die Analyse der vielfältigen Auswirkungen auf Leistung und Effektivität aufgrund der vielschichtigen Wechselwirkungen erfordert Entwurf und Bewertung anhand einer System-of-Systems-Vorgehensweise. In dieser Arbeit wird ein Tool für den Konzeptentwurf von senkrecht startenden und landenden Luftfahrzeugen als Teil einer agentenbasierten Simulationsumgebung entwickelt, welche für den System-of-Systems-Flottenbetrieb verwendet wird. In diesem Zusammenhang wird das aufstrebende Luftfahrtsegment Urban Air Mobility für die Demonstration betrachtet, bei dem zwei grundverschiedene elektrische senkrecht start- und landefähige Luftfahrzeugarchitekturen (d. h. Multikopter und Kipprotorflugzeug) entworfen und hinsichtlich der Leistung und Effektivität bewertet werden. Dabei werden Sensitivitäten des Subsystem- und System-/Luftfahrzeugentwurfs sowie deren Auswirkungen auf System-of-Systems-Ebene aufgezeigt.

Patrick Ratei

Title of the Thesis
Development of a Vertical Take-Off and Landing Aircraft Design Tool for the Application in a System of Systems Simulation Framework

Keywords
Conceptual Aircraft Design, Initial Sizing, Design Tool, Vertical Take-Off and Landing, Urban Air Mobility, System of Systems

Abstract

Aeronautical system architectures and aviation use cases feature complex interactions of several subsystems, systems and operational concepts or tactics. The evaluation of manifold impacts on performance and effectiveness due to the multi-level interdependencies necessitate system of systems design and assessment. In this thesis, a tool for conceptual design of vertical take-off and landing aircraft is developed as part of an agent-based simulation framework for system of systems fleet operations. For demonstration, the emerging aviation segment urban air mobility is considered, where two disparate electric vertical take-off and landing aircraft architectures (i.e., multirotor and tiltrotor) are designed and assessed regarding performance and effectiveness. Sensitivities of the subsystem and system/aircraft design and their impacts on the system of systems level are shown.

If you are in trouble anywhere in the world, an airplane can fly over and drop flowers, but a helicopter can land and save your life.

— Igor I. Sikorsky [1]

Acknowledgements

Contents

List of Figures

List of Tables

List of Abbreviations and Symbols

Abbreviations

AAM	Advanced Air Mobility
ABS	Agent-Based Simulation
AD	Aircraft Design
CFD	Computational Fluid Dynamics
CONOPS	Concept of Operations
CPACS	Common Parametric Aircraft Configuration Schema
CS	Certification Specifications
CSV	Comma-Separated Values
CTOL	Conventional Take-Off and Landing
DEP	Distributed Electric Propulsion
DLR	German Aerospace Center
DoD	Department of Defense
DoE	Design of Experiments
EASA	European Union Aviation Safety Agency
EIS	Entry Into Service
EU	European Union
eVTOL	Electric Vertical Take-Off and Landing
FAA	Federal Aviation Administration
FCAS	Future Combat Air System
INCOSE	International Council on Systems Engineering
IPCC	Intergovernmental Panel on Climate Change
ISA	International Standard Atmosphere
JSON	JavaScript Object Notation
LCA	Life Cycle Assessment
MDO	Multi-disciplinary Design Optimization
MoC	Means of Compliance
MoE	Measure of Effectiveness

MoP	Measure of Performance
MSL	Mean Sea Level
MTOM	Maximum Take-Off Mass
NASA	National Aeronautics and Space Administration
NDARC	NASA Design and Analysis of Rotorcraft
OpenVSP	Open Vehicle Sketch Pad
PAX	Passenger
PEM	Proton Exchange Membrane
POB	Person(s) On Board
RAM	Regional Air Mobility
RCE	Remote Component Environment
SA	Software Architecture
SD	System Dynamics
SE	Systems Engineering
SoI	System of Interest
SoS	System(s) of Systems
SoSE	System of Systems Engineering
SPL	Sound Pressure Level
STOL	Short Take-Off and Landing
SUAVE	Stanford University Aerospace Vehicle Environment
TLAR	Top Level Aircraft Requirement
TPP	Technical Performance Parameter
UAM	Urban Air Mobility
UAV	Unmanned Aerial Vehicle
UML	Unified Modeling Language
UN	United Nations
VFS	Vertical Flight Society
VLM	Vortex Lattice Method
VTOL	Vertical Take-Off and Landing
XLSX	Microsoft Excel Open XML Spreadsheet

Latin Symbols

A	Rotor disk area
A_b	Blade area
AR	Wing aspect ratio
AR_H	Horizontal tail aspect ratio
AR_V	Vertical tail aspect ratio
a	Acceleration
b	Wing span
C_D	Drag coefficient
$C_{D,0}$	Zero-lift drag coefficient
$C_{D,i}$	Induced drag coefficient
$C_{d,0}$	Blade zero-lift drag coefficient
C_f	Flat-plate skin friction drag coefficient
C_L	Lift coefficient
$C_{L,max}$	Maximum lift coefficient
$C_{L,md}$	Minimum drag lift coefficient
$C_{L,mp}$	Minimum power lift coefficient
$\overline{C_l}$	Rotor mean lift coefficient
C_P	Power coefficient
$C_{P,0}$	Parasite power coefficient
$C_{P,c}$	Climb power coefficient
$C_{P,i}$	Induced power coefficient
$C_{P,p}$	Profile power coefficient
C_T	Thrust coefficient
C_W	Weight coefficient
c	Wing chord
c_b	Blade chord
D	Drag
D	Fuselage diameter
D	Rotor diameter
D_{cc}	Cruise climb distance
D_{cr}	Cruise distance
D_{tot}	Total distance
DL	Disk loading, T/A
E	Energy

E_{bat}	Battery energy
E_{hdg}	Hydrogen energy
E_{krs}	Kerosene energy
e	Oswald efficiency
FF	Form factor
FOM	Figure of Merit
f	Equivalent flat plate area
f_{af}	Airframe mass fraction
f_e	Empty mass fraction
f_{egy}	Energy mass fraction
f_{obs}	Onboard systems mass fraction
f_{pl}	Payload mass fraction
f_{zf}	Zero-fuel mass fraction
g	Gravitational acceleration
H	Altitude
H_{ad}	Aerodrome altitude
H_{cr}	Cruise altitude
L	Lift
L_1	Fuselage nose length
L_2	Fuselage center length
L_3	Fuselage tail length
L_F	Fuselage length
L_H	Horizontal tail arm
L_T	Tail arm
L_V	Vertical tail arm
L/D	Lift-to-drag ratio, WV/P
m	Mass
m_{af}	Airframe mass
m_{bat}	Battery mass
m_{emp}	Empennage mass
m_{fus}	Fuselage mass
m_{hdg}	Hydrogen mass
m_{krs}	Kerosene mass
m_{lg}	Landing gear mass
m_{mto}	Maximum take-off mass
m_{obs}	Onboard systems mass

m_{os}	Other systems mass
m_{pc}	Powertrain component mass
m_{pl}	Payload mass
m_w	Wing mass
N	Number of rotors
N_b	Number of blades
N_{ult}	Ultimate load factor
N_{wheel}	Number of wheels
P	Power
$P_{bat,max}$	Battery maximum required power
P_{cc}	Cruise climb power
P_{cr}	Cruise power
P_{ho}	Hover power
P_{in}	Required power
P_{lo}	Loiter power
P_{out}	Provided power
$P_{pc,max}$	Powertrain component maximum required power
P_s	Segment power
P_t	Segment time
P_{tr}	Transition power
P_{tx}	Taxi power
P_{vc}	Vertical climb power
PL	Power loading, T/P
Q	Interference factor
q	Dynamic pressure
R	Rotor radius
R_1	Wing fuselage radius
R_2	Empennage fuselage radius
ROC	Rate of climb
S	Wing area
SE	Specific energy
SE_{bat}	Battery specific energy
SE_{hdg}	Hydrogen specific energy
SE_{krs}	Kerosene specific energy
S_H	Horizontal tail area
SP	Specific power

SP_{bat}	Battery specific power
SP_{pc}	Powertrain component specific power
S_{ref}	Reference area
S_V	Vertical tail area
S_{wet}	Wetted area
$S_{wet,F}$	Fuselage wetted area
T	Thrust
t	Time
t_{cc}	Cruise climb time
t_{cr}	Cruise time
t_{lo}	Loiter time
t_{tr}	Transition time
t_{tx}	Taxi time
t_{vc}	Vertical climb time
t_{vd}	Vertical descent time
V	Forward flight speed
V_{be}	Best endurance speed
V_{br}	Best range speed
V_c	Climb speed
V_{gs}	Ground speed
V_H	Horizontal tail volume
V_{hw}	Headwind speed
V_s	Stall speed
V_t	Rotor tip speed
V_V	Vertical tail volume
V_{vc}	Vertical climb speed
v_{ho}	Hover induced velocity
W	Weight
W	Work
WL	Wing loading, W/S

Greek Symbols

α	Angle of attack
Δ	Difference
ε	Convergence
η	Efficiency
η_{pc}	Powertrain component efficiency
η_{tot}	Total powertrain efficiency
κ	Induced power factor
λ_c	Climb induced inflow ratio
λ	Induced inflow ratio
ρ	Density of air
σ	Rotor solidity

1 Introduction

1.1 Motivation

Aeronautical engineering and science has ever since, and even before, the birth of aviation been a complex and challenging field of research and development. While many discipline-specific physical principals and natural phenomena as well as technologies and system architectures are well understood and manageable thanks to past and ongoing activities in aeronautics research and development, further research and innovation is needed to address today's environmental, societal and technical needs.

Facing the worldwide threats of continuing anthropogenic global warming as projected and described by the Intergovernmental Panel on Climate Change (IPCC) [2], the European Commission has defined goals for climate impact reduction and net zero greenhouse gas emissions or climate neutrality by 2050 in the European Union (EU). Therefore, the policy concept and initiative aims at a new era beyond fossil fuel subsidies and towards a progressive and economically as well as environmentally sustainable global competitor by decoupling economic growth and resource use. To reach this overall goal, the EU-wide transport sector is required to reduced its emissions by as much as 90%. Therefore, the European as well as global aviation system, which currently contributes about 3.5% to global anthropogenic greenhouse gas emissions [3], needs to research, develop and implement aspirational mobility as well as technology changes. [4]

In this context, the German Aerospace Center (DLR) has published its aviation strategy on the research contributions and development pathways towards a vision of zero-emission aviation. Following the historical phases of (early) pioneering, industrialization and exponential growth, the present challenge of aviation is the purposeful transition into an efficient, integrated and sustainable means of transport, as described above. The DLR acts as a "virtual original equipment manufacturer" researching and developing, e.g., air vehicle concepts, green propulsion systems or components, enabling technologies and methods as well as processes for the development and assessment of novel climate-neutral aviation products or use cases. Together with other international research organizations and the aviation industry, the DLR addresses four main pillars or fields of research: low-emission propulsion systems, energy-efficient aircraft, reduced-emission air transport system and digitalization. [5]

The aforementioned research domains already represent a challenge in themselves, but also the interaction of these domains opens up another layer of complexity. Firstly, subsystem (e.g. propulsion system) design involves the development of enabling technologies as well as component design and connection. Secondly, the system (e.g. air vehicle) architecture design defines the system's overall layout or structure. Lastly, the overall system (e.g. air transport system), technically referred to as System of Systems (SoS), includes the composition of systems and their operational interaction while tracing and managing the inter-level dependencies of the subsystem, system and overall system levels. Consequently, the integrated connection of the three levels may not only bring together the related domain expertise in a joint framework, but also enhance and increase the available knowledge during the development or evaluation process as part of the digital data thread while considering, respecting and collaborating with the relevant research domains and experts, of course.

Thus, aeronautical system architectures and aviation use cases feature a broad as well as complex interaction of several subsystems, systems and operational concepts or tactics. The evaluation of manifold impacts on their performance and effectiveness due to the multi-level interdependencies necessitate SoS design and assessment. Furthermore, this approach cannot only be applied to existing products and services in order to get a better understanding of the interrelations and interactions, but is particularly useful for developing innovative products and services.

The emerging concept of Urban Air Mobility (UAM), which promises time-saving, affordable and zero-emission air taxi passenger transport, urban rescue and emergency services, delivery of time-critical (medical) goods, and other use cases in densely populated major city areas, serves as a very suitable field of application for this approach. The air taxi vehicles or drones are technically referred to as electric Vertical Take-Off and Landing (eVTOL) aircraft due to their mostly fully electric powertrain architectures as well as Vertical Take-Off and Landing (VTOL) capabilities. These eVTOL aircraft do not only have to overcome hurdles on the subsystem and system level regarding air vehicle and powertrain architectures with the concerns of energy-efficiency, noise and safety, but also considering their integration and operations on the overall air transport level which all demands a holistic SoS approach. Eventually, this SoS approach will not only be useful for UAM in particular, but is also expected to be applicable to further novel as well as existing aviation use cases, which makes this topic relevant to aeronautical research and engineering, in general.

While different methods and tools can be applied for this purpose, agent-based simulations are commonly used to model transport systems including vehicles and their performance as well as the interplay between individual vehicles or systems. Therefore, a DLR in-house agent-based simulation framework for the purpose of SoS design and assessment in the field of UAM and further aviation use cases is currently under development and requires

an aircraft design tool to be contributed and connected by the means of this thesis, whereas specific thesis objectives are described in the subsequent section.

1.2 Objectives

The objectives of this thesis follow the previously mentioned motivation and are mostly set on the development of a software tool for the conceptual design and assessment of VTOL aircraft. Since the thesis is linked to the DLR-internal research project HorizonUAM, the main focus of the VTOL aircraft design tool is on UAM, thus novel eVTOL aircraft architectures or configurations must be designed and evaluated for their aircraft performance and SoS effectiveness.

Due to the large design space of eVTOL aircraft architectures in UAM, a literature review must be conducted considering the different characteristics of typical design options. In this regard, methods and methodologies for conceptual aircraft design must be researched and selected for the consequent development of the design tool in the programming language Python. Particular interests and main focuses are set on the initial sizing and performance evaluation of fundamentally different eVTOL aircraft architectures, which also includes different powertrain topologies or architectures. Thereby, a compromise between user-friendliness and level of fidelity or details should be made in order to allow many users other than just users worked into eVTOL aircraft design to be able to apply the tool.

Furthermore, the tool integration into the holistic SoS simulation framework, which is developed within HorizonUAM, must be considered. This means that the internal and external interfaces between the involved tools must be carefully coordinated and matched. Eventually, the design tool must be demonstrated not only specifically on the tool level, but also as part of the SoS simulation framework. Here, an eVTOL aircraft must be designed as well as assessed for its individual performance and also its effectiveness within the SoS context.

Focusing on the expected relevance and impact of this thesis, the underlying work develops and delivers a puzzle piece for an even broader framework. The eVTOL aircraft design tool must respect and implement a state-of-the-art methodology from aircraft design handbooks as well as domain-specific literature for sizing and performance. Relevance and impact beyond state-of-the-art is expected to be achieved through the overarching SoS simulation framework. At this, the connection of multiple expert domains, ranging from subsystem over system to the overall system, for holistic SoS design and assessment, is expected to contribute new knowledge to the (aeronautical) science community, the industry and last but not least the society.

For reference, the formal thesis task, as originally defined and submitted, can be found in Appendix A. Herein, the thesis goals are described and specific working steps are requested.

1.3 Approach

The approach and outline of this thesis follow the required or proposed steps from the task description (see Appendix A). For clarity, a comparatively standard outline of a technical report is chosen that first describes the problem as well as establishes context, then develops a solution as well as demonstrates the results, and finally summarizes the findings and potentials for future work.

Chapter 1 describes the general motivation as well as the context in which this thesis is being conducted in. Further, the objectives of this work are established in line with the official thesis task. Additionally, the expected relevance and impact of this thesis are highlighted for a better understanding of its uniqueness.

This introduction is followed in Chapter 2 by the presentation of background and literature review for the main aspects of this thesis, namely and written-out Vertical Take-Off and Landing as well as electric Vertical Take-Off and Landing aircraft, Urban Air Mobility and System of Systems. The context within the research project HorizonUAM, the eVTOL aircraft design literature review and the SoS simulation framework are of particular importance for the subsequent design tool development.

Chapter 3 elaborates on the used methodology and implementation of the eVTOL aircraft design tool. Therein, the general design aspiration and approach are explained. The methodology is explained with regard to the involved aircraft design disciplines, e.g. aerodynamics, propulsion, structures. Furthermore, a broad overview of the general tool implementation and a closer look on the interface set up and required user inputs are provided. Eventually, limitations of the methodology are summarized.

Subsequently, Chapter 4 demonstrates the tool and its integration within the SoS simulation framework in the field of UAM. The design of two disparate eVTOL aircraft architectures, i.e. multirotor and tiltrotor, is carried out with regard to typical UAM use cases and related requirements. The results involve aircraft design as well as SoS sensitivities. Thereby, different features of the design tool are demonstrated and validated.

Finally, Chapter 5 presents the conclusion of this thesis. It summarizes the general findings on each level within the SoS, respectively. Furthermore, ideas on potential future work are provided, not only with regard to the design tool but also the SoS simulation framework research and development.

2 Background

2.1 Vertical Take-Off and Landing Aircraft

2.1.1 General Perspective

In the following sections, a general, historical and subsequently prospective view on VTOL aircraft will be given following a similar narrative as in the earlier compiled overview and description of this special aircraft class in the project report by the same author [6].

Generally, aircraft or air vehicles have always been developed and utilized for operations in a wide variety of aviation use cases. These use cases can be vastly different from each other which makes most aircraft designs unique and distinct from the others just as the environments or settings they have been developed for. In this context, very striking and unique features of air vehicles are VTOL capabilities. Compared to Conventional Take-Off and Landing (CTOL) aircraft, the hover and vertical flight attributes make VTOL aircraft very versatile in their operations. Thus, this type of aircraft can operate independently of large and mostly fixed infrastructures and runways, and many times permits operations in rough environments or densely built-up areas where no or only limited infrastructure might be available. Exemplary use cases in which VTOL aircraft operate range from air patrol, medical emergency services, search and rescue, aerial firefighting, disaster relief, and passenger or cargo transport in both civil as well as military applications.

Commonly, VTOL capabilities are directly associated with rotary-wing air vehicles or more specifically helicopters. Helicopters consist of one or more powered horizontally-spinning rotors to produce both lift as well as thrust and also to control the flight attitude. In the modern history of aviation this special class of air vehicles has been introduced after the early pioneering stage of fixed-wing aircraft. Since then, helicopters have evolved in many configurations such as tandem, side-by-side, co-axial and compound helicopters. Regarding the conventional or single main rotor helicopter configuration which consists of a single lift as well as thrust producing main rotor and an anti-torque tail rotor, limitations with regard to forward flight efficiency and speed arise due to the inherent aerodynamics of the main rotor. [7]

While the requirements of versatility and extended hover endurance prevailing in some aviation use cases definitely favor rotorcraft, their aerodynamic efficiency, measured in terms of equivalent lift-to-drag ratio, typically stays well below the potentials of fixed-wing aircraft

[8]. On the one side, by their large rotor disk area, conventional helicopters can achieve a comparably low disk loading (weight over rotor disk area) which also permits a desirable high power loading (weight over power), resulting in efficient hover flight. On the other side, "retreating blade stall" is usually the most common restricting factor that limits the forward airspeed of rotorcraft. To understand the aerodynamic effect behind the technical term, the general lift generation of a helicopter must be fundamentally comprehended and will be explained with reference to Leishman [7]. In principle, the horizontally-spinning main rotor acts as an aerodynamic profile that shows a blade-wise linear speed distribution with the maximum local speed occurring at the rotor tip. In hover, the tip speed all around the rotor disk is constant and well below the speed of sound. However, as soon as the rotor disk or helicopter moves forward, the blade-wise speed distribution shifts due to the oncoming air flow. Hence, the advancing blade (i.e. moves forward with respect to the direction of flight) has a significantly higher tip speed compared to the retreating blade (i.e. moves backwards with respect to the direction of flight). Therefore, the advancing blade may experience very high tip speeds which are even beyond the speed of sound and suffers from compressibility effects. Additionally, some local blade profiles of the retreating blade will stall, thus produce less lift. All this causes dissymmetry of lift leading to instability and is a well-known aerodynamic condition of the helicopter's main rotor which can be somewhat alleviated in the design. However, the forward speed of rotorcraft will still have to be limited and typically leaves them behind fixed-wing aircraft.

2.1.2 Historical Development and Challenges

Following the previously identified drawbacks of helicopters and fixed-wing aircraft, a combination of capabilities is desirable for certain aviation use cases with many of them located in the military sector. This is also reflected in the mainly military-driven developments for different use cases, e.g. aircraft carrier and remote. Initial air vehicle concepts that allow this combination of vertical flight and fixed-wing cruising flight have already been researched and developed during the Second World War. This was just at the same time when the first production helicopter, the Sikorsky R-4 laid out in a nowadays conventional configuration, entered into US military services [9]. However, none of the VTOL aircraft concepts was able to enter this stage due to technical hurdles.

Following that time period of initial design concepts, the 1950s and 1960s proved as a highly developmental time full of different prototypes where research and development of VTOL and also Short Take-Off and Landing (STOL) aircraft presumably reached its peak. Many design approaches of combining vertical lift as well as fixed-wing cruising flight considering both jet and propeller/rotor (often referred to as proprotor) propulsion systems have been investigated by prototypes. The developed V/STOL aircraft have been summarized and categorized by their means of propulsion in the "V/STOL wheel" (see Figure 2.1). The
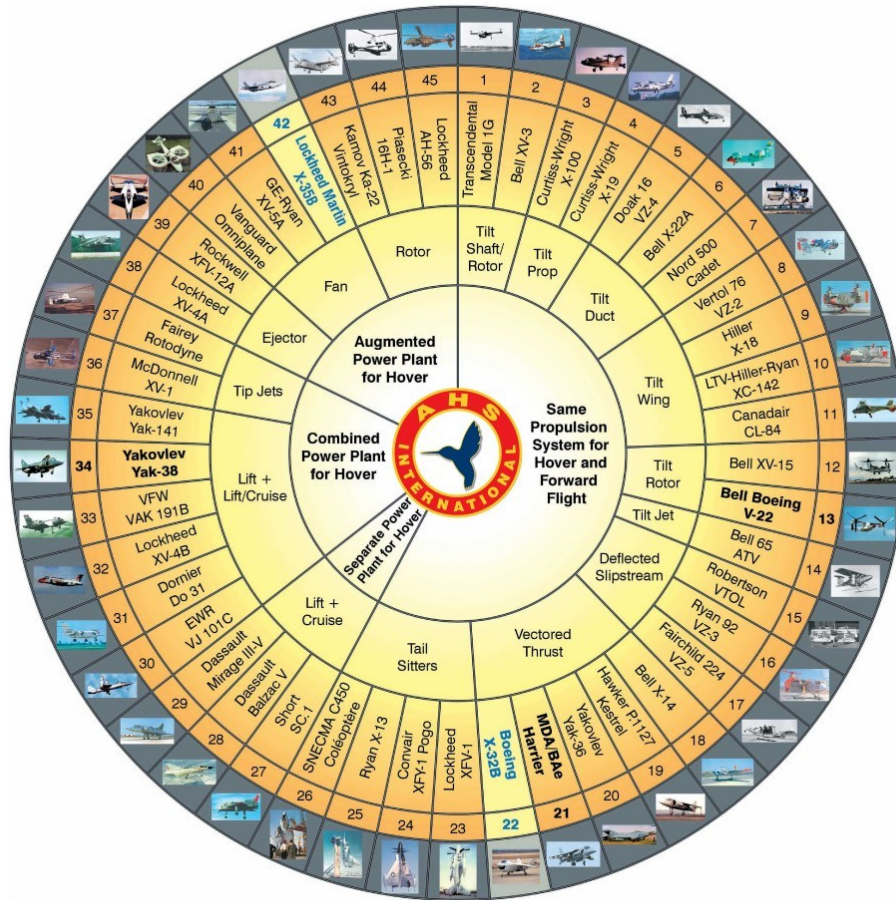
Figure 2.1: Classification of V/STOL Aircraft Configuration by the V/STOL Wheel [10]

relevant classifications for this thesis will be discussed later. For a detailed explanation of each aircraft as well as its characteristics, the reader is directed to [10].

As mentioned, many of the air vehicles have been investigated on a prototype level, but never matured beyond. Therefore, the overview of V/STOL aircraft is sometimes extended to "V/STOL wheel of misfortune". The main reasons for V/STOL aircraft development hurdles and issues have been summarized by Hirschberg, executive director of the Vertical Flight Society (VFS) originally founded as the American Helicopter Society [11]:

- **Thrust or power requirement mismatch** between vertical and cruising flight resulting in oversized propulsion systems driven by the vertical flight requirements

- **Thrust or power distribution** along the aircraft's longitudinal and lateral axis to achieve hover flight stability

- **Complex mechanical powertrains** to enable the thrust or power distribution by several engines or shaft connections

- **Low fuel efficiency**, firstly due to the aerodynamics in vertical flight, and secondly the mechanically complex propulsion systems with overall depleted efficiencies

Further investigations of the historic V/STOL aircraft designs and the lessons learned are summarized in a National Aeronautics and Space Administration (NASA) report by Anderson [8]. For further in-depth insights on aerodynamics, propulsion, flight dynamics and controls, operating problems, and testing techniques on the general class of V/STOL aircraft and specific designs, the reader is directed to this report.

Due to these challenges only few of the entire collection of 45 V/STOL aircraft have been further pursued and despite the often continuing challenges successfully accomplished their Entry Into Service (EIS) in the military. These aircraft are highlighted in Figure 2.1 and comprise of the British MDA/BAe Harrier (EIS 1969), the Soviet Yakovlev Yak-38 (EIS 1977), the Bell Boeing V-22 (EIS 2005) and the Lockheed Martin F-35B (EIS 2015), with the latter two from the USA. The further development of the propulsion technology was of great importance, as this increased the reliability of the engines and consequently reduced the required redundancy as can be especially seen for the latter two and comparatively recently introduced aircraft. [11]

2.1.3 Advancements and Prospects

Since all the previously mentioned V/STOL aircraft are specifically designed for military services, another ongoing and advanced development of a civil VTOL aircraft to be mentioned is the Next-Generation Civil Tiltrotor research and innovation project lead by Leonardo as part of the EU Clean Sky 2 program (see Figure 2.2). This project aims at the development a modern VTOL aircraft demonstrator by the year 2023. The design of this VTOL aircraft particularly focuses on passenger and cargo transportation, and compared to the historic technologies promises increased aerodynamic efficiency and reduced emissions also including acoustics. [12, 13]

This previously mentioned tiltrotor research project still features a conventional propulsion system, i.e. turboprop engine [14], which may be needed for the very near term EIS, and the desired payload and range characteristics. However, changes and advancements in powertrain technology are all around within the transportation sector with the automotive segment as a general example. Also for aviation, electrified propulsion systems are strongly on the rise. For example, Harbour Air, a Canadian seaplane airline operator, is in the process of retrofitting its seaplanes with battery-electric powertrains for the goal of clean, efficient and more quiet air transport [15]. In addition, the Slovenian light aircraft manufacturer Pipistrel recently obtained a type-certificate for its Velis Electro making it the world's first and currently only type-certified electric aircraft [16].

Key benefits of fully electric aircraft are their (local) zero emission potential including greenhouse gases and pollutants, their reduced noise emission potential due to electric

Figure 2.2: Rendering of the Next-Generation Civil Tiltrotor Concept [13]

motors, and their high powertrain component efficiencies. However, some drawbacks exist especially with regard to the battery technology where not only the specific energy (Wh/kg) as well as energy density (Wh/l), but also the specific power (W/kg) is often limited by state-of-the-art battery technology. The former typically limit the aircraft's range by adding too much weight (potentially also size), and the latter impact the maximum possible power draw (e.g. flight performance) as well as supply (e.g. recharging). Despite these drawbacks, the feasibility of electric aircraft for certain short-range missions or aviation use cases is definitely given with current technology levels. Further discussions on the challenges and opportunities of battery-powered aircraft can be found in [17].

Additionally, to battery-electric aircraft, the potentials of other reduced emission or even zero-emission electric powertrain architectures have already been shown years ago, e.g. by Hepperle [18]. The combination of different energy sources, e.g. kerosene and battery, may provide higher ranges, improved performance and additional capabilities. However, involving fossil fuels or carbon energy sources in hybrid-electric topologies may mostly be considered a bridging technology only until zero-emission powertrain architectures have further matured. Besides batteries, hydrogen fuel cells provide another opportunity to achieve zero-emission aviation and are key parts of current (aeronautical) research and development (see e.g. [19]).

In this context, Distributed Electric Propulsion (DEP) is an enabling technology and disruptive concept for advancements not only but especially in VTOL aircraft design allowing the designers to arrange multiple electric motor-driven propulsors longitudinally and laterally across the airframe to enhance control and stability in vertical and also forward flight. This concept also reduces the mechanical complexity, as most drive shafts can be replaced

Figure 2.3: Classifcation of eVTOL Aircraft Configurations by the eVTOL Wheel [21]

by electrical wiring and highly efficient electric powertrain components. By using scalable light-weight motors, large mass penalties as known formerly can typically be avoided, and often aero-propulsive benefits due to propeller-wing interaction can be achieved by deliberate design. In order to further exploit the potential, research on different (hybrid-)electric powertrain architectures and battery technology is needed. [20]

These developments lead to the design of several eVTOL concepts for passenger and cargo transportation. Due to the strong rise of concepts, demonstrators and prototypes, another summary and classification of these aircraft has been created by the VFS. Due to the high hopes and expectations for those novel aircraft, it received the name "eVTOL wheel of fortune", as a contrasting reference to the earlier shown and mentioned V/STOL wheel (see Figure 2.1). Consequently, the eVTOL wheel is shown in Figure 2.3 which does not only give an (outdated) overview of eVTOL aircraft concepts but also helps with a state-of-the-art classification of those with respect to their thrust type (note that an updated overview of eVTOL aircraft concepts will be provided subsequently).

Regarding and explaining the classification, the majority of all shown eVTOL aircraft fall into the class "vectored thrust", more generally also known as convertiplane. Therein, historically known concepts such as tiltwing, tiltrotor and tiltduct are brought back to light. In these concepts, typically the same propulsion system is utilized for vertical and forward flight whereas the transition between these phases is facilitated by respective tilting mechanisms. Next, the class "lift + cruise" features separate propulsors for the two different

flight phases allowing specifically adapted propulsor designs for both, vertical and forward flight. Eventually, the "multirotor" class is the only wingless eVTOL aircraft configuration with a multiple of rotors experiencing axial and edgewise flow conditions in vertical and forward flight, respectively. For a more general perspective of VTOL aircraft configurations using distributed propulsion (not limited to DEP only), the reader is directed to the review paper by Finger et al. [22].

For the sake of completeness, Unmanned Aerial Vehicles (UAVs) must also be mentioned in the context of advancing VTOL aircraft. UAVs often feature VTOL capabilities and are used over a large span of aviation activities where several UAV specific classifications exist. While VTOL UAVs, commonly known as drones, have been mostly used for military services in the past, these air vehicles are nowadays more and more often also designed for consumer and general aviation use cases. The utilized powertrains range from conventional up to electrified, such as battery-electric or hydrogen fuel cell, powertrains. Thanks to the advances in unmanned and even autonomous flight, such enabling technologies might be transferable from UAVs to other aviation use cases which could enable highly automated or even autonomous flight. For further textbook reading on UAVs, the reader is referred to [23].

2.2 Urban Air Mobility

2.2.1 Vision and Challenges

Urban Air Mobility has already been mentioned in the introductory sections of this thesis (see Chapter 1). It should be noted that the term Advanced Air Mobility (AAM) is sometimes used in a similar context. Basically, AAM considers similar aviation use cases but typically goes beyond the purely urban air transportation aspects, thus also addresses Regional Air Mobility (RAM) and other than only mobility-related use cases.

Further on, additional background information on the concept and vision of UAM, the DLR's ongoing internal research project HorizonUAM, and a literature review on UAM or eVTOL aircraft design will be given in the following sections to provide a better understanding of the domain.

Generally, UAM is an emerging concept of air taxi operations that promises affordable and not only scheduled but also on-demand air transportation within as well as around busy and congested metropolitan cities. The trends on which this concept is based on are the continuing urbanization as observed and predicted by the UN [24], for example, and also people's mobility demands in ground congested major cities across the globe. Herein, road traffic congestion is monitored and analyzed, for example, by the annually published INRIX Global Traffic Scorecard [25]. Therefore, the idea is to extend urban mobility into

the airspace in order to escape surface congestions and add another mode of transportation to the already existing mobility options.

However, there is nothing new under the sun. The idea of air taxi services in metropolitan areas has been evolving from the 1950s onwards with the first use case for airport shuttle operations in New York City as shown by the historical overview and comparison of air taxi concepts then and now by Vascik [26]. According to Vascik's findings from past air taxi operations using helicopters, the scaling of operations was constraint by several issues including availability of infrastructure, overloaded air traffic management, community acceptance due to noise, safety issues and the associated public opinion, operational limitations in adverse weather conditions, unfavorably high direct operating costs especially due to maintenance, energy, and staff costs, demand and fleet management as part of the network logistics, and eventually uncertain regulations [26].

Despite the aforementioned challenges, the research, trial and implementations of this general concept has steadily continued involving on-demand aviation research by NASA [27, 28], on-demand civil VTOL operations also by NASA [29] and on-demand UAM helicopter operations available via mobile booking apps developed by the US ride-sharing company Uber. The operations are performed by Blade in New York City, USA [30], and by Voom, which is Airbus' innovation subsidiary Acubed, in São Paulo, Brazil and further major cities in the Americas [31]. The latter UAM helicopter service company, Voom, ceased operations during the coronavirus pandemic in 2020 handing over the insights of this around two-year practical experience to Airbus' UAM branch [32].

Beyond these individual examples, the UAM vision was given a huge boost thanks to the very influential white paper on on-demand urban air transportation published by Uber Elevate in 2016 [33]. Uber Elevate's vision considered airport shuttle and intra-city operations between so-called vertiports (aerodromes for vertical take-off and landing operations) for which eVTOL aircraft should be used. Since then, the domain has gained a lot of international attention by start up as well as established aircraft manufacturers, prospective operators and service providers, infrastructure developers, consulting companies, investors, authorities, and academia as well as research. The start of initial UAM operations and EIS of the required aircraft is foreseen in the near future around the year 2025. Market research by Roland Berger [34] has projected that, after initial low-scale production and correspondingly high ticket prices, a large market growth may reach a global fleet size of 160,000 air taxis and a yearly revenue of USD 90 billion within the entire UAM industry by the year 2050.

With these prospects, however, the previously mentioned scaling constraints of past air taxi operations as summarized by Vascik [26] must be considered again. Thus, a re-evaluation for the modern understanding of UAM needs to be carried out. Due to the technology advancements that have been described in the previous Section 2.1.3 on eVTOL aircraft, the vehicle technology itself is developing and may not be the most crucial limiting factor for

UAM operations. However, the also discussed limitations concerning battery technology and also certification remain in place and will be discussed in the separate Section 2.2.3. Accordingly, Uber Elevate has identified several scaling constraints including some already listed historical aspects as well as pilot training or aircraft automation, aircraft certification, battery technology, in addition. Here also, the infrastructure availability of the so-called vertiports has been rated the most significant barrier for large-scale operations [33]. Vascik [26] has also identified and addressed the hurdle of infrastructure limitations with the special consideration of take-off and landing area development to maximize the traffic throughput. Moreover, the aforementioned author has developed strategies for efficient air traffic management and division of airspace for UAM operations. Other research findings from Rothfeld et al. [35] have further emphasized the eventual limitations due to a lack of infrastructure by an air transport network simulation which revealed that the promised time savings may not be generally achievable if the network is not set up sensibly, i.e. deployment of a large number and distribution of quickly reachable vertiports.

However, to overcome and tackle these challenges, a very vibrant research and development community has formed, where regular workshops, conferences, projects, etc. help to push the newly developing technologies. Here, also cooperations between industry and research as well as academia must be mentioned for different aspects of UAM development. In regard to the eVTOL aircraft design and operations, especially close collaboration with the supposedly most relevant aviation authorities, namely the US Federal Aviation Administration (FAA) and the European Union Aviation Safety Agency (EASA), is of importance to comply with aviation's high safety standards and develop pathways for eVTOL aircraft certification. In this context, the EASA is actively developing a special condition for small-category VTOL aircraft in the SC-VTOL-01 [36] and a corresponding set of Means of Compliance (MoC) as per cording MOC-2 SC-VTOL [37]. Thus, it shows positive that this challenge is being actively addressed.

To tackle some major challenges and to reach the presented vision in Germany, the concept of AAM is now being driven forward by the recently launched Air Mobility Initiative project led by Airbus. Therein, a large consortium of the most relevant stakeholders is brought together for a three-year project with a total budget of EUR 86 million. The project contents mainly concern eVTOL aircraft design, air traffic management of unmanned aircraft, and infrastructure integration in cities and at airports [38].

2.2.2 Research Project HorizonUAM

Even before the start of the aforementioned Air Mobility Initiative project, another UAM project associated to Germany has already been running since mid-2020. This is the DLR internal research project HorizonUAM, in the context of which also this thesis has been prepared. HorizonUAM addresses many of the previously mentioned challenges which UAM is facing. Accordingly, a consortium of domain experts has been brought together
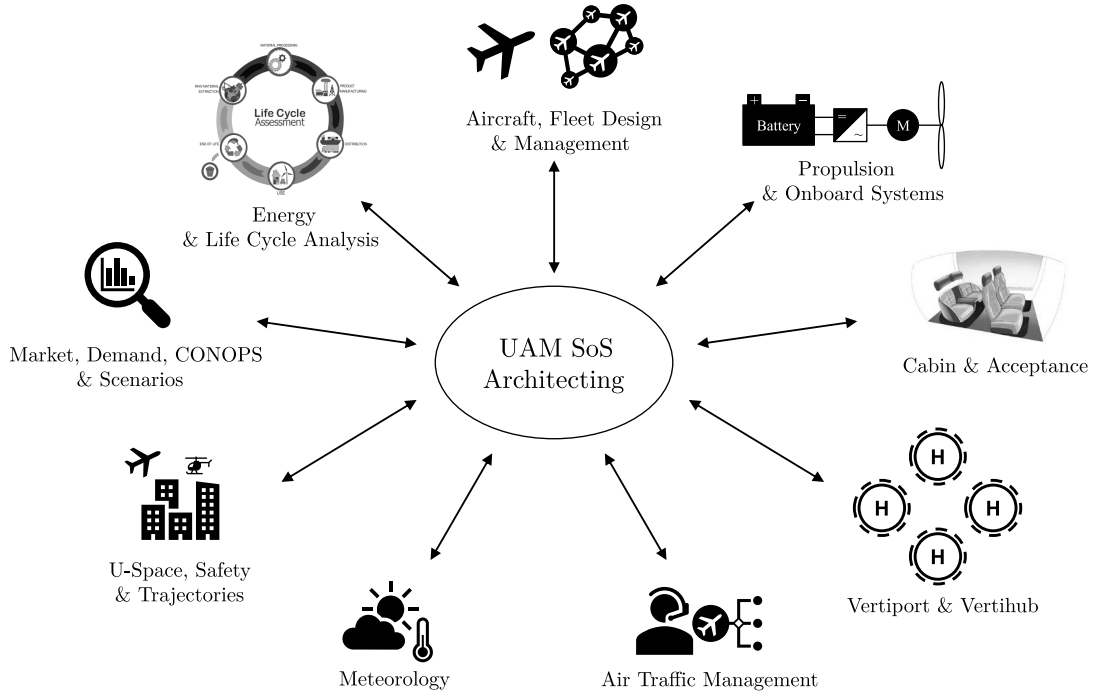
Figure 2.4: UAM Systems, Stakeholders or Research and Development Domains. Adapted from [40].
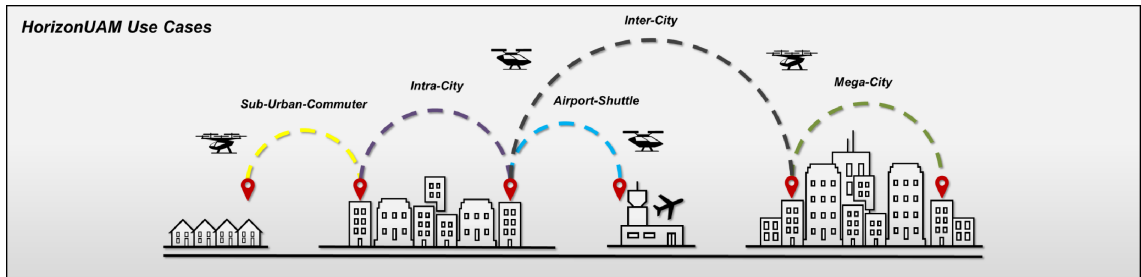
Figure 2.5: Schematic Representation of the HorizonUAM Use Cases [41]

for a runtime of three years to explore and investigate the potentials and limitations of the emerging aviation segment (see Figure 2.4). In this context, Schuchardt et al. [39] have published a dedicated overview of the project scope while stressing the importance of efficiency, safety, feasibility, sustainability, and affordability as key metrics for UAM on which the research project aims to provide insights.

A broad variety of UAM use cases is considered in the project. The use cases have been developed as well as summarized by Asmer et al. [41] and are illustrated in Figure 2.5. Those use cases all have their own characteristics and challenges with regard to aircraft as well as infrastructure design and operations. The use cases also feature different Concepts of Operations (CONOPS) which include scheduled and on-demand air transport services. Further, it should be noted that the use cases do not consider STOL-, but VTOL-capable aircraft only. Hence, certain requirements for the eVTOL aircraft design can be derived concerning the conceptual design process, in subsequent sections of this thesis.

Addressing the challenges of infrastructure or vertidrome development as well as the airside operations are a major part of HorizonUAM in order to investigate this often mentioned limiting factor. Here, especially the airside arrival and departure sector are examined and transferred into operational procedures or CONOPS while investigating the traffic flow as described by Schweiger et al. [42]. Further considerations of UAM integration at airports are paid attention to by the analyses of air taxi operations at Hamburg airport by Ahrenhold et al. [43] that suggest integration by separate vertiports in the airport area. In this context, it should be noted that Hamburg is taken as a reference scenario or city within the HorizonUAM project.

Beyond infrastructure-related considerations, further airspace challenges are also part of the project. Those concern the urban air traffic management including trajectory and airspace modeling and simulation. An initial airspace-related study has shown that air taxi transport may provide time savings of up to 50% compared to ground-based taxi transportation [44]. Furthermore, due to the highly interlinked automation, communication and navigation systems involved in UAM operations, not only the safety, but also security of these systems must be regarded which has initially been addressed by Torens et al. [45].

Eventually, the overall discipline of eVTOL aircraft design is split up into different domains ranging from conceptual aircraft design with different fidelity levels, onboard systems design, and cabin design. The intended workflow is presented in Figure 2.6. As mentioned before, assumptions and requirements are mostly derived from the scenario and use case definitions. Accordingly, the conceptual aircraft designs are developed, where the vehicle architecture design and assessment seeks for a low-fidelity approach in order to discover a range of eVTOL aircraft and derive family concepts. This conceptual design process is highly iterative, of course, where cooperation between vehicle architecture, onboard systems and cabin design is required resulting in the presented collaborative workflow. Hence, the interdependencies of the involved disciplines pose requirements for the design tool that will be developed in this thesis. Additionally, higher-fidelity design insights are taken into consideration from outside the workflow illustrated in Figure 2.6 by another conceptual design work package dedicated to multirotor configurations. Recently, the work contents have been extended by another work package which focuses on the maintenance aspects of eVTOL aircraft. Thus, important aspects regarding the aircraft and powertrain architecture design as well as the aircraft and fleet operations will be analyzed and fed back into the design loop.

2.2.3 Electric Vertical Take-Off and Landing Aircraft Design

This section focuses on the conceptual design of eVTOL aircraft for UAM applications with the main emphasis on a literature review of existing research on this topic. However, in the first part of this section, a brief overview of the eVTOL aircraft designs from the industry is given.
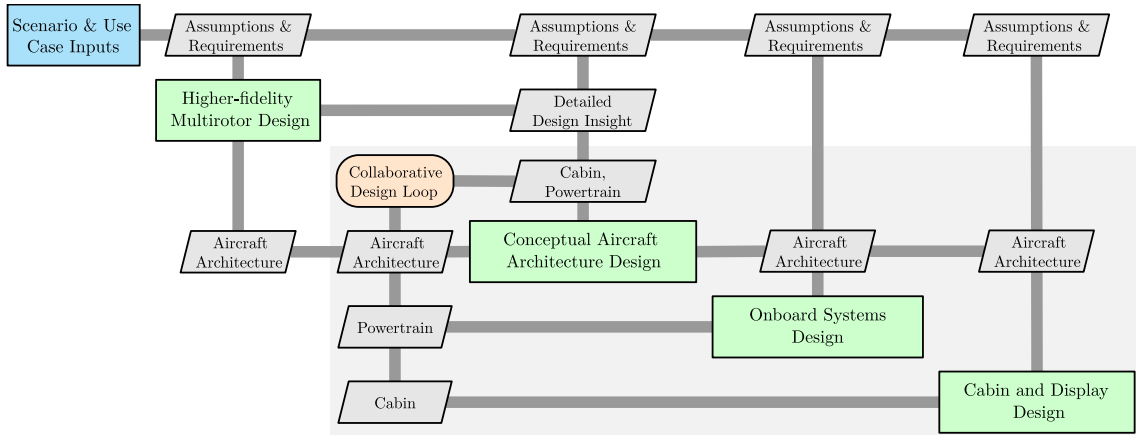
Figure 2.6: HorizonUAM eVTOL Aircraft Design Workflow

The aforementioned UAM hype has started a boom in the domain of eVTOL aircraft design. This can be seen by the chronological overview published online by the VFS on their dedicated eVTOL website, named Electric VTOL News, which also features a database or directory of eVTOL aircraft concepts [46]. Thus, Figure 2.7 shows the strong growth of this eVTOL directory after the release of Uber Elevate's white paper in 2016, as mentioned earlier.

An overview of the developed concepts can be found in Figure 2.8, which is a collection of the most relevant AAM aircraft concepts in development (including VTOL- as well as STOL-capable aircraft) as summarized and compiled by the Advanced Air Mobility Reality Index developed by the SMG Consulting company [48]. Additionally, the aircraft are annotated with the company name in bold and the aircraft concept name in regular print. This website also provides a ranking of the different companies and concepts, further allowing insights into the funding situations, the expected EIS, and the orders of the emerging UAM businesses and aircraft developments.

Finally, since the most relevant eVTOL aircraft and their design features as well as characteristics have already been generally mentioned in the previous sections and have more extensively been discussed in a preceding report by the author [6], only the graphical overview of the eVTOL aircraft specifications in terms of cruise speed, range and seat capacity is updated with respect to current industry concepts and shown in Figure 2.9. It can be found that Airbus' recently presented CityAirbus NextGen eVTOL aircraft [49] is now mapped in a different position compared to before. The aircraft remains a four-seater all-electric air taxi, however, the earlier multirotor configuration has been omitted and replaced by a winged lift + cruise configuration. This design change may potentially enable higher cruise speed, operational range, and aerodynamic efficiency, as also discussed in Section 2.1.1.
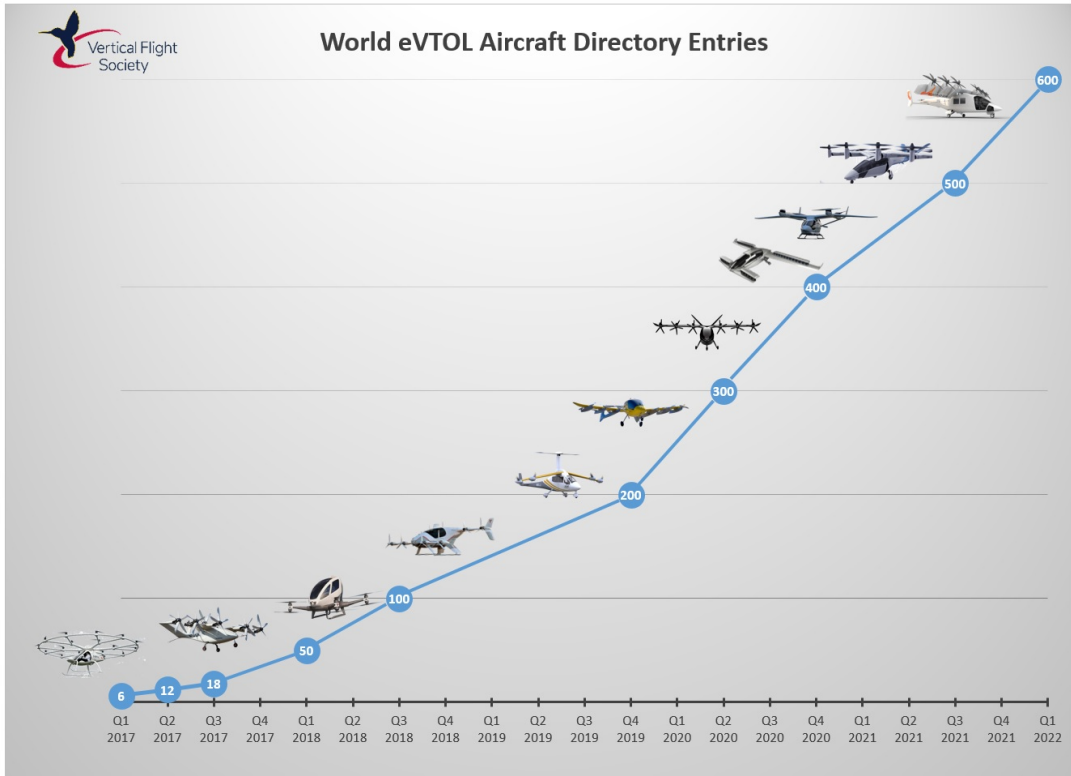
Figure 2.7: Chronological Overview of the eVTOL Aircraft Concept Boom [47]

Figure 2.8: Composition of Different AAM Aircraft Concepts. Adapted from [48].
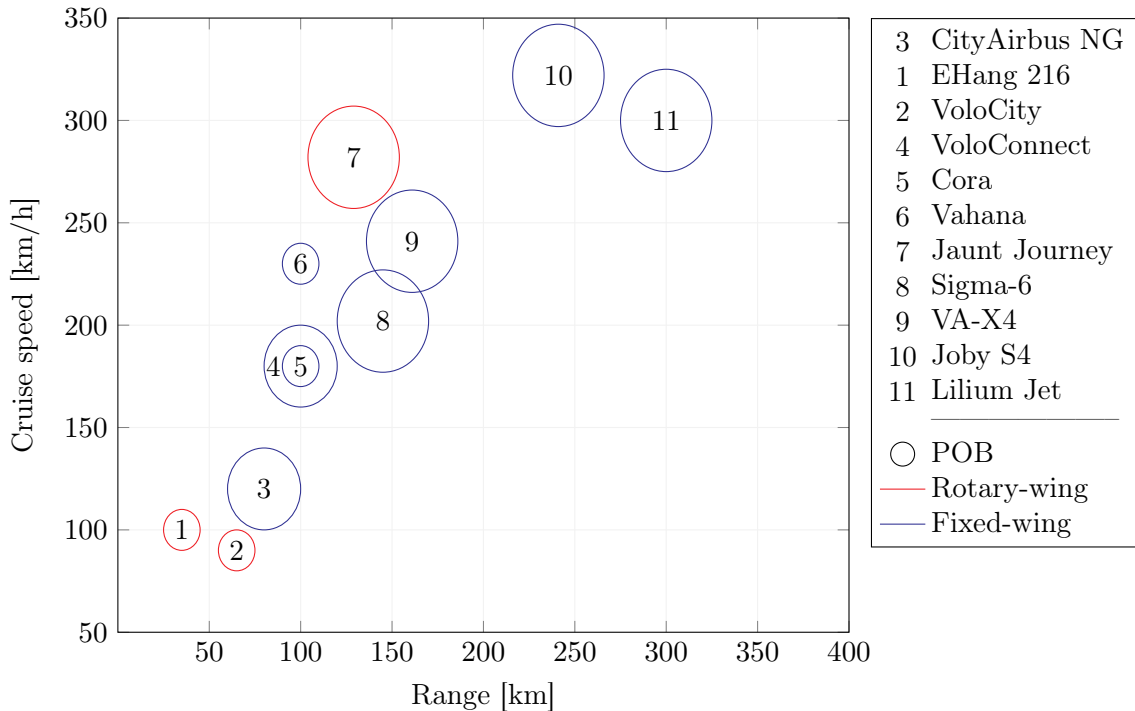
Figure 2.9: Specifications of Exemplary eVTOL Aircraft from the Industry. Data Collected from eVTOL News [46]. Adapted from [6].

For further background information on eVTOL aircraft development companies, characteristics and specifications of eVTOL aircraft under development, the reader is directed to the project report by this author which provides a summary of the most relevant eVTOL aircraft concepts [6]. An online directory of all proposed eVTOL aircraft concepts can be found on the eVTOL aircraft directory by the VFS [46] and an overview as well as ranking of AAM aircraft in development is available online from the AAM Reality Index [48].

Beyond the industry concepts, a lot of research work has also been carried out in this specific aircraft design domain and has also seen a strong rise similar to the eVTOL aircraft concepts as shown in the earlier Figure 2.7. The strongly increasing relevance in the UAM research community has been shown by the chronological overview of research publications on the topic revealing a strong increase of publications as shown in the project report by this author [6].

Transitioning from industry to research, a recent assessment study of eVTOL aircraft concepts from the industry has been conducted by Sripad & Viswanathan [50]. The study is based on simple aircraft design methods and analyzes not only the energy efficiency of different winged eVTOL aircraft concepts, but also investigates their feasibility by computing a range of the required battery parameters to meet their published aircraft performance specifications. Thereby, Sripad & Viswanathan have shown that the energy consumption of different eVTOL aircraft depends not only on the load factor, but also on the mission range. This is due to the high power demand in the vertical flight phases, which is more

dominant on shorter mission ranges, of course. Moreover, the study also suggests that eV-TOL aircraft may potentially be in a similar range of energy efficiency as terrestrial internal combustion engine vehicles and may even be able to compete with electric vehicles. Yet, only if deployed for longer operating ranges and high occupancy missions. Concerning the assessment of required battery technology levels, it is shown that most of the concepts are mapped at the edge of current or even prototype levels. Especially, the tiltduct Lilium Jet appears to be way beyond current or novel battery technologies which would be required to meet the announced aircraft performance specifications. [50]

The latter finding concerning the Lilium Jet represents an ongoing debate about the feasibility of this particular eVTOL aircraft concept. In this context, the German start-up company has already been trying to defend their concept by providing more (high-level) insights into their conceptual aircraft design assumptions, considerations and performance assessment [51]. In the end, it remains to be seen and demonstrated by successful certification and deployment.

Generally, the use of simple methods as part of the before mentioned study by Sripad & Viswanathan has been part of the very first assessments of different eVTOL aircraft configurations ranging from helicopter over multirotor and lift + cuise to tiltduct concepts. In this regard, McDonald & German [52] have presented a methodology for eVTOL aircraft mission and energy analysis that considered the most relevant configurations and derived basic performance design spaces regarding the vertical and forward flight characteristics by ranges of disk loading and lift-to-drag ratio, respectively.

Considering design tools that facilitate the use of mixed-fidelity aircraft design methods, the Stanford University Aerospace Vehicle Environment (SUAVE) design tool provides a powerful open-source toolbox for novel air vehicle classes such as eVTOL aircraft [53]. SUAVE does allow for the modeling, design, assessment and optimization of air vehicles, however, the tool has a high learning curve and does actually require already (initially) sized aircraft as an input. Thus, the tool may be very usable after the initial sizing process. Clarke & Alonso [53] have been demonstrating SUAVE's capabilities in the field of UAM research, where they modeled different battery-electric UAM aircraft configurations and assessed them for their performance and noise characteristics. In a further study, Clarke & Alonso [54] set particular focus on the battery discharge as well as degradation modeling available through SUAVE. As a key result, they found that the usable battery capacity of electric aircraft reduces over its operating life and may impose limitations to the operational flexibility in terms of actual feasible range compared to the original design range. Thus, the authors suggested considering the battery degradation and associated range reductions not only in the design, but also in the operational planning and strategies for UAM network development.

Beyond battery-electric powertrain architectures for eVTOL aircraft, also research on hydrogen fuel cell powered aircraft exists. In this context, Datta [19] has prepared a sophisti-

cated model for Proton Exchange Membrane (PEM) fuel cell systems specifically dedicated to and demonstrated for the conceptual design of hydrogen eVTOL aircraft. Basically, a PEM fuel cell is an electrochemical system that converts hydrogen together with air to electricity (unused air, water, and heat). In the developed model by Datta [19], not only the fuel cell stack, which is a set of fuel cells, but also the auxiliary required subsystems involving the hydrogen tank are considered. Thus, also hydrogen fuel cells are to be investigated for eVTOL aircraft due to the intensified research around hydrogen as a potentially renewable energy carrier on the rise in several industry countries.

Also, NASA [55] has been developing a set of VTOL aircraft considering a variety of powertrain architectures for their AAM campaign. According to their Top Level Aircraft Requirements (TLARs), compared to UAM, high ranges of 140 km must be achievable. Thus, multirotor, co-axial helicopter, lift + cruise, and tiltwing concepts with powertrain options involving turbo-electric or full-electric architectures have been developed. For the initial sizing and conceptual design, NASA researchers use their in-house design tool called NASA Design and Analysis of Rotorcraft (NDARC) which is a very sophisticated design tool for rotorcraft. Beyond NASA's conceptual design development, André & Hajek [56] have also evaluated the aforementioned NASA concepts for their sustainability which must represent important factor for the deployment of UAM, of course. Herein, a Life Cycle Assessment (LCA) study has been conducted, where certain seat utilization is assumed. Among other influencing factors, the importance of renewable energy production as well as intensified battery technology research is highlighted in order to reach sustainable UAM in the future.

As can be found from the previously reviewed research on eVTOL aircraft design, several methodologies and tools for the conceptual design of eVTOL aircraft are utilized. Some of the aforementioned methodologies are provided together with some not yet mentioned works in Table 2.1, which represents an adaptation and extension from [57]. It can be seen most methodologies focus on full-electric aircraft of different configurations where commonly computationally cheap semi-empirical methods are utilized for the aerodynamics modeling (e.g. assumed aerodynamic characteristics or basic parabolic drag polar). Only few authors have been using higher-fidelity methods such as Vortex Lattice Method (VLM) and Computational Fluid Dynamics (CFD) for the conceptual design. Moreover, most airframe models are based on semi-empirical methods either using take-off or more refined component weight build-up approaches. Despite the high importance of noise in the field of UAM, only two tools have an acoustics model implemented as part of the conceptual design process. Supposedly, the other authors rely on either design considerations for reduced noise and/or higher-fidelity noise assessment of the conceptual eVTOL aircraft design. The use of optimizers is more often represented in the conceptual design process as shown in the summary.

Table 2.1: Summary of Conceptual Design Methodologies for Electric Vertical Take-off and Landing Aircraft. Adapted from [57].

Configuration	Powertrain	Aero Model	Airframe Model	Acoustics Model	Opt.	Ref.
Tiltrotor	Full-electric	VLM and CFD	Semi-empirical	No	Yes	[58]
Helicopter	Full-electric	Semi-empirical	Component weight build-up	No	No	[59]
Helicopter, multirotor, lift + cruise, tiltwing, tiltrotor	Full-electric	Semi-empirical	Component weight build-up	No	No	[60]
Helicopter, lift + cruise, tiltwing, tiltrotor	Full-electric	Semi-empirical and assumed characteristics	Take-off weight build-up	Yes	Yes	[61, 62]
Tiltwing	Full- and hybrid-electric	CFD	Take-off weight build-up	No	No	[63]
Helicopter, multirotor, lift + cruise, tiltwing	Hybrid- and full-electric	Semi-empirical	Detailed component weight build-up	No	Yes	[64, 65]
Multirotor, lift + cruise, tiltwing	Full-electric	Semi-empirical and VLM	Component weight build-up	Yes	Yes	[53, 54, 66, 67]

In summary, the review of research work on the design of eVTOL aircraft shows that only few methods are either directly implementable or available as open source tools. Therefore, an in-house tool must be developed with methodologies derived from this literature review. Moreover, the initial sizing with the consideration of multiple eVTOL aircraft configurations is only part of few of the reviewed methodologies. In the further course of this work, focus will be set on the use of semi-empirical and component-weight build-up methods for disparate eVTOL aircraft configurations, e.g. multirotor and tiltrotor, which are available from the summarized papers in Table 2.1. Accordingly, especially the models presented

by Kadhiresan & Duffy [60] and Brown & Harris [61, 62] will be considered for the tool development.

2.3 System of Systems

2.3.1 Contextual and Historical Perspective

In order to give a broad overview of SoS as a further research domain relevant for this thesis due to the involved SoS simulation framework, the background associated to the chronology, definitions, application areas and approaches of SoS are presented in the following.

For other reasons, but also thanks to Systems Engineering (SE), *system* and *subsystem* may represent ordinary terms or notions with a clear meaning and understanding in (aeronautical) research as well as engineering. A brief recapitulation of the mentioned terms will still be provided in a common definition: according to the International Council on Systems Engineering (INCOSE) a system is "an integrated set of elements, subsystems, or assemblies that accomplish a defined objective. The elements include products (hardware, software, firmware), processes, people, information, techniques, facilities, services, and other support elements" [68]. However, the term *system of systems* seems to be comparatively less common and is still a fairly new concept in aeronautical research and industry despite its prevalence in recent decades.

A large literature review on the related discipline of System of Systems Engineering (SoSE) by Gorod et al. has shown that the domain of SE began several decades before SoS and SoSE came up. A timeline of the modern history of SoS is provided in Figure 2.10. Although some early mentions of SoS appeared even earlier, academic work on the modern understanding of SoS began in the early 1990s. A decade later, industry and government agencies also began to embrace the emerging concept, while at the same time a great amount of academic work was being conducted and published. [69]

Another comprehensive literature review performed a histogram analysis of the SoS field and titled the time frame from 1990 until 2011 the "revolution of SoS", due to the significant developments where several definitions, characteristics, perspectives and methodologies have been proposed for SoS. Thanks to the high frequency of studies and exchanges in that time frame, some convergence could be achieved in terms of SoS characteristics. [70]

Furthermore, state-of-the-art resources in terms of general textbooks on methodology and various case studies [71], knowledge sources [72], modeling and simulation handbook contributions [73] and guiding materials [74] have been compiled since then.
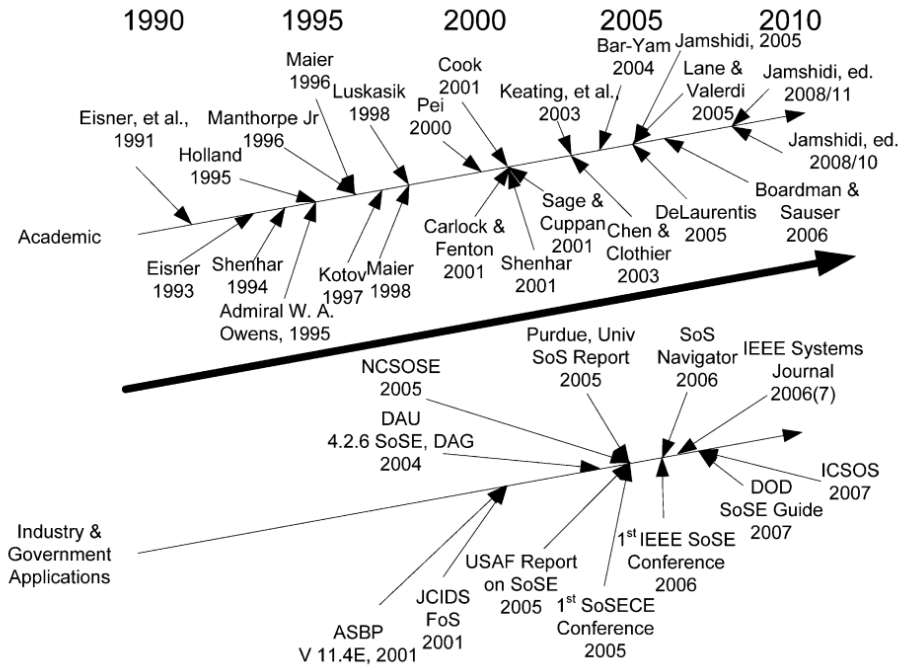
Figure 2.10: Chronological Overview of the Modern History of SoS [69]

2.3.2 Definitions and Characteristics

The term *system of systems* has been mentioned and paraphrased multiple times in the introduction of this thesis (see Chapter 1). However, a formal definition is yet to be given and will be established in this section which will provide the reader with a clearer understanding of SoS.

As for definitions of SoS, in the early 20th century, during the extensive formulation phase of the field mentioned earlier, several definitions and descriptions were developed depending on the context and application of SoS, some of which were discussed by Jamshidi [75]. Within the comparatively recently formulated standard ISO/IEC/IEEE 21839:2019 [76] the following terms and definitions are given and shall be recognized in this thesis:

> "System of Systems (SoS) — set of systems or system elements that interact to provide a unique capability that none of the constituent systems can accomplish on its own"

> "Constituent System — independent system that forms part of a System of Systems (SoS)"

Also, the latter definition implies that each constituent system requires SE activities and processes over all its life-cycle stages, e.g. development, manufacturing, use, service, etc. [76]

Additionally, another relevant definition can be found in ISO/IEC/IEEE 15288:2015 [77]:

> "System of Interest (SoI) — system whose life cycle is under consideration in the context of this document."

Aside from definitions, different characteristics have been found to identify and distinguish SoS. Maier, the apparently most influential researcher in the field of SoS, formulated properties of SoS that are commonly referred to when (complex) systems need to be distinguished from SoS. Maier has postulated these traits first in 1996 [78], while further refinement followed in 1998 [79]. The five SoS key characteristics, sometimes abbreviated by the acronym OMGEE, are as follows [79]:

1. **Operational Independence of the Constituent Systems**: The constituent systems must be able to operate independently of other constituent systems while being dispersed from the SoS.

2. **Managerial Independence of Constituent Systems**: Apart from the ability to be operationally independent, the component systems do actually work independently of each other.

3. **Geographic Distribution**: The constituent systems are geographically distributed over a wide area.

4. **Emergent Behavior**: Assembled as an SoS, the collaborating constituent systems are able to achieve unique capabilities beyond those achievable by any constituent system.

5. **Evolutionary Development**: The SoS is never finished, but changes and develops further over time.

Especially, the operational and managerial independence are the crucial characteristics that a collaborative SoS must have in order to differentiate from systems, regardless of their complexity [79]. Accordingly, an individual aircraft, which may be regarded as a complex system and a set of multiple complex subsystems, would not classify as an SoS due to the lack of operational and managerial independence.

Also note that in this context, *complex* is not equivalent to *complicated*. Rather, complicated systems can be understood through the fixed relationships of their parts and can be decomposed into simpler parts. However, complex systems are more difficult to understand and predict because of all interactions and emergent behaviors involved. [68]

Further characteristics which aid for distinction between (complex) systems and SoS are shown in Table 2.2 which summarizes the findings from a review of common SoS characteristics by Boardman & Sauser [80].

It can be stated that the five given properties to distinguish systems and SoS go with the same flow as Maier's OMGEE characteristics. Therefore, these properties are widely accepted and are important for understanding the SoS concept and thinking.

Table 2.2: Differences of Systems and System of Systems [80]

Element	System	System of Systems
Autonomy	Autonomy is ceded by parts in order to grant autonomy to the system.	Autonomy is exercised by constituent systems in order to fulfill the purpose of the SoS.
Belonging	Parts are akin to family members; they did not choose themselves but came from parents. Belonging of parts is in their nature.	Constituent systems choose to belong on a cost/benefits basis; also in order to cause greater fulfillment of their own purposes, and because of belief in the SoS supra purpose.
Connectivity	Prescient design, along with parts, with high connectivity hidden in elements, and minimum connectivity among major subsystems.	Dynamically supplied by constituent systems with every possibility of myriad connections between constituent systems, possibly via a net-centric architecture, to enhance SoS capability.
Diversity	Managed i.e. reduced or minimized by modular hierarchy; parts' diversity encapsulated to create a known discrete module whose nature is to project simplicity into the next level of the hierarchy.	Increased diversity in SoS capability achieved by released autonomy, committed belonging, and open connectivity.
Emergence	Foreseen, both good and bad behavior, and designed in or tested out as appropriate.	Enhanced by deliberately not being foreseen, though its crucial importance is, and by creating an emergence capability climate, that will support early detection and elimination of bad behaviors.

2.3.3 Application Areas and Approaches

In this section, the previous review of somewhat abstract SoS definitions and characteristics will be elucidated by few exemplary application areas, whereas different domains in addition to aeronautics are considered. Together with the aeronautical applications, few relevant approaches are highlighted and explained.

Exemplary application areas collected within the public and science community are the service industry (e.g. infrastructure systems), electric power grids (e.g. renewable energy grid), transportation systems (e.g. railway network), human health care systems (smart health care), aerospace systems (e.g. space exploration missions), communication systems (e.g. Internet of Things), etc.

In general, the defense or military domain must be recognized as an early adopter of the SoS concept with the first introduction by Owens [81] in 1995. As summarized by Gorod et al., the United States Department of Denfense (DoD) has further worked on and contributed to the SoS domain, e.g. publishing the before cited SoSE guiding materials [74]. Since most military systems or services can be recognized as parts of SoS [82], the application areas are very broad in this domain. Applications listed by the DoD range from army, air force, navy, intelligence up to joint defense activities [74]. A very prominent and highly joint military development within the EU is the Future Combat Air Systems (FCAS) [83], which forms a heterogeneous air defense SoS consisting of fighters, UAVs, satellites, air tanker and transport aircraft, etc.

Another central work in the military SoS domain has been created by Biltgen [84] who developed a methodology for the technology evaluation for military or more specifically air force SoS applications. In his methodology, Biltgen differentiates between Measure of Performance (MoP) and Measure of Effectiveness (MoE), where MoPs are used for system-level performance metrics (e.g. speed, range, payload, etc.) and MoEs for higher-level capability goals of SoS (e.g. time expenditure, resource spending, etc.), recalling term explanations from IEEE Standard 1220-2005 [85]. Moreover, Biltgen [84] has used a mission simulation-driven approach to analyze the interrelations and influences of different levels ranging from subsystem to system and SoS level as illustrated in Figure 2.11.

Considering civil aviation, DeLaurentis [86] has introduced SoS thinking in the aeronautical research and engineering community in 2005 where he not only introduced and characterized the general SoS concept, but also mapped the proposed characteristics to the (air) transportation system. The traits are in large agreement with the already shown SoS characteristics by Maier [79] and Boardman & Sauser [80].

The previously mentioned transportation sector is often referred to as an illustrative SoS example. The before referenced standard ISO/IEC/IEEE 21839:2019 also provides a short example of an SoS related to aviation: here, the SoS is defined as the air transport level which consists of multiple constituent systems, e.g., airports, air traffic control systems
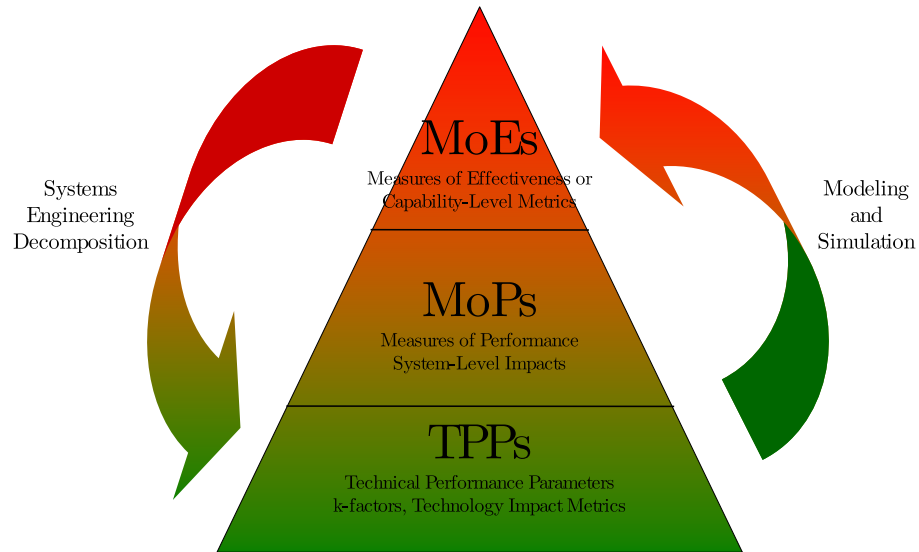
Figure 2.11: SoS Levels in the Military Domain. Adapted from [84].

and air vehicles [76]. This example can also be found in the INCOSE Systems Engineering Handbook [68] where the air transport system is presented as an SoS within the overall transport SoS (see Figure 2.12).

Already during the introduction of SoS concept for air transportation in 2005, DeLaurentis proposed two methods that were mostly new to the aeronautical community for the modeling of transportation systems: System Dynamics (SD) and Agent-Based Simulation (ABS). While SD as a mathematical modeling approach for nonlinear problems definitely supports the understanding of complex systems and its behaviors, it is limited by the ability to explore emergent behaviors of the SoS. Therefore, ABS appears to be a more promising option, since the interactions of individual agents that represent constituent systems of the SoS are able to predict emergent behaviors. Limitations are stated with regard to validation of ABS results. [86]

In technical terms, an agent represents an individual constituent system and is modeled as an autonomous decision-making entity. All agents act independently of each other whereas decisions follow predefined rules. Thus, nonlinear behaviors and couplings can be discovered in research and engineering applications that yield the potential of emergence. Further drivers for ABS are the modeling of flows, i.e. moving agents such as a traffic scenario, and diverse systems consisting of heterogeneous agents. The difficulties in ABS range from the purposeful creation of the model and set of rules, to the difficulty of modeling human agents, eventually to the computational cost. [87]

Other aviation-related application examples involving ABS have been presented by Ranque et al. [88] as well as Papageorgiou et al. [89]. While Ranque et al. [88] consider aerial firefighting in addition, both use cases focus on maritime surveillance using UAVs, where even radars are modeled in the ABS as part of the subsystem domain. In this exemplary
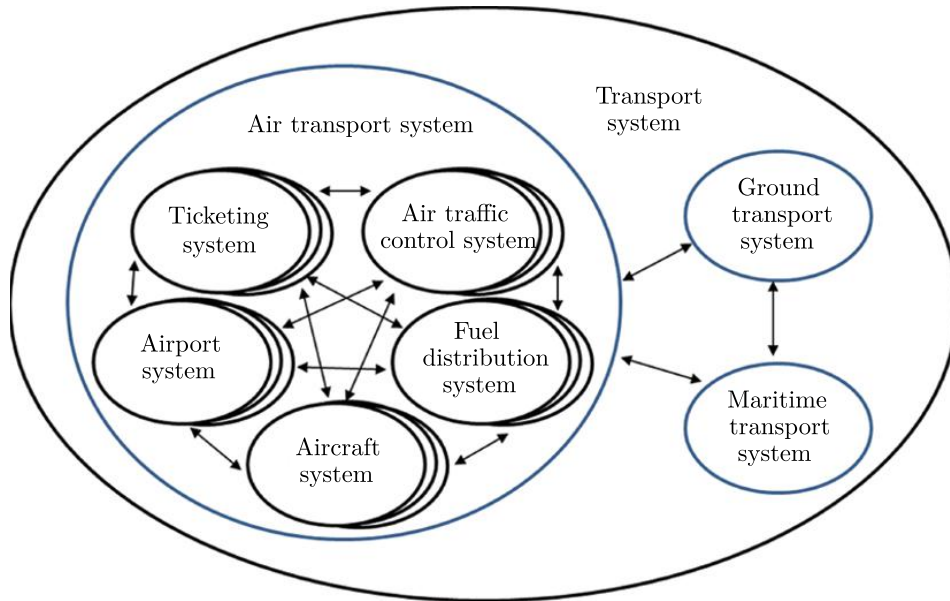
Figure 2.12: Air Transport SoS within the Overall Transport SoS. Adapted from [68, 72].
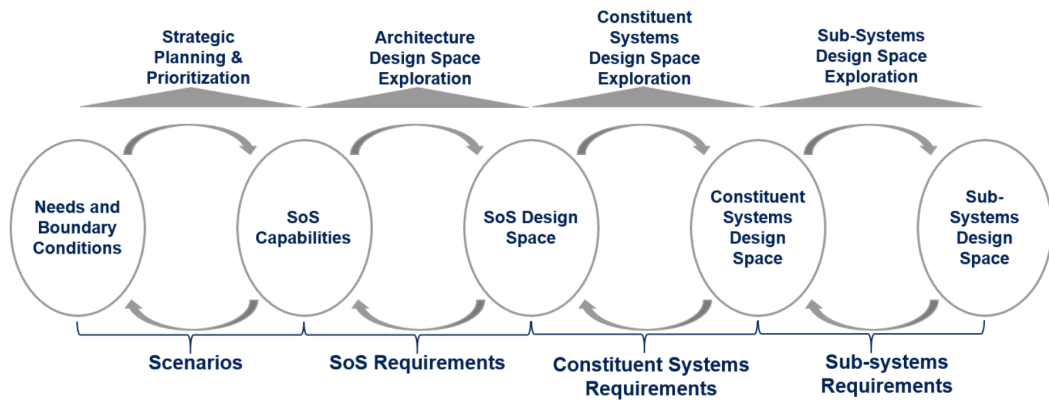
Figure 2.13: Holistic SoS Design Process [90]

case study, Papageorgiou et al.[89] follow a holistic SoS design process proposed by Staack et al. [90]. The process is depicted in Figure 2.13 and can be decomposed into five coupled phases that range from the top-level needs and boundaries over the SoS capabilities to the design space on SoS, constituent system, and subsystem level. This systematic approach enables approaching SoS problems from a holistic point of view, thus considering and understanding all relevant parts of the SoS, from high-level needs and SoS capabilities to the subsystem design space, is supported as well as promoted. Thus, the basic idea of the presented design process should ideally be followed in this work, too.

For further SoS aviation and aircraft design related perspectives and progresses with regard to applications as well as modeling and simulations methods, the reader is directed to an extensive review article by Liu et al. [91] which was published in 2015 and still appears to be relevant.

2.3.4 Agent-Based Simulation Framework

Connecting the overview of the HorizonUAM research project in Section 2.2.2 and the review of SoS definitions in Section 2.3.2 as well as SoS application areas in Section 2.3.3, the SoS simulation framework and approach will be explained. Thereby, the purpose and approach of the underlying SoS simulation framework will be justified.

Initially, Table 2.3 picks up the SoS characteristics and descriptions shown in Table 2.2 and provides basic explanations why UAM can be recognized as an SoS. It should be noted that the descriptions consider the UAM aircraft as the SoI, thus focus mostly on the aircraft design perspective within the overall SoS context. Further constituent systems of the UAM SoS have already been presented in Section 2.2.2 (see Figure 2.4).

With regard to the existing literature on SoS definitions and application areas, it can be generally stated that the SoS concept does not prescribe specific methods, but rather enables another way of thinking and approaching complex interlinked and interacting systems. To tackle the complexity of SoS research and engineering requires new methods and additional tools compared to the design and assessment of individual (complex) systems.

Typically, modeling and simulation are required for SoS design and assessment of various engineering application [73]. As described by DeLaurentis [86], a system of autonomous agents, i.e., aircraft operating in an air transportation system, ABS are used since the approach closely matches the previously described SoS characteristics. Especially, the operational and managerial indecency of constituent systems can be directly traced and modeled by the agents. As described earlier, their decisions follow a set of rules which are implemented by simulation algorithms.

In order to consider all the expert domains of the HorizonUAM project as explained in Section 2.2.2, the overall UAM SoS simulation framework is collaboratively developed and work in progress considering the integration of demand modeling, cost modeling, vertiport, airspace and trajectory management modeling, and maintenance operations modeling. In this context, Niklaß et al. [92] have proposed a collaborative framework for UAM modeling and simulation (also involving ABS), where data schemes, interfaces, and workflows are proposed. This approach is one of several bases for the development of an overall UAM simulation framework within HorizonUAM. Subsequently, a visual representation of the overall UAM SoS simulation framework for aircraft design proposed by Shiva Prakasha et al. [40] is depicted in Figure 2.14. The structure of the framework enables a similarly holistic design space exploration as suggested by Staack et al. [90], where needs and constraints are expressed as input parameters not only for the system and subsystem design, but also for the SoS fleet design and assessment simulations, thus enabling different SoS architectural solutions and design space explorations (for comparison, see Figure 2.13).

However, the initial studies have been already conducted with regard to the modeling and simulation of UAM aircraft and fleet operations. Thus, this specific aircraft and fleet design

Table 2.3: Urban Air Mobility as a System of Systems extended from [80]

Element	System of Systems	Urban Air Mobility
Autonomy	Autonomy is exercised by constituent systems in order to fulfill the purpose of the SoS.	Aircraft operate autonomously to transport passengers as one of many constituent systems of the urban air transportation system. Modeling must enable aircraft movements and passenger transport.
Belonging	Constituent systems choose to belong on a cost/benefits basis; also in order to cause greater fulfillment of their own purposes, and because of belief in the SoS supra purpose.	Aircraft operate autonomously and are in fact operationally independent but still belong to the airspace and its management systems. Hence, they belong to the urban air traffic management to ensure smooth and safe operations. Modeling must enable urban air traffic management.
Connectivity	Dynamically supplied by constituent systems with every possibility of myriad connections between constituent systems, possibly via a net-centric architecture, to enhance SoS capability.	Aircraft operate as part of a connected fleet and are assigned to passengers flight requests by a (central) dispatcher. Modeling must account for the (net-centric) connection of aircraft.
Diversity	Increased diversity in SoS capability achieved by released autonomy, committed belonging, and open connectivity.	Aircraft operate not only in homogeneous, but often in heterogeneous fleets. Those fleets can evolve over time so that diverse capabilities are added to increase the urban air transportation capability. Modeling has to consider heterogeneous fleets.
Emergence	Enhanced by deliberately not being foreseen, though its crucial importance is, and by creating an emergence capability climate, that will support early detection and elimination of bad behaviors.	Aircraft operate as on-demand air transportation services. Herein, the passenger waiting times depend on various factors such as aircraft availability and dispatch readiness. Modeling must account for cascading effects of passenger waiting times.
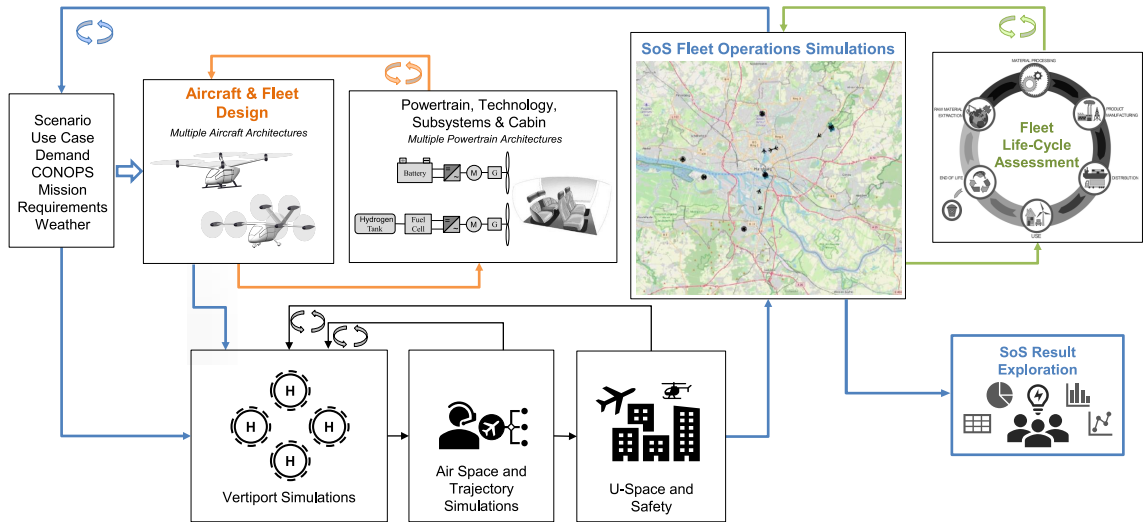
Figure 2.14: UAM SoS Simulation Framework. Adapted and Extended from [40, 93].

and assessment simulation framework deploys an ABS for the modeling and simulation of UAM aircraft that operate in an urban air transport network where air taxi passenger operations are performed. The ABS is developed as a branch of the general purpose SoS aircraft design and simulation toolkit presented by Kilkis et al. [94]. The derived UAM framework has first been presented in 2021 by Shiva Prakasha et al. [40] where initial proof of concept studies for the initial demonstration of this approach have been shown considering different near- as well as far-term scenarios that include eVTOL aircraft configurations, mobility demands, regulatory uncertainties, subsystem technologies, etc. Not only UAM specific MoPs, e.g. cruise speed, payload, and energy efficiency, but also MoEs, e.g. fleet size, network throughput, and passenger waiting time, are considered. By this approach, the complex interplay and impacts between the subsystem, system, and SoS level can be analyzed by sensitivity studies which is visualized in Figure 2.15.

Further studies by Shiva Prakasha et al. [93] that involved the aforementioned UAM aircraft and fleet design and assessment simulation framework have also been conducted with regard to modeling different powertrain architectures of UAM aircraft. Herein, the design and operations of different fully battery-electric and series hybrid-electric UAM aircraft configurations have been considered and analyzed by sensitivities regarding battery technology. Accordingly, the results suggest that fully battery-electric UAM aircraft may be advantageous compared to conventional or mild-hybrid powertrain architectures due to the high powertrain efficiency and further improved due to advancing battery technologies. Those results were found by subsystem, system, and SoS design and assessment.

Apart from that, the LCA of UAM aircraft design and operations has a high priority for efficient and prospectively sustainable deployment as well as operations. Accordingly, Shiva Prakasha et al. [95] have also extended the UAM aircraft and fleet design and assessment simulation framework to consider LCA by SoS simulations. Involving ABS in the process of LCA allows directly deriving assessment metrics such as aircraft utilization rates, load
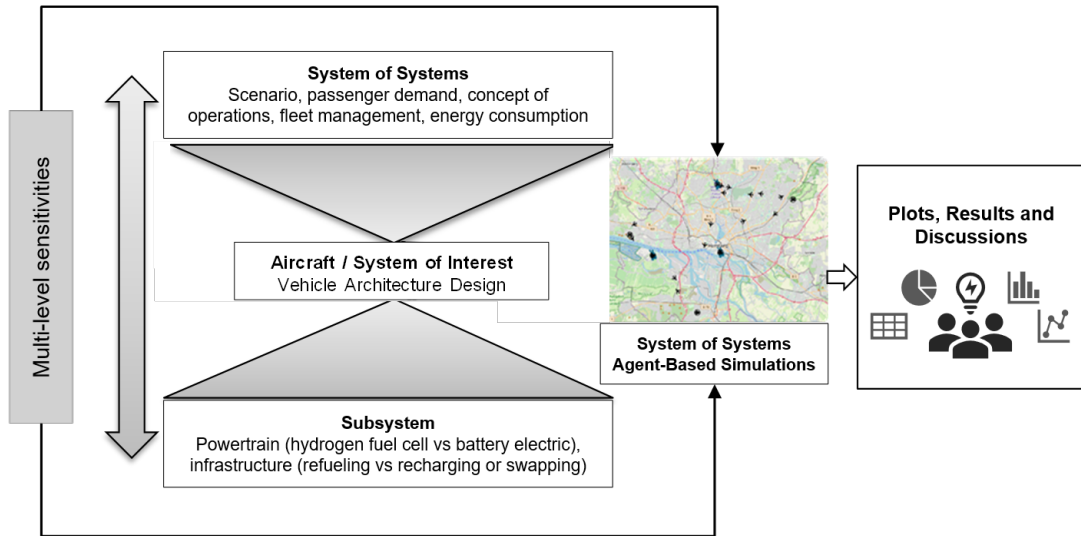
Figure 2.15: UAM SoS Multi-level Sensitivity Analysis. Adapted and Extended from [40].

factors, and energy consumption, for which assumptions must often otherwise be made. In their research paper, Shiva Prakasha et al. [95] considered different battery-electric UAM aircraft configurations, locations, use cases, and battery technologies over different time frames. Thus, sensitivity analyses for UAM SoS fleet operations and the associated LCA regarding battery production and operations are presented.

Similar research approaches for the modeling and simulation of UAM transport networks are limited with regard to fleet dispatch and/or aircraft performance modeling. More precisely, Rothfeld et al. [35, 96] model a UAM network by the assumption that aircraft are available for dispatch at every vertiport at all times. Also, a rather superficial UAM aircraft performance model, relying on aircraft properties such as vertical as well as cruising speeds and maximum range, is utilized. Kohlman et al. [97] have developed a more profound dispatching model and also the performance model follows a more refined, yet, assumption based approach. Here, the performance is based on power loading assumptions for different mission segments. Since the network as well as the aircraft performance modeling impact the UAM SoS, the developed ABS by Shiva Prakasha et al. [40] considers both, a finite fleet or number of aircraft, thus, requiring empty deadhead flights to fulfill the transport requests, and also a representative UAM aircraft sizing as well as performance model.

Since the development of the overall UAM SoS simulation framework is still ongoing, the first approach relied on assumptions and/or simplified models for the respective expert domains. Also, the involved aircraft design tool has been of low fidelity where the aircraft sizing and performance computations are mostly performance according to assumed eVTOL aircraft characteristics. Therefore, the UAM or eVTOL aircraft design tool requires further development as well as extensions in order to provide a robust and more sophisticated building block to the overall UAM SoS simulation framework.

Finally, the presented ABS framework for UAM SoS aircraft and fleet design and assessment is part of a literature review in the context of SoS software architectures [98]. Accordingly, the framework is suitable for the assessment of several conceptual SoS architectures involving an executable model allowing for detailed analysis of the architectural solution. Apart from that, the review provides an overview of different approaches: while scenario-based approaches involving workshops and questionnaires are used sometimes, most SoS architectures are approached by mathematical modeling and simulation where trade space exploration, event-based simulation, and graph theory are utilized besides ABS. Thus, the need for a simulation-driven framework further justifies the development of the UAM SoS simulation framework which shall be suitable for analyses of architectural solutions. This also necessitates the continued development of the eVTOL aircraft design tool in order to implement further architectural design options such as hydrogen-powered aircraft.

3 Design Tool

3.1 Conceptual Aircraft Design and Development Approach

For the development of the tool for VTOL aircraft design, which will be abbreviated by the acronym VTOL-AD in the following, the scope and objectives are to be defined before the explanation of the implemented methodology and the developed software architecture. Therefore, this section will provide an overview about the approach which is located in conceptual aircraft design, sometimes known as predesign, of the VTOL aircraft architecture.

Traditionally, the aircraft design process can be divided into three phases, which follow an initial set up of needs and requirements, namely conceptual, preliminary, and detailed aircraft design [99]. During the very first steps of the conceptual aircraft design phase, only limited knowledge about the aircraft is available. Yet, the commitment, typically measured by committed cost, is already quite high [100].

Therefore, Raymer [99] highlights the importance to start with a broad view on different aircraft configurations as well as feasible architectures, and to perform numerous trade-off and sensitivity studies of those with regard to requirements, involved technologies, performance, cost, etc. All this makes the conceptual aircraft design process an extremely iterative process which typically involves comparatively low- to medium-fidelity methods and necessitates the use of software tools in order to compute and manage the large amount of design points. Consequently, a conceptual aircraft design approach typically involves textbook, handbook and additional topic-specific methods. Eventually, the aircraft designer should always have the objective of a design freeze for the initiation of the preliminary and eventually detailed design processes in mind.

The development scope of the VTOL-AD tool is driven by the thesis objectives which are mostly derived from the needs for the HorizonUAM research project as explained in Sections 1.2 and 2.2.2, respectively. Thus, different objectives must be met while also reasonable compromises in terms of the design fidelity level have to be made. The requirements or development objectives are summarized and restated below. Note that for clarity and traceability the design tool development requirements are divided into two categories, namely Aircraft Design (AD) and Software Architecture (SA).

The VTOL-AD tool ...

AD.1 must perform initial sizing of eVTOL aircraft.

AD.2 must consider different eVTOL aircraft configurations.

AD.3 must alleviate existing limitations of previously utilized tools.

AD.4 must compute the mission performance of the sized eVTOL aircraft.

AD.5 must allow design trade-off studies considering powertrain and cabin design.

AD.6 must be easily operable also by eVTOL aircraft design newcomers.

SA.1 must be written in the programming language Python 3.

SA.2 must be executable by a standalone version.

SA.3 must match and adapt the interfaces with the SoS simulation framework.

SA.4 must match and adapt the interfaces with the powertrain design tool.

SA.5 must be integrated into the DLR's remote component environment.

Also note that the acronym VTOL-AD is deliberately chosen despite its specific application and development in the domain of eVTOL aircraft design. This is reasoned by the general applicability of the methods and extension potentials to VTOL aircraft design in general, thus this broad and descriptive acronym is preferred over a too narrow and specific one.

Subsequently, the chosen methods as programmed in the VTOL-AD tool will be presented, followed by the software architecture implementation. Eventually, limitations concerning the methodology as well as the software tool will be stated.

3.2 Methodology

3.2.1 Sizing Loop

For the initial sizing of different eVTOL aircraft configuration a common sizing loop is defined. This sizing loop is depicted in Figure 3.1 and shows the conceptual set up of the computational process which is inspired by Leishman [7]. Basically, the process is initialized by defining few input parameters with regard to the mission, the rotor, the wing, and the fuselage or cabin sizing. Exemplary parameters are provided in Figure 3.1 showing that the loop is initiated by an arbitrary guess value for the Maximum Take-Off Mass (MTOM). Based on all those inputs, the first iteration is started where the sizing and performance computations are conducted. The first step starts with rotor and wing sizing as well as performance. Here, the aircraft's geometry, aerodynamics and mission performance are computed. In the second step, the component weights or masses are estimated concerning two major groups, namely airframe and onboard systems which also
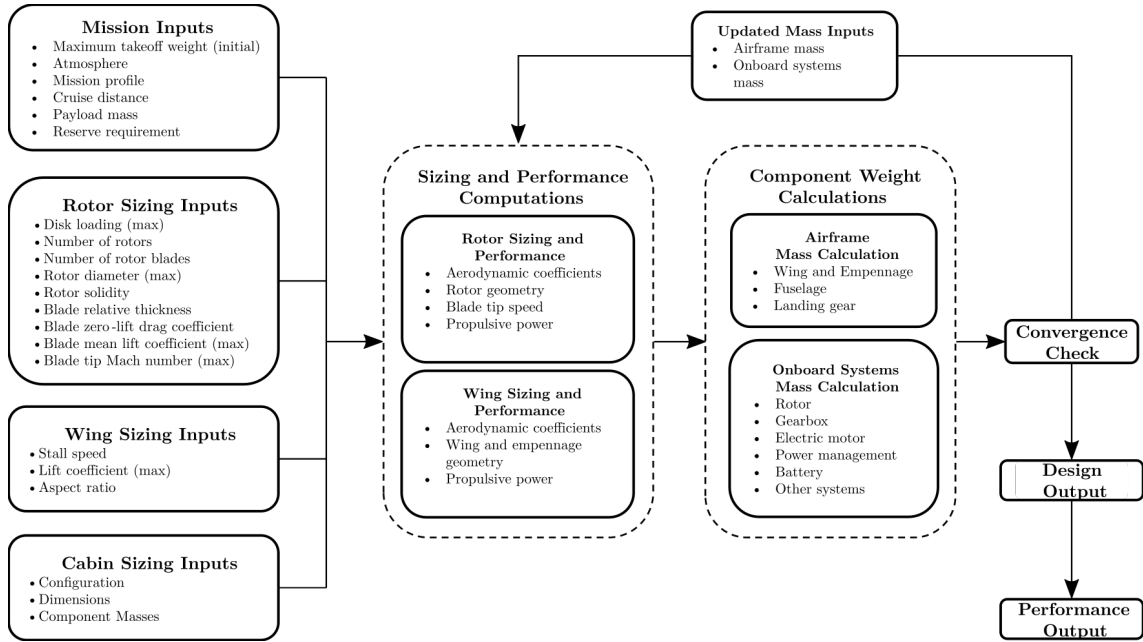
Figure 3.1: Sizing Loop for the Conceptual VTOL Aircraft Design. Adapted from [7, 93].

include the propulsion and powertrain modeling. Based on these two steps, a convergence check can be undertaken. The sizing or convergence loop is simply based on the absolute value of the MTOM and is achieved as soon as the following equation is fulfilled:

$$\left| \text{MTOM}_n - \text{MTOM}_{n+1} \right| < \varepsilon. \tag{3.1}$$

Thus, in each check, the MTOM of the $(n+1)$th iteration is subtracted from the MTOM of the preceding nth iteration, whereas in the very first computation run, the initial MTOM guess value is taken as MTOM_n. Only if the absolute value of this subtraction is smaller than the defined convergence criterion ε, convergence is achieved. However, more than one iteration is usually required. Hence, the MTOM is updated by the airframe as well as onboard systems masses that have just been computed and the loop is run again with the subsequent sizing and performance calculations. As soon as Equation 3.1 is fulfilled, the loop is successfully exited resulting in the aircraft design output. Furthermore, the aircraft performance is evaluated in a post-processing step in order to provide data for design evaluation and to feed the ABS with the required aircraft performance inputs.

This setup and description of the sizing loop fulfills requirement AD.1 and sets the basis for further explanations of the involved methodology which will be presented in the subsequent sections.

3.2.2 Geometry

For the geometry calculations the fuselage or cabin, the rotor and wing sizing are explained. To estimate the fuselage geometry including its surface or wetted area, a method as described by Gudmundsson [101] is used. Here, the fuselage length L_F is divided into three parts L_1 (nose), L_2 (center) and L_3 (tail), which can be simply summed up:

$$L_F = L_1 + L_2 + L_3. \tag{3.2}$$

Eventually, the fuselage wetted area $S_{wet,F}$ is computed as a pod-style fuselage

$$S_{wet,F} = \frac{\pi D}{4} \left(\frac{1}{3L_1^2} \left[\left(4L_1^2 + \frac{D^2}{4} \right)^{1.5} - \frac{D^3}{8} \right] - D + 4L_2 + 2\sqrt{L_3^2 + \frac{D^2}{4}} \right), \tag{3.3}$$

where the nose is modeled as a paraboloid, the center as a cylinder and the tail as a cone. Also, it should be noted that D represents the maximum diameter of the fuselage. By modeling different fuselage geometries, the cabin sizing inputs can be considered in the aircraft sizing process which contributes to the fulfillment of requirement AD.5. Also, the fuselage is always modeled by this approach no matter which configuration is considered.

In order to fulfill requirement AD.2, the eVTOL aircraft configurations are divided into two major configurations, namely wingless and winged eVTOL aircraft (see Section 2.1.3). Consequently, the methodology will be presented with regard to those two disparate configurations. The further geometry sizing explanations will first explain the rotor sizing as part of the wingless configurations (even though it is also used for winged eVTOL aircraft configurations).

Wingless

The following fundamental explanations regarding the geometry and sizing of VTOL aircraft are reproduced according to Leishman [7]. For the wingless as well as winged eVTOL aircraft configurations, the disk loading DL or T/A is an important design parameter which indicates the ratio of rotor thrust T and rotor disk area A. Since the thrust is essentially the weight W of the hovering aircraft, it can be determined using the MTOM or m_{mto} as well as the gravitational acceleration $g = 9.81\,\mathrm{m/s^2}$ and is computed by

$$DL = \frac{T}{A} = \frac{W}{A} = \frac{m_{mto}g}{A}. \tag{3.4}$$

The rotor disk area is simply

$$A = N\frac{\pi D^2}{4}N, \tag{3.5}$$

where N is the number of rotors and D is the rotor diameter. The rotor thrust T and the ideal rotor power P are related to each other by $P = Tv_{ho}$. The rotor induced velocity in

hover v_{ho} can be computed by

$$v_{ho} = \sqrt{\frac{T}{2\rho A}} = \sqrt{\frac{1}{2\rho}DL}, \tag{3.6}$$

where in addition the desity of air ρ is used. Hence, the power loading PL or T/P is of further importance to understand the impact of disk loading on the eVTOL aircraft sizing. Similar to DL, the parameter PL is defined by

$$PL = \frac{T}{P} = \frac{W}{P} = \frac{m_{mto}g}{P}. \tag{3.7}$$

Recalling that $P = Tv_{ho}$ and combining it with Equation 3.6, the relation between disk loading and power loading becomes clear and shows that power loading is inversely proportional to the rotor induced velocity in hover:

$$v_{ho} = \sqrt{\frac{1}{2\rho}\left(\frac{T}{A}\right)} = \frac{P}{T}, \tag{3.8}$$

$$= \sqrt{\frac{1}{2\rho}DL} = (PL)^{-1}. \tag{3.9}$$

Thus, the relationship also explains the hover efficiency of a VTOL aircraft meaning that a low DL, thus high PL allows achieving high hover efficiency and long hover endurance. Here, the helicopter is a perfect example when it comes to high efficiency in hover, as already mentioned in Section 3.3.1.

Winged

Regarding the winged aircraft configurations, the basic equations and relations are recalled from Raymer [99]. Thus, similar to the rotor disk loading DL, initially, the wing loading WL is explained which is defined as the aircraft weight W divided by the wing area S. Typically, the MTOM or m_{mto} is used in the context of wing sizing. The basic equation is presented below:

$$WL = \frac{W}{S} = \frac{m_{mto}g}{S}. \tag{3.10}$$

Accordingly, the wing loading is higher for smaller wing aircraft when comparing aircraft of same weight. Further, the wing area is simply modeled by a rectangular plan form and can be computed by

$$S = bc, \tag{3.11}$$

where the wing span b is multiplied by the wing chord c. No sweep is intended since eVTOL aircraft normally operate in subsonic speeds. Next, the wing aspect ratio AR can be computed by

$$AR = \frac{b^2}{S} \tag{3.12}$$

which is not only a pure geometry parameter, but is also relevant for the wing aerodynamics as will be explained later. Due to the high power requirement in vertical flight, the wing is mostly considered to be sized based on the stall speed V_s which is defined as

$$V_s = \sqrt{\frac{2m_{mto}g}{\rho S C_{L,max}}} = \sqrt{\frac{2}{\rho C_{L,max}} WL},$$
(3.13)

where ρ is the density of air. The aircraft's maximum lift coefficient $C_{L,max}$ depends on the wing and high-lift system design and is expected to be in a range of 1.5 to 2.0 [99].

After the wing sizing, the empennage or tail geometry has to be computed. Here, the initial estimation of the horizontal and vertical tail is based on their volumes V_H and V_V, respectively. As can be found in Gudmundsson [101], the volumes are defined as

$$V_H = \frac{L_H S_H}{Sc},$$
(3.14)

where L_H is the horizontal tail arm and S_H is the horizontal tail area. Similarly,

$$V_V = \frac{L_V S_V}{Sb},$$
(3.15)

where L_V is the vertical tail arm and S_V is the vertical tail area. In both cases, wing parameters are used in the denominator. It should be noted that the wing chord is relevant for the horizontal tail and the wing span for the vertical tail. Raymer [99] provides values for the volume parameters applicable for initial sizing: horizontal tail volume $V_H = 0.80$ and the vertical tail volume $V_H = 0.07$ taken from twin-engine general aviation aircraft. These values are used for the sizing consequently, however, the tail arms are still missing. Therefore, a method from Gudmundsson [101] is used to determine the tail arm L_T as replicated below:

$$L_T = \sqrt{\frac{2S(V_H c + V_V b)}{\pi(R_1 + R_2)}}.$$
(3.16)

Here, R_1 and R_2 stand for the fuselage radii at the wing and the empennage position. The horizontal and vertical tail geometry is also modeled by rectangular planforms so that the same equations given for the wing geometry are applicable for the sizing (see Equations 3.11 and 3.12)

3.2.3 Aerodynamics

The methodology regarding aerodynamics is divided into three parts, namely hover and vertical flight, wingless forward flight, and winged forward flight. Firstly, the hover flight model will be presented in the following which is relevant for both, wingless and winged eVTOL aircraft configurations.

Hover and Vertical Flight

Aerodynamics in hover are modeled according to momentum theory in order to determine thrust and power correlations. This methodology follows the developed model by Brown & Harris [61, 62] and is described with regard to Leishman [7]. Also, note that the methodology does not model conventional helicopters since no tail rotor power is considered. Initially, the aerodynamic coefficients are defined. Here, the thrust and power coefficients, C_T and C_P, are defined as

$$C_T = \frac{T}{\rho A V_t^2}, \tag{3.17}$$

$$C_P = \frac{P}{\rho A V_t^3}, \tag{3.18}$$

where thrust and power are represented as T and P, respectively. Furthermore, ρ is the density of air, A is the reference or rotor disk area, and V_t is the rotor tip speed.

Furthermore, the power coefficient can be broken down into the sum of the induced power coefficient and profile power coefficient, $C_{P,i}$ and $C_{P,p}$, respectively. Since $C_{P,i}$ only represents the ideal power, it is corrected by the induced power factor κ as shown below:

$$C_P = \kappa C_{P,i} + C_{P,p}. \tag{3.19}$$

Typical values for κ are in range of 1.1 to 1.2 as found in [7], thus $\kappa = 1.15$ is chosen. The just introduced rotor power coefficients are computed by

$$C_{P,i} = \frac{C_T^{3/2}}{\sqrt{2}}, \tag{3.20}$$

$$C_{P,p} = \frac{\sigma C_{d,0}}{8}. \tag{3.21}$$

Here, the blade zero-lift drag coefficient $C_{d,0} = 0.01$ and the rotor solidity $\sigma = 0.1$ are used as default parameters. The rotor solidity, which represents the ratio of the rotor blade area A_b compared to the rotor area A, is determined by

$$\sigma = \frac{A_b}{A} = \frac{N_b c_b R}{\pi R^2}, \tag{3.22}$$

where N_b is the number of rotor blades, c_b is the rotor chord and R is the rotor radius.

Another important parameter for the rotor aerodynamics is the rotor mean lift coefficient $\overline{C_l}$ which is calculated by

$$\overline{C_l} = \frac{6C_T}{\sigma}. \tag{3.23}$$

This parameter depends on the eVTOL aircraft configuration and is one of the rotor sizing constraints representing the lower limit for the rotor tip speed.

Eventually, the figure of merit FOM represents the rotor efficiency by comparing the (ideal) induced power coefficient computed in Equation 3.20 with the total power coefficient including the induced power factor as determined by Equation 3.19. Thus, FOM can be computed by

$$FOM = \frac{C_{P,i}}{C_P}. \tag{3.24}$$

Following the hover aerodynamics, the required power for vertical flight or climb can be computed by the following equation as given by Leishman [7]:

$$\frac{P_{vc}}{P_{ho}} = \frac{V_{vc}}{v_{ho}} + \sqrt{\left(\frac{V_{vc}}{v_{ho}}\right)^2 + 1}. \tag{3.25}$$

Here, the ratio of vertical climb power P_{vc} and hover power P_{ho} is computed, where V_{vc} is the vertical climb speed and v_{ho} is the rotor induced velocity in hover.

Wingless Forward Flight

The methodology for wingless eVTOL aircraft in forward flight also follows momentum theory and is basically similar to the hover performance despite the additional terms to consider the rotor performance in edgewise flight. A simplified model has been proposed by Kadhiresan & Duffy for the modeling of different eVTOL aircraft configurations [60]. The methodology is explained with regard to the theoretical background provided by Leishman [7]. Thus, two additional power coefficients, namely the parasite power coefficient $C_{P,0}$ and the climb power coefficient $C_{P,c}$ have to be considered as well. Accordingly, power coefficient C_P is now computed by

$$C_P = C_{P,i} + C_{P,0} + C_{P,p} + C_{P,c}, \tag{3.26}$$

where

$$C_{P,i} = \frac{\kappa C_T^2}{2\sqrt{\lambda^2 + \mu^2}}, \tag{3.27}$$

$$C_{P,0} = \frac{1}{2}\left(\frac{f}{A}\right)\mu^3, \tag{3.28}$$

$$C_{P,p} = \frac{\sigma C_{d,0}}{8}(1 + K\mu^2), \tag{3.29}$$

$$C_{P,c} = \lambda_c C_W. \tag{3.30}$$

In the above power coefficients, additional non-dimensional parameters are introduced. Basically, Equation 3.27 is an extended form of the induced power coefficient in hover. Here, the induced inflow ratio λ is introduced and, according to Kadhiresan & Duffy [60],

simplified as follows:

$$\lambda = \sqrt{\frac{C_T}{2}} \tag{3.31}$$

Furthermore, the advance ratio μ is introduce in order to model the forward flight. It is computed by

$$\mu = \frac{V\cos(\alpha)}{V_t} \approx \frac{V}{V_t}, \tag{3.32}$$

where the approximation for small rotor angles of attack α is assumed ($W \approx T$) to simplify the computational process as proposed by Kadhiresan & Duffy [60]. Thus, the advance ratio is simplified to the ratio of flight speed V and tip speed V_t. As can be found, $C_{P,i}$, $C_{P,0}$, and $C_{P,p}$ are all dependent on μ. Furthermore, to determine $C_{P,0}$, the equivalent flat-plate area of the aircraft must be known which can be estimated in different ways as will be shown later. Also, the computation of $C_{P,p}$ is extended compared to the hover aerodynamics. Here, the factor K has be accounted for. According to Leishman [7] the numerical value of K lies in a range from 4.5 to 5 and varies with different advance ratios and aerodynamic models. Eventually, $K = 4.7$ is used as proposed in the model by Kadhiresan & Duffy [60]. Eventually, $C_{P,c}$ is computed by the induced climb inflow ratio λ_c and the weight coefficient C_W. This expression basically models the climb by accounting for the additional power required $P = WV_c$ when climbing with an aircraft weight W and climb speed V_c.

To estimate the parasite power of multirotors, Kadhiresan & Duffy [60] have proposed an empirical relation for wingless eVTOL aircraft configurations which is derived from different multirotors and allows roughly estimating the equivalent flat-plate area f by

$$f = 0.0327 m_{mto}^{0.8903}, \tag{3.33}$$

where the empirical equation models the equivalent flat-plate area purely based on the MTOM. It should also be noted that the parameter m_{mto} is in imperial units, i.e. lb, and must be converted to SI units, i.e. kg. This method may provide an initial estimation and may also ease the process for easily utilizing the presented methodology as intended for the fulfillment of requirement AD.6, but more sophisticated methods are needed for the parasite drag estimation and will, among others, be introduced in the context of the winged forward flight aerodynamics.

Winged Forward Flight

For winged forward flight additional coefficients have to be given. In case of winged aircraft, the aircraft lift and drag coefficients, C_L and C_D, are essential parameters for the aerodynamics. Those parameters are defined by the following equations:

$$C_L = \frac{L}{qS} = \frac{L}{\frac{1}{2}\rho V^2 S}, \tag{3.34}$$

$$C_D = \frac{D}{qS} = \frac{D}{\frac{1}{2}\rho V^2 S}. \tag{3.35}$$

Here, aircraft lift L and drag D forces are divided by the dynamic pressure q and the reference or wing area S. The dynamic pressure is a function of air density ρ and flight speed V.

The overall drag coefficient is modeled according to a quadratic drag polar consisting of the parasite or zero-lift drag coefficient $C_{D,0}$ and the lift-induced drag coefficient $C_{D,i}$. Hence,

$$C_D = C_{D,0} + C_{D,i}, \tag{3.36}$$

where $C_{D,0}$ related to aircraft geometry, flight speed and atmospheric conditions and has to be carefully determined. The zero-lift drag coefficient can also be better understood as the ratio of an equivalent flat-plate area f and the reference area S_{ref} which is the wing area S in this case and the rotor disk area A in the case of wingless configurations. Consequently, this drag coefficient can be also expressed as

$$C_{D,0} = \frac{f}{S_{ref}} = \frac{f}{S}. \tag{3.37}$$

Kadhiresan & Duffy [60] have proposed and validated an empirical relation for winged eVTOL aircraft configurations which is derived from historic VTOL aircraft and allows roughly estimating the equivalent flat-plate area by

$$f = 1.6\left(\frac{m_{mto}}{1000}\right)^{2/3}. \tag{3.38}$$

As can be seen from the above equation, the empirical equation models the equivalent flat-plate area fully based on the MTOM. It should also be noted that the parameter m_{mto} is in imperial units, i.e. lb, and must be converted to SI units, i.e. kg. This method may provide an initial estimation and also ease the process for easily utilizing the presented methodology as intended for the fulfillment of requirement AD.6, however, further methods should be considered for the drag estimation. Thus, a component drag build up method, as described by Raymer [99], may offer a higher accuracy for the drag prediction. For this method, the flat-plate skin friction drag coefficient C_f, the form factor FF, the interference factor Q, and the wetted area S_{wet} are needed for each drag component. Consequently,

$$C_{D,0} = \frac{\sum\left(C_{f,c}FF_cQ_cS_{wet,c}\right)}{S_{ref}}, \tag{3.39}$$

where the subscript c stands for each drag component that has to be accounted for.

Furthermore, regarding the second part of the quadratic drag polar shown in Equation 3.36, $C_{D,i}$ depends on the aircraft lift coefficient as follows:

$$C_{D,i} = \frac{C_L^2}{\pi e AR}. \tag{3.40}$$

According to Raymer [99] the span efficiency or Oswald efficiency e can be computed by

$$e = 1.78(1 - 0.045AR^{0.68}) - 0.64, \tag{3.41}$$

which takes the influence of the wing aspect ratio into account. However, the zero-lift drag coefficient

Eventually, the use of the presented class II methods for the aerodynamics modeling represents an improvement compared to the previously utilized tool for eVTOL aircraft sizing [40] that relied purely on constant lift-to-drag ratios of different eVTOL aircraft configurations. Thus, this methodology contributes to fulfilling requirement AD.3.

3.2.4 Acoustics

While the eVTOL aircraft noise assessment does not make a part of this thesis and is mostly considered by certain aircraft architecture and design considerations for reduced noise, it plays an important role in the design and deployment of aircraft in general, but is especially pivotal for eVTOL aircraft due to the intended operations in urban environments. Therefore, the tool can easily allow for low-fidelity assessment of rotor acoustics. This can be enabled by the methodology derived by Brown & Harris [61] which can be utilized in the post-processing stage of the eVTOL aircraft design.

As mentioned already before, the noise of (non-hybrid) eVTOL aircraft has fewer contributing powertrain components due to the lack of gas turbines, piston-engines and sometimes also gearboxes. Subsequently, the aforementioned methodology considers three main sources of rotor noise for eVTOL aircraft, namely blade slap noise, rotational noise, and vortex noise, which are briefly summarized in the next paragraph with reference to Brown & Harris [61] in order to provide an insight into the rotor acoustics model and insights gained from it.

Brown & Harris discuss the causes of blade slap, i.e. shockwave formation, blade stall, and blade-vortex interaction, and conclude that through certain design considerations, i.e. low tip Mach numbers, reasonable blade mean lift coefficients, and optimized departure as well as arrival procedures, respectively, the blade slap noise is neglected in this low-fidelity assessment. Next, rotational noise can be evaluated by modeling loading noise and thickness noise, and can be computed as Sound Pressure Level (SPL). The model used by Brown & Harris does rely on few input parameters which have to be assumed in addition to the computed results from the rotor sizing as explained in Section 3.2.2. However, Brown & Harris have found that rotational noise is negligible in contrast to vortex noise not only directly underneath, but also at close and distant observer positions diagonally underneath the rotor. Thus, vortex noise is of greater importance. The referred derivation and model for vortex noise shows some trends and design considerations that must be paid attention to in the eVTOL aircraft design. Accordingly, decreasing rotor tip
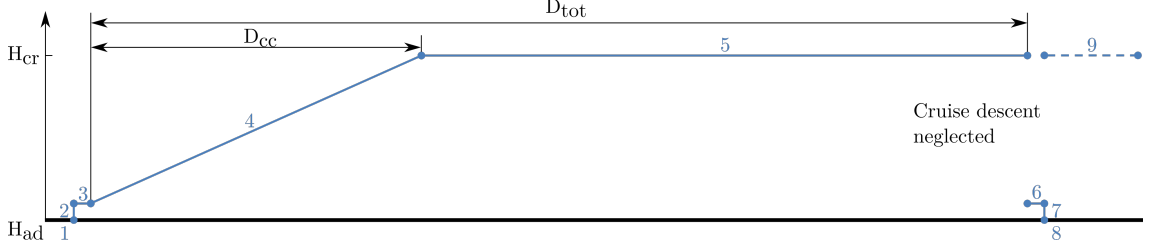
Figure 3.2: Generic Mission Profile for VTOL Aircraft Design

speed as well as rotor disk loading and increasing rotor solidity benefit the vortex noise reduction. Finally, the computed SPL is adjusted by the A-weighting scheme in order to better model the human hearing characteristics by accounting for different responses over different sound frequencies. Due to the peak of the A-weighting scheme at 600 Hz, Brown & Harris suggest avoiding this frequency by careful attention in the design. Since the model considers isolated open rotors only, limitations with regard to deviating eVTOL aircraft configurations or special design considerations are stated. [61]

3.2.5 Mission

In order to size the eVTOL aircraft, a representative (sizing) mission has to be defined. Accordingly, the generic mission definition of this methodology is established with regard to NASA's [102] and Uber's [103] mission profiles for eVTOL aircraft. The derived mission profile is presented in Figure 3.2 and consists of 9 individual segments, namely taxi out (1), vertical climb (2), transition (3), cruise climb (4), cruise (5), re-transtion (6), vertical descent (7), taxi in (8), and loiter (9). An arbitrary definition of segment altitudes is feasible, whereas the atmosphere modeling follows the International Standard Atmosphere (ISA).

The single segments are successively explained by the following equations. Starting with both taxi segments which are simply defined as a fixed period of taxi time $t_{tx} = const.$ over which a taxi power

$$P_{tx} = 0.1P_{ho} = const. \tag{3.42}$$

is applied which is basically defined as 10% hover power P_{ho}.

Consequently, the vertical climb phase is entered, where a vertical climb power $P_{vc} = const.$ is applied over a period of vertical climb time t_{vc} computed as

$$t_{vc} = \left(\frac{\Delta H}{RoC}\right)_{vc}, \tag{3.43}$$

which models a vertical climb at a constant rate of climb RoC over a predefined difference of altitude ΔH. Note that the vertical descent time t_{vd} is set equal to t_{vc}.

In order to transition to forward flight, the aircraft has to accelerate which is modeled by an acceleration $a = const$. Accordingly, the time to accelerate the aircraft is computed by the difference of flight speed ΔV, which is zero at the start and reaches forward flight speed V at the end of the transition segment, so that the transition time t_{tr} is computed by

$$t_{tr} = \frac{\Delta V}{a} = \frac{V}{a}. \tag{3.44}$$

It should be noted that this segment is also modeled by a constant transition power $P_{tr} = const.$, similarly as before. The distance traveled during acceleration is neglected in this methodology. Furthermore, the re-transition time is modeled in the same way, whereas the aircraft decelerates here, though the same methodology applies.

Also, during the cruise climb segment, a constant power $P_{cc} = const.$ is applied. Further, it represents mission segment, where $RoC = const.$ and the resulting cruise climb time t_{cc} is simply calculated by

$$t_{cc} = \left(\frac{\Delta H}{RoC} \right)_{cc}. \tag{3.45}$$

The distance traveled during the cruise climb time D_{cc} is considered by

$$D_{cc} = V_{gs} t_{cc} = (V - V_{hw}) t_{cc}, \tag{3.46}$$

where the ground speed V_{gs} must be multiplied with t_{cc}. Accordingly, V_{gs} is obtained by the difference of flight speed V, representing the true air speed, and the headwind speed V_{hw}. Since the difference of altitude also leads to a change of air density and power required, the cruise climb power P_{cc} is evaluated at the aerodrome altitude $(P_{cc})_{H,ad}$ and cruise altitude $(P_{cc})_{H,cr}$. Subsequently, the mean value is computed by

$$P_{cc} = \frac{(P_{cc})_{H,ad} + (P_{cc})_{H,cr}}{2}. \tag{3.47}$$

Similar as for t_{cc}, the cruise time t_{cr} is computed considering V_{hw} by

$$t_{cr} = \frac{D_{cr}}{V_{gs}} = \frac{D_{cr}}{V - V_{hw}}, \tag{3.48}$$

where the cruise distance D_{cr} must be calculated accounting for D_{cc}. Thus,

$$D_{cr} = D_{tot} - D_{cc}, \tag{3.49}$$

basically taking the desired total distance D_{tot} as a basis which is reduced by the distance traveled during cruise climb. As for all segments, the computed cruise power $P_{cr} = const.$

The cruise descent is neglected which is a common procedure in the conceptual aircraft design stage, e.g. see Raymer [99]. Accordingly, this approach leads to a more conservative

estimation of required mission energy and may give some flexibility in the continuing design process.

As stated before, the remaining mission segments, namely re-transition, vertical descent, and taxi in, are simply mirrored by their counterparts at the start of the mission.

The final mission segment which must be considered in the loiter segment which stands for the mission reserve. Here, the computed loiter power $P_{lo} = const.$ is applied over a fixed period of loiter time t_{lo} which can be defined arbitrarily.

3.2.6 Performance

Generally the performance considers all mission performance as well as additional aircraft performance aspects. Herein, the required powers and energies for all mission segments are computed according to the aerodynamics methodology which was presented in Section 3.2.3. This is not only needed for the sizing process but also for the ABS where the aircraft performance must be input. Therefore, the aircraft's mission performance is evaluated after the design output is reached as explained in Section 3.2.1. Hence, the performance evaluation considers all possible load factors from empty up to the full payload of the aircraft, whereas the aircraft piloting can also be specified as an input variable. Eventually, the performance over all segments and load factors is computed where also deviating atmospheric conditions in comparison to the sizing mission can be considered. It should be noted that, in the computational process, the aircraft MTOM is assumed to be constant over the entire mission time, even for hydrogen- or kerosene-based propulsion systems. Due to the comparably small fuel masses, the influence is considered negligible.

In this context, a distinction is made in the performance evaluation of pitch and speed controlled rotors. For (classic) pitch controlled rotors, the tip speed is constant and change in thrust is generated through the change of the blade pitch. However, for speed controlled rotors, which are increasingly used for multirotor air vehicles, the aerodynamic coefficients remain constant, thus change in thrust is generated through the change of tip speed. Accordingly, this is considered by the model where either the thrust coefficient or tip speed are recomputed, respectively.

As the speeds for best range V_{br} and V_{be} are important aircraft characteristics for efficient operations of energy-constraint eVTOL aircraft, the speeds are computed as part of the performance. From graphical analyses of the aircraft's power curve (power over flight speed), V_{br} represents the speed at which a line passing the origin of the graph is tangential to the power curve. Further, V_{be} can be simply found as the minimum of the power curve. Those characteristic speeds are computed differently depending on wingless or winged aircraft configurations and the corresponding equations are shown in the following. It should be noted that the speeds are calculated based on the MTOM, thus are not updated in respect of different load factors.

Wingless

As given in Leishman [7] for example, V_{br} and V_{be} can be simply calculated from already available aircraft parameters. For wingless aircraft, the induced velocity in hover flight needs to be input so that both speeds can be computed as follows:

$$V_{br} = v_{ho}\left(\frac{4\kappa}{f/A}\right)^{1/4} = \sqrt{\frac{W}{2\rho A}}\left(\frac{4\kappa}{f/A}\right)^{1/4}, \tag{3.50}$$

$$V_{be} = v_{ho}\left(\frac{4\kappa}{3f/A}\right)^{1/4} = \sqrt{\frac{W}{2\rho A}}\left(\frac{4\kappa}{3f/A}\right)^{1/4}. \tag{3.51}$$

Winged

For the winged eVTOL aircraft configurations, for example, Raymer [99] gives the following equations for V_{br} and V_{be}, respectively:

$$V_{br} = \sqrt{\frac{2W}{\rho S C_{L,md}}} = \sqrt{\frac{2W}{\rho S}}\left(\frac{k}{C_{D,0}}\right)^{1/4}, \tag{3.52}$$

and

$$V_{be} = \sqrt{\frac{2W}{\rho S C_{L,mp}}} = \sqrt{\frac{2W}{\rho S}}\left(\frac{k}{3C_{D,0}}\right)^{1/4}, \tag{3.53}$$

which involve the lift coefficient for minimum drag $C_{L,md}$ and the lift coefficient for minimum power $C_{L,mp}$, respectively.

Eventually, the proposed performance methodology allows computing or evaluating the performance of the design output or sized eVTOL aircraft so that all required inputs for the ABS are obtained. Correspondingly, requirement AD.4 can be fulfilled.

3.2.7 Airframe

The airframe components and associated weights or masses are estimated based on a set of methods proposed for conceptual eVTOL aircraft design by Kadhiresan & Duffy [60]. The methods are taken from empirical weight and design correlations based on historical fixed-wing and rotary-wing aircraft, where Roskam [104] and Prouty [105] are referred to, respectively. Eventually, the following equations are derived.

The equation for the fuselage mass m_{fus} is based on both, Roskam [104] and Prouty [105]. Accordingly, the methodology by Kadhiresan & Duffy [60] suggests that

$$m_{fus} = 6.9\left(\frac{m_{mto}}{1000}\right)^{0.49} L_F^{0.61} S_{wet,F}^{0.25}, \tag{3.54}$$

where the computed parameters for MTOM, fuselage length and fuselage wetted area are inserted. Next, the landing gear mass m_{lg} also follows a combination of the methods by Roskam [104] and Prouty [105]. Thus, Kadhiresan & Duffy [60] presented the following equation, where the influencing parameters are the MTOM and the number of wheels N_{wheel} which is set to 2, as proposed in the methodology:

$$m_{lg} = 40\left(\frac{m_{mto}}{1000}\right)^{0.67} N_{wheel}^{0.54}. \tag{3.55}$$

The two latter equations are used for wingless and winged eVTOL aircraft configurations, while for the wingless ones, only these two aircraft components are modeled.

Additionally, for the winged eVTOL aircraft configuration, the wing and empennage masses have to be estimated. The wing mass m_w depends on the computed MTOM, the computed wing area, the specified wing aspect ratio, and the ultimate load factor N_{ult}, which is derived from EASA's Certification Specifications (CS) 23 normal aeroplanes and set to 5.7, accordingly. Thus, the wing mass is computed according to [104] by

$$m_w = 0.04674 m_{mto}^{0.347} S^{0.36} N_{ult}^{0.397} AR^{1.712}. \tag{3.56}$$

Further on, the empennage mass m_{emp} including horizontal and vertical tail is computed as Kadhiresan & Duffy [60] derived from Roskam [104] and Prouty [105]:

$$m_{emp} = 0.72 S_H^{1.2} AR_H^{0.32} + 1.05 S_V^{0.94} AR_V^{0.53}. \tag{3.57}$$

Here, the computed areas of both components are inserted together with the horizontal and vertical tail aspect ratio AR_H and AR_V, respectively. These parameters are set to $AR_H = 2$ and $AR_V = 1.3$ as proposed by Kadhiresan & Duffy [60].

It should be noted that all the parameters of the above airframe estimation equations are in imperial units, i.e. lb, ft, etc., and must be converted to SI units, i.e. kg, m, etc.

Eventually, the use of the presented class II methods for the airframe mass estimations represents an improvement compared to the previously utilized tool for eVTOL aircraft sizing [40] that relied purely on historical mass fractions to account for the structural group as described in [61, 62]. Thus, this methodology contributes to fulfilling requirement AD.3.

3.2.8 Propulsion and Onboard Systems

The modeling of propulsion and onboard systems for conceptual eVTOL aircraft design has been developed by Bertram et al. [106, 107] as part of the HorizonUAM research project. In this context, it should be noted that onboard systems comprise all powertrain components (e.g. rotor, motor, battery, etc.) as well as other systems (e.g. avionics,
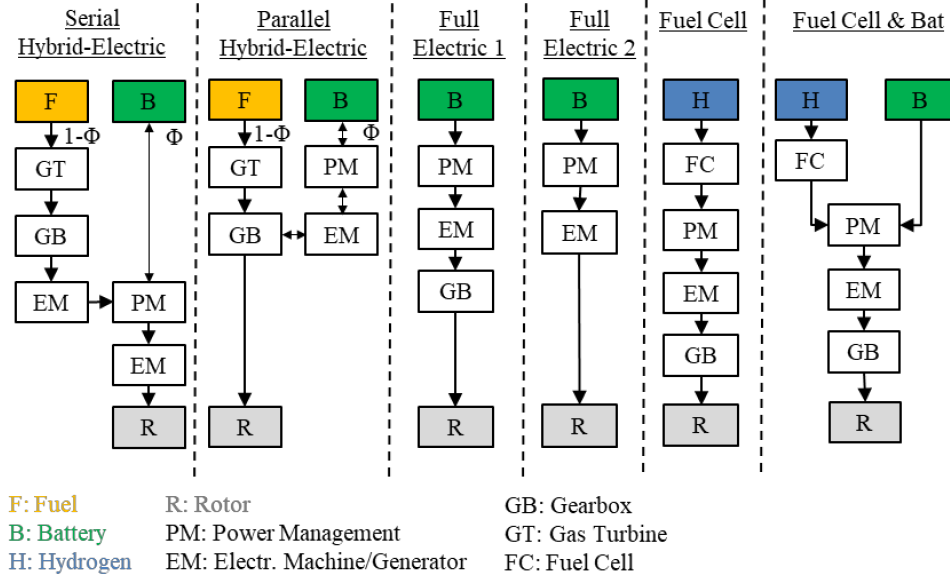
Figure 3.3: Overview of the Modeled Powertrain Architectures [107]

furnishings, environmental control system, etc.) and is used as the main technical term subsequently.

Bertram et al. [107] propose a basic model for different powertrain architectures that can be investigated for eVTOL aircraft. The modeling considers hybrid-electric (serial and parallel), battery-electric (with and without gearbox), and fuel-cell powered (with and without battery) powertrain architectures. Subsequently, Figure 3.3 shows the different architectures including each powertrain component involved.

Furthermore, technical specifications or characteristics of the involved powertrain components have be found. Bertram et al. [107] have compiled and proposed a set of parameters that is replicated in Table 3.1. The given parameters consider state-of-the-art technology levels.

Table 3.1: Powertrain Component Characteristics [107]

Powertrain Component	SP, kW/kg	SE, kWh/kg	η
Gas Turbine	8.2	—	0.5
Gearbox	5	—	0.98
Rotor/Propeller	3	—	0.87/0.8
Generator	4	—	0.95
Power Management	5	—	0.98
Electric Motors	4	—	0.95
Fuel Cell Stack	0.6	—	0.5
Kerosene	—	11.8	—
Hydrogen	—	33.3	—
Battery	0.625	0.25	0.96

From Table:3.1 it can be seen that the powertrain components are represented by their specific power SP, specific energy SE, and efficiency η which is assumed to be constant over the entire mission. As can be seen, the electric powertrain components, aside for the basic PEM fuel cell model, show comparably high efficiencies. However, the battery shows severe limitations in terms of specific energy when compared to kerosene or hydrogen. Also, the usable battery energy is further reduced in this linear battery model in order to account for the non-linear battery discharge behavior in the low and high states of charge which leads to a maximum depth of discharge or usable battery capacity of 80%. In this context, the battery discharge is generally limited to 2.5C which can be found from dividing the battery's specific power by specific energy.

Moreover, regarding the fuel cell stack (set of multiple fuel cells), limitations with regard to its specific power may be expected. This is also the reason why the combination of fuel cell and battery may provide benefits as the battery could support the high power requirements during vertical flight and the fuel cell could provide a more or less constant power during stationary cruising flight benefiting from the high specific energy of hydrogen to enable increased ranges compared to battery-electric eVTOL aircraft. Some of these aspects have been already shown in the results from Bertram et al. [107].

Eventually, it should also be noted that the rotor and propeller efficiencies are just listed for completeness, but are already considered within the aerodynamics model.

The analytical powertrain model presented by Bertram et al. [107] is based on the de Vries' work on the modeling of different hybrid-electric aircraft [108]. In this model, the flight performance as explained in Sections 3.2.3, 3.2.5 and 3.2.6, is the required input to compute the power required by each powertrain component. According, the efficiency of powertrain components η_{pc} as given in Table 3.1 must be considered so that

$$P_{out} = \eta_{pc} \sum P_{in}, \tag{3.58}$$

where P_{out} represents the provided power and P_{in} the required power by the powertrain component. Eventually, the mass of each powertrain component m_{pc} can be found from the maximum required powertrain component power $P_{pc,max}$ divided by its specific power SP_{pc} as shown in Table 3.1:

$$m_{pc} = \frac{P_{pc,max}}{SP_{pc}}. \tag{3.59}$$

Beyond the powertrain components that are sized according to their maximum required powers, the energy sources, namely battery, hydrogen, and kerosene, require another input which is the required energy, of course. Therefore, the basic physical relationship between work W, power P and time t is shown by the following integral equation:

$$W = \int_{t_0}^{t_1} P(t)\mathrm{d}t. \tag{3.60}$$

Since the mission performance model only considers constant powers for each mission segment, the integral can be simplified to a sum formula,

$$E = \frac{1}{\eta_{tot}} \sum_s P_s t_s, \tag{3.61}$$

where the energy E is computed by summing the products of segment power and time, P_s and t_s, over all segments, respectively. The total powertrain efficiency η_{tot} must also be accounted for, of course.

Subsequently, the masses of the energy storage systems can be computed. Here, the battery mass depends on both, specific energy and power, SE_{bat} and SP_{bat}, so that the maximum required battery power $P_{bat,max}$ and battery energy E_{bat} must be considered. Eventually, the battery mass m_{bat} is sized according to the maximum of both evaluations, as shown below:

$$m_{bat} = \max\left(\frac{P_{bat,max}}{SP_{bat}}, \frac{E_{bat}}{SE_{bat}}\right). \tag{3.62}$$

Since hydrogen and kerosene do not have limitations with regard to specific power, their mass, m_{hdg} and m_{krs}, can be simply computed by required energy, E_{hdg} and E_{krs}, and specific energy, SE_{hdg} and SE_{krs}, as follows:

$$m_{hdg} = \frac{E_{hdg}}{SE_{hdg}}, \tag{3.63}$$

$$m_{krs} = \frac{E_{krs}}{SE_{krs}}. \tag{3.64}$$

Since the previously sized components only consider the powertrain, further onboard systems are summarized under the designation of other systems. Here, a linear fitted equation is used to account for the masses of systems such as flight controls, avionics, environmental control, furnishings and equipment, instruments, and electrical components. [66]. It should be noted that the parameters are in imperial units, i.e. lb, ft, etc., and must be converted to SI units, i.e. kg, m, etc. The equation to estimate the other systems mass m_{os} is as follows:

$$m_{os} = 0.0239 m_{mto} + 195.71. \tag{3.65}$$

Since the before equation has been derived and analyzed for a two-seater eVTOL aircraft by the authors of the previously cited work, the mass m_{os} is increased by 15 kg for every additional seat onboard of the aircraft.

Finally, the use of this model does contribute to the fulfillment of requirement AD.5 where different powertrain architectures can be modeled in the conceptual eVTOL aircraft design process. Furthermore, different cabin designs can be modeled with respect to the increasing mass impact of other systems as required in AD.5. Also, this model overcomes limitations that were present in the earlier utilized eVTOL aircraft design tool which only considers

battery-electric architectures and does not allow deriving a powertrain component break down [40]. Thus, this methodology also contributes to requirement AD.3.

3.2.9 Masses

This section considers mass groups and fractions which will be briefly described in the following. Firstly, the MTOM is computed as the sum of the airframe mass m_{af}, the onboard systems mass m_{obs}, and the payload mass m_{pl}:

$$m_{mto} = m_{af} + m_{obs} + m_{pl}. \tag{3.66}$$

Next, the group airframe mass is further broken down and can be computed from the airframe component masses shown in Section 3.2.7:

$$m_{af} = m_w + m_{emp} + m_{fus} + m_{lg}. \tag{3.67}$$

Similarly, the onboard systems mass considers all powertrain components m_{pc}, the other systems mass, and the masses for energy storage as presented in Section 3.2.8:

$$m_{obs} = \left(\sum_{pc=1}^{n} m_{pc} \right) + m_{os} + m_{bat} + m_{hdg} + m_{krs}. \tag{3.68}$$

Besides the shown mass groups, several fractions can be defined. Starting with the empty mass fraction f_e which is computed by

$$f_e = \frac{m_{af} + m_{obs} - m_{bat} - m_{hgd} - m_{krs}}{m_{mto}}, \tag{3.69}$$

and represents an empty aircraft without any energy masses onboard. The naming may be misleading at the first glance but the fraction can serve for comparison with non-eletric aircraft. Moreover, the zero-fuel fraction f_{zf} is computed as expected, thus

$$f_{zf} = \frac{m_{af} + m_{obs} - m_{hgd} - m_{krs}}{m_{mto}}, \tag{3.70}$$

where only the consumable energy masses, namely the hydrogen and kerosene masses are subtracted, leaving the aircraft at zero fuel. Eventually, the energy mass fraction f_{egy} is computed by the masses of all available energy storage components. It shows that

$$f_{egy} = \frac{m_{bat} + m_{hgd} + m_{krs}}{m_{mto}} = f_{bat} + f_{hdg} + f_{krs}, \tag{3.71}$$

where the single fraction can also be decomposed into the sum of the constituent mass fractions for battery f_{bat}, hydrogen f_{hdg}, and kerosene f_{krs}.

The subsequent mass fractions require no further explanation. Hence, equations 3.72, 3.73, and 3.74 present the calculations of the airframe mass fraction f_{af}, the onboard systems mass fraction f_{obs}, and the payload mass fraction f_{pl}, respectively:

$$f_{af} = \frac{m_{af}}{m_{mto}}, \tag{3.72}$$

$$f_{obs} = \frac{m_{obs}}{m_{mto}}, \tag{3.73}$$

$$f_{pl} = \frac{m_{pl}}{m_{mto}}, \tag{3.74}$$

3.3 Software Architecture

3.3.1 Overview

As stated in Section 3.1, several requirements must be met for the technical implementation. First, to fulfill requirement SA.1 the tool is coded in Python 3 [109] which is a free and open source programming language that support Object-Oriented Programming (OOP). As Python has become very popular in general as well as within science and engineering, probably thanks to its emphasize on code readability and the wide range of additionally available packages, choosing this programming language definitely makes sense. Moreover, the ABS for SoS fleet assessment is also written in Python which is expected to ease the utilization and maintenance of the VTOL-AD tool, since other developers can use and modify it, too.

The VTOL-AD tool makes use of OOP as a programming paradigm that basically utilizes classes to set up data (variables) and methods (functions). Thereby, the so-called objects are instances of classes. Accordingly, the developed software architecture is depicted in Figure 3.4 as a Unified Modeling Language (UML) class diagram. The tool utilizes one central class, the `Vehicle` class, that holds all the vehicle related variables as a non-frozen data class, whereas few exemplary variables such as *maximum_ takeoff_ mass*, *disk_ area* and *wing_ area* are shown in Figure 3.4. As shown in the UML diagram, further classes and modules are grouped around the central `Vehicle` class and will be explained subsequently.

While the tool mostly makes use of commonly utilized Python packages such as numpy, pandas, etc., a special mention in regard to the handling of units must be given. Since many of the variables stored in `Vehicle` class the have units and often wrong or forgotten unit conversions lead to incorrect results in science and engineering, the package pint is imported to allow the assignment of units and enable automatic unit checking as well as conversions. The unit registry is initialized in the `units.py` module and used in all other modules.
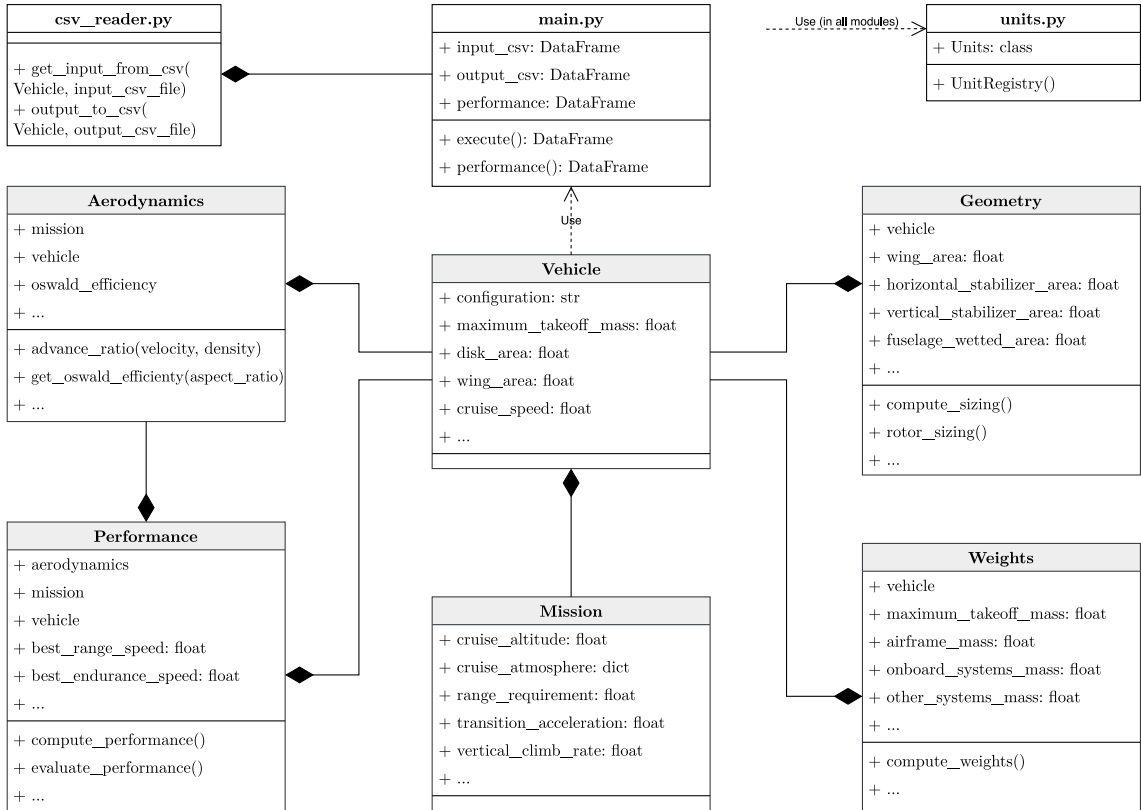
Figure 3.4: Developed Software Architecture Represented as UML Class Diagram

Next, the `Mission` class contains all the variables and computations that are relevant to the set-up of the sizing mission. It mostly incorporates the variables and simple computations presented in Section 3.2.5 which among others include the *cruise_altitude* and the *cruise_atmosphere*. Moreover, the class also imports another method from Brown & Harris [62] which directly interpolates and returns the requested ISA parameters, e.g. air density, from a look-up table.

The remaining classes mostly implement the previously presented methodology by methods. Starting with the `Geometry` class: here, the most of the sizing is performance where different variables such as the *wing_area, disk_area* and *fuselage_wetted_area* are computed (see Section 3.2.2). Also, the class directly imports the rotor model developed by Brown & Harris [62] for the rotor sizing process which is formulated as a geometric program for optimization and implemented by the Python package GPkit [110]. Slightly different compared to the earlier presented structure for the VTOL-AD tool's methodology (see Section 3.2), the `Weights` class comprises all the computations with regard to component weights or masses including powertrain and onboard systems as well as airframe components (see Sections 3.2.8 and 3.2.7). It should be noted that the standalone version of the VTOL-AD tool incorporates a fully electric powertrain architecture as described in the associated methodology. The two remaining classes, i.e. `Aerodynamics` class and `Performance` class, implement the corresponding methods as explained before in Sections 3.2.3 and 3.2.6, respectively. Here, it should be noted that the latter two classes are

also interconnected in order to make use of reusable methods that are implemented in the aerodynamics modeling, but mostly utilized within the performance computations.

Eventually, the VTOL-AD tool is bundled by the main.py module that imports all the other classes and modules, thus provides the executable file for the initial sizing loop and performance evaluation process including the definitions of input and output directories. In the following, an excerpt of the code implemented in the main.py module is shown to illustrate the implementation of the initial sizing loop as conceptually shown in Figure 3.1 (see Section 3.2.1). It should be noted that the presented code snippet provides only a shortened overview of the main.py module. However, all relevant lines of code for running the initial sizing loop are compiled and presented in this snippet. For further reference, the fully executable code of the VTOL-AD tool can be found in the digital appendix which is structured as described in Appendix C.

```python
1   from aerodynamics import Aerodynamics
2   from geometry import Sizing
3   from mission import Mission
4   from performance import Performance
5   from units import Units
6   from vehicle import Vehicle
7   from weights import ComponentWeightSizing
8
9
10  def main():
11      """
12      This function executes the initial vehicle sizing loop.
13      """
14      # Initialize vehicle classes
15      mission = Mission()
16      vehicle = Vehicle(mission)
17
18      # Initialize sizing classes
19      geometry = Sizing(vehicle)
20      weight = ComponentWeightSizing(vehicle)
21      aerodynamics = Aerodynamics(vehicle)
22      performance = Performance(vehicle, aerodynamics)
23
24      # Initialize sizing loop
25      iteration = 0
26      convergence = 999 * Units.kg
27      convergence_criterion = 0.001 * Units.kg
28
29      # Performance sizing until convergence
30      while (convergence > convergence_criterion or
31          convergence < -convergence_criterion):
32        maximum_takeoff_mass = vehicle.maximum_takeoff_mass
33        geometry.compute_sizing()
34        performance.compute_performance()
35        weights.compute_airframe_weights()
```

```
36        weights.compute_onboard_systems_weights()
37        weights.compute_weights()
38
39        convergence = (maximum_takeoff_mass - vehicle.maximum_takeoff_mass)
40        iteration += 1
41
42    # Evaluate performance
43    performance.evaluate_performance()
```

In order to enable easily accessible user interaction with the tool, the vehicle parameters are input and output in Comma Separated Values (CSV) files that can be modified in Excel or other spreadsheet software programs. Eventually, the `csv_reader.py` module, which is inherited from the SoS simulation toolkit, reads the inputs from the CSV file and creates a separate output CSV file after the sizing loop has converged. In this process, the module also takes care of unit conversions which are also indicated in the header of the CSV file. Further information on the user input and output variables as well as handling will be provided in the following Section 3.3.2.

In summary, the developed software architecture fulfills requirement SA.2 by providing a fully executable software tool which does not require additional interfaces to other tools but can be run as a standalone version of its own.

3.3.2 User Input and Output

As explained before, the user input and output handling is mostly done through CSV files. An exemplary input CSV file named *aircraft_input.csv* is shown in Table 3.2. While it only provides an excerpt of the even larger data file, a complete list of variables is provided in Appendix B. Even if it was part of the requirements concerning the aircraft design methodology, the learning curve for newcomers to eVTOL aircraft design is mitigated by requiring only relatively few input variables and providing default input variables that are part of the provided input files for both, wingless as well as winged eVTOL aircraft configurations. Further information on default input variables can be found in Appendix B. Thus, requirement AD.6 can be fulfilled.

Table 3.2: Input and Output CSV File of the VTOL-AD Tool (Excerpt Only)

0	study	config	is_winged	max_disk_loading	disk_loading	hover_power
1	dimensionless	dimensionless	N/m**2	N/m**2	N/m**2	kW
2	None	None	None	None	None	tuple
3	str	str	bool	float64	float64	float64
4	Validation	LiftCruise	True	750	0	()

Table 3.2 shows the header of the file where the first row defines the variable name, the second row the variable's unit, the third row the sequence type (e.g. list, tuple), and the

fourth row the data type (e.g. str, bool, float64). Below, the actual variables are defined with some default values already inserted. Furthermore, the user can input separate design points by simply adding additional rows. Typically, no special care must be taken of the initial *maximum_ takeoff_ mass* input variable or guess value, since the tool usually reaches convergence after less than 10 s per design point if a feasible solution can be found according to the given constraints. After user manipulations, the CSV file must be saved and closed in order to start the sizing process within the VTOL-AD tool by executing the `main.py` module. During the tool run, the user can find information on the converged sizing loops of each design point via the console. The displayed information contain the number of iterations, the final convergence value, and the resulting MTOM. Afterwards, the user receives an additional CSV file named *aircraft_ output.csv* and saved in the same directory as the input file. Thus, all vehicle variables are updated and shown together with the inputs. However, the mission parameters which are utilized for the sizing process are currently input through the `Mission` class and the corresponding file. This present limitation is also discussed in Section 3.4.

3.3.3 Interfaces

The remaining three requirements for the software architecture SA.3 to SA.5 concern the interfaces of the VTOL-AD tool.

SoS Simulation Framework

First of all, the connection within the SoS simulation framework must be assured. Currently, the overall SoS simulation framework is still under development, however, the earlier described ABS for SoS fleet assessment is readily available at this institute for an indirect connection through input and output files. To match the interface, the VTOL-AD tool contains a `json_reader.py` module in order to provide a JavaScript Object Notation (JSON) file, which is a frequently utilized file format for data exchange between different tools. An examplary JSON file of a fully battery-electric lift + cruise configuration is presented in the below excerpt.

```
1  {
2    "study": "validation",
3    "config": "liftcruise",
4    "powertrain_architecture": "FullElectric1",
5    "icon": "aeroplane.svg",
6    "flow_rate": 1.2, # m^3/s
7    "can_scoop": true,
8    "mtom": 3721.462, # kg
9    "payload": 540.0, # kg
10   "persons_on_board": 6,
11   "flight_velocity": 61.946, # m/s
12   "battery_specific_energy": 500.0, # Wh/kg
```

```
13    "fuel_cell_specific_energy": 0.0, # W/kg
14    "powertrain_efficiency": 0.912,
15    "total_energy": 1547286.656, # kJ
16    "total_usable_energy": 1237829.325, # kJ
17    "reserve_energy": 305975.901, # kJ
18    "battery_mass_fraction": 0.231,
19    "hover_power": [
20      629.358,
21      656.252,
22      683.518,
23      711.152,
24      739.148,
25      767.503,
26      796.211
27    ], # kW
28
29    [...]
30
31    "charging_power": 450.0, # kW
32    "taxi_time": 30.0, # s
33    "transition_time": 31.584, # s
34    "vertical_climb_altitude": 15.24, # m
35    "cruise_climb_altitude": 609.6, # m
36    "vertical_climb_rate": 0.508, # m/s
37    "vertical_descent_rate": 0.508, # m/s
38    "cruise_climb_rate": 4.572, # m/s
39    "cruise_descent_rate": -3.81, # m/s
40 }
```

As can be seen from the given data structure, it is an easily readable file that transfers all the relevant aircraft parameters to the ABS. Some parameters (see lines 6, 7 and 38) are actually not used in the UAM simulation but are required inputs for the wildfire suppression simulation which conveniently uses the same JSON file format. Since the aircraft performance is modeled in the ABS, the required inputs comprise energy and power. Therefore, the three energy values are provided, namely *total_energy*, *total_usable_energy* and *reserve_energy*. Here, the *total_usable_energy* is the *total_energy* reduced due to the maximum battery discharge as introduced in the battery modeling (see Section 3.2.8). Aircraft without batteries will not be affected, of course. Eventually, each aircraft agent within the ABS has the *total_usable_energy* minus the *reserve_energy* available for its normal revenue flight mission. The energy consumption of each agent is represented by a constant power for each mission segment and load factor. Accordingly, the exemplary six-seat aircraft shows six different values for the *hover_power* considering all possible load factors including autonomous or remote-piloted aircraft (lines 20 and 26 represent the power values of an empty and fully loaded aircraft, respectively). While the excerpt only shows the *hover_power* for the associated segment, further powers of other segments are not shown for abbreviation as indicated by the ellipsis points in line 29. Another power value important for the agent's energy modeling and very relevant during the turnaround is

the *charging_ power*. Since all the powers are directly provided considering the powertrain efficiency, the powers can be directly applied to the agent's energy source. Also, since the ABS performs calculation or simulation steps based on seconds, the powers can be directly subtracted from the agent's energy source due to the unit usage of kW for power and kJ or kWs for energy. However, the units cannot be directly asserted to the output values, thus the `json_reader.py` module applies all the required conversions according to the units commented in the file before outputting the values. Further mission defintions are provided in lines 32 to 38. In this context, it should be noted that the *cruise_ descent_ rate* parameter is currently only used in the wildfire simulation and cruise descent is not yet implemented in the UAM simulation at the current development stage of the ABS. Eventually, requirement SA.3 is completely fulfilled by the explained JSON file transfer.

Onboard Systems Design

Furthermore, different onboard systems or powertrain architectures for eVTOL aircraft must be implemented by an interface to the tool for conceptual design of onboard systems, named ConOBS. Since the tool is developed by a partner institute within the HorizonUAM project, the connection must be enabled remotely. Therefore, the DLR has developed a software which allows connecting multiple tools in the so-called Remote Component Environment (RCE) where tools can be integrated, shared, connected and executed in work flows [111]. This approach does not only allow the involved tool developers to keep their code but also allows the remote connection of partnering domain expert tools to design and assess complex engineering problems through RCE.

The ConOBS tool uses Microsoft Excel Open XML Spreadsheet (XLSX) files for input and output. The input consists of a simple spreadsheet that must provide the shaft powers in kW, the durations in h, the aircraft weight or mass in kg, and the names of all computed sizing mission segments, respectively (see Table 3.3). All the required inputs can be easily provided by the VTOL-AD tool.

Table 3.3: XLSX Input File Template to the ConOBS Tool

power	duration	aircraftWeight	missionSegment
4.362	0.0166	1958.317	taxi_power
320.157	0.0166	1958.317	vertical_climb_power
320.157	0.0134	1958.317	transition_power
108.448	0.3685	1958.317	cruise_climb_power
43.617	0.4128	1958.317	cruise_power
19.417	0.3333	1958.317	loiter_power
166.62	0.0134	1958.317	retransition_power
320.157	0.0166	1958.317	vertical_descent_power
4.362	0.0166	1958.317	taxi_power

After running its sizing computations, the ConOBS tool provides a large XSLX output file that contains the sizing results for different powertrain architectures as presented in Section 3.2.8. The VTOL-AD tool is extended accordingly, to read these outputs and update the variables of the `Vehicle` class. An excerpt of the output file template from the ConOBS tool is shown in Table 3.4. It should also be noted that the presented values of Tables 3.4 and 3.4 do neither correspond to each other nor represent meaningful results, but are rather meant for demonstration and explanation purposes. Accordingly, a concept for the connection can be found by adopting the input and output formats of the ConOBS tool, whereby the requirement SA.4 can be fulfilled.

Table 3.4: XLSX Output File Template from the ConOBS Tool (Excerpt Only)

	Study 0	Study 1	Study 2	Study 3
Powertrain Characteristics	—	—	—	—
Architecture Type	Serial	Parallel	FullElectric1	FullElectric2
Efficiency	0.533	0.575	0.912	0.931
Reliability	0.943	0.944	0.857	0.902
Shaft Power Ratio (phi)	1	0	0	1
Supplied Power Ratio (PHI)	0.2	0.2	1	1
Battery Specific Energy [Wh/kg]	250	250	250	250
Fuel Cell Specific Power [kW/kg]	1.6	1.6	1.6	1.6
Weights	—	—	—	—
Onboard Systems Weight [kg]	652.19	510.21	849.81	784.32
Other Systems Weight [kg]	128.65	128.65	128.65	128.65
Powertrain Weight [kg]	523.54	381.56	721.16	655.67
Gasturbine [kg]	49.96	46.34	0	0
Gearbox [kg]	41.06	55.82	55.82	0
Rotor 1 [kg]	0	91.18	91.18	0
Rotor 2 [kg]	91.18	0	0	91.18
Power Mgmt [kg]	58.76	19.05	59.96	58.76
Eletr. Mach. 1 [kg]	50.30	23.33	73.45	0
Eletr. Mach. 2 [kg]	71.98	0	0	71.98
Fuel Cell [kg]	0	0	0	0
Reformer [kg]	0	0	0	0
Battery [kg]	153.91	139.92	440.75	433.75
Kerosene [kg]	6.38	5.92	0	0
Hydrogen [kg]	0	0	0	0

However, the integration and technical implementation of the collaborative sizing loop must still be realized as an RCE workflow. Consequently, an illustrated guide for the RCE integration of the VTOL-AD tool as well as the set up of the workflow will be presented in order to fulfill requirement SA.5.

Firstly, both tools do not follow the DLR's common language or data definition and exchange format for aircraft design, named Common Parametric Aircraft Configuration Schema (CPACS) [112], but rather implement ad-hoc data structures as explained before
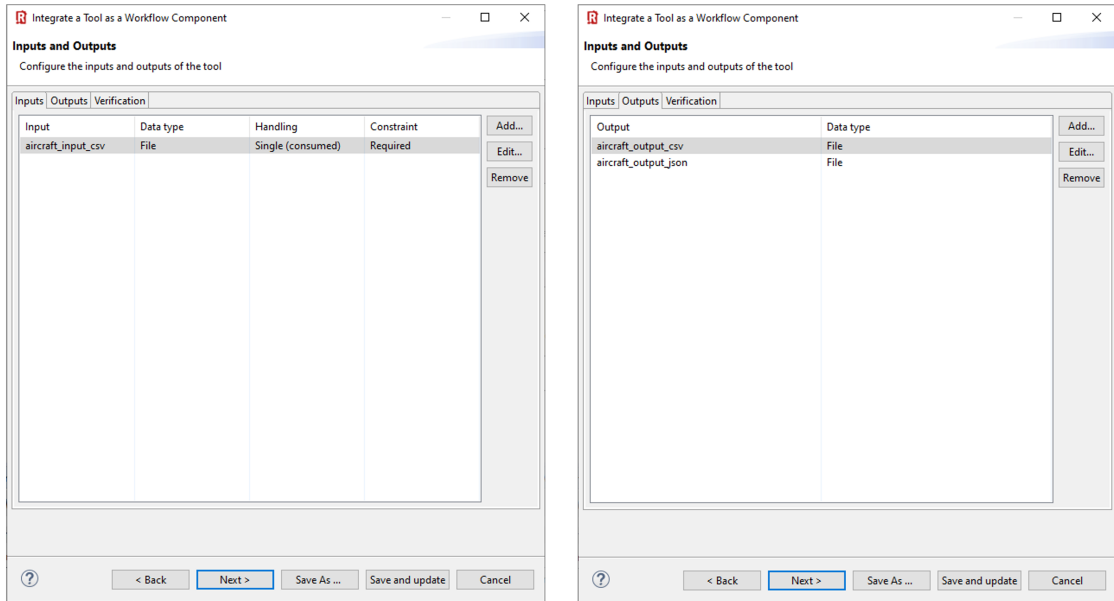
Figure 3.5: RCE Tool Integration Input and Output Settings

in order to reach swift development and implementation of the connection. Therefore, the VTOL-AD must be integrated as a new tool that does not follow the CPACS configuration. Next, the tool description is defined by adding the tool name, and further tool characteristics such as description and contact information. The configuration of inputs and outputs is shown in Figure 3.5. Those have to be set up accordingly to open up the tool interfaces. It should be noted that the input file is a required input, of course. It is important to keep the associated input and output files within the directory `VTOL-AD/data/RCE` so that the VTOL-AD tool can find them.

Figure 3.6 shows the launch settings configuration of the VTOL-AD tool. First, the tool has to be added by the definition of its directory where the `main.py` module must be located. The tool copying behavior is set so that the runtime is reduced, thus copying is disabled. Moreover, it is important to keep the tool in its original directory to maintain the intended input and output file handling. The remaining launch settings depend on the user's own preferences.

Finally, to run VTOL-AD within RCE, the execution configuration must be defined. Here, the command to execute the tool is shown in the left window in Figure 3.7. The `main.py` module must be called together with the additional bool `True` which tells the VTOL-AD tool that it is executed via RCE. This clear distinction of runtime environments is possible through the implementation of the `main.py` module. Also, a pre execution script is defined which is mainly meant to copy the input CSV file to the tool directory `VTOL-AD/data/RCE` where the VTOL-AD expects and reads it.

After the integration, the workflow has to be setup. Therefore, the VTOL-AD tool can be directly added from the available tools in the sidebar. Access to the ConOBS tool
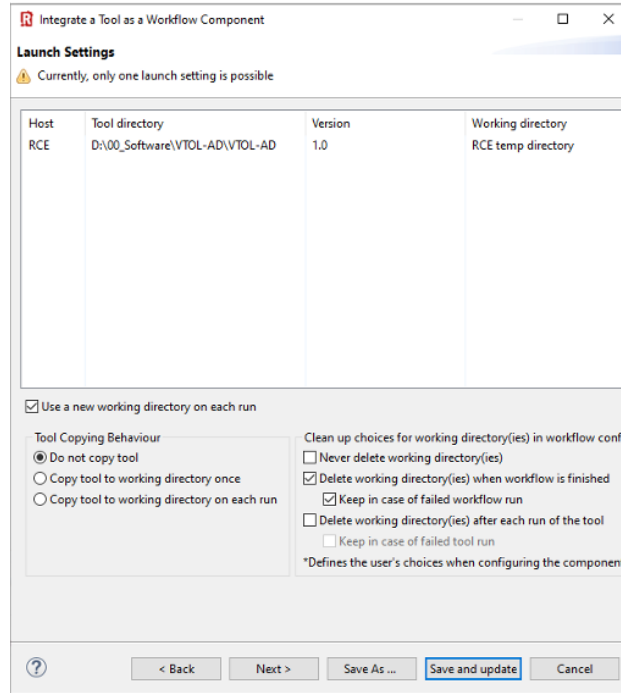
Figure 3.6: RCE Tool Integration Launch Settings
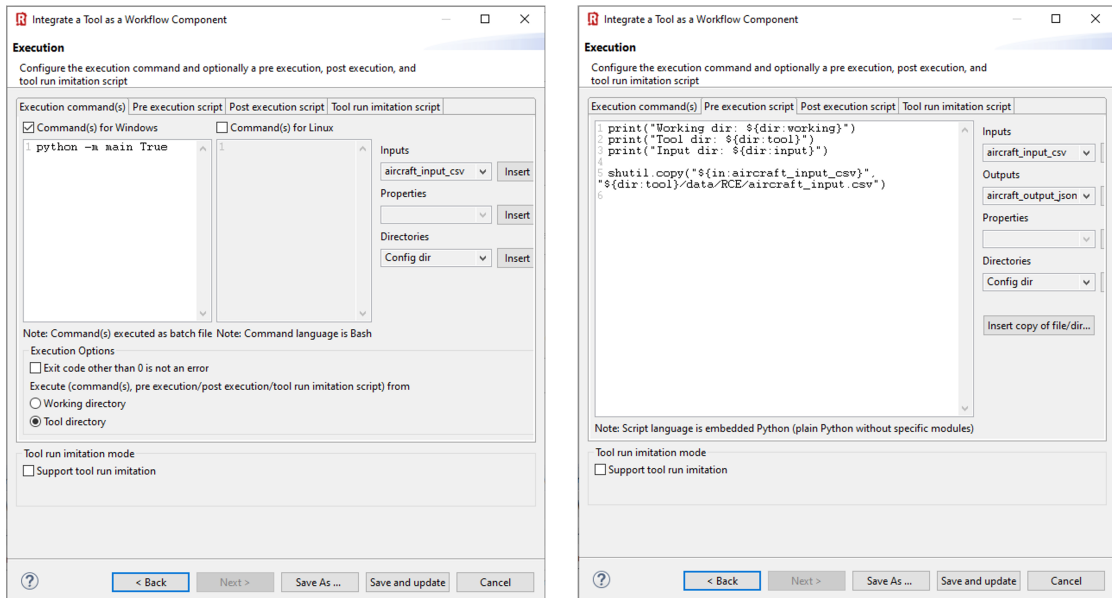
Figure 3.7: RCE Tool Integration Execution Settings
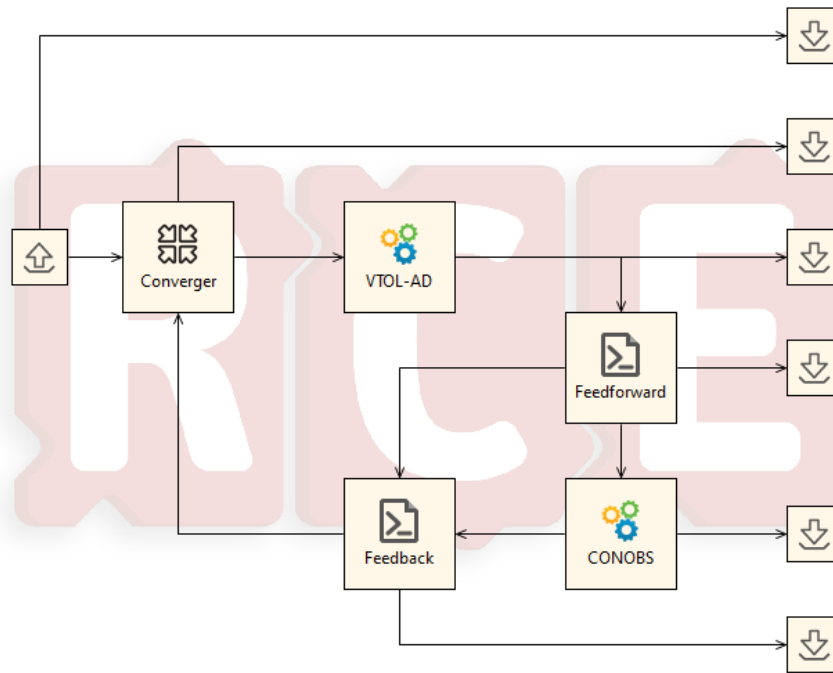
Figure 3.8: Collaborative RCE Workflow Involving VTOL-AD and ConOBS

is obtained through a network connection with the partner institute's RCE server. The workflow is depicted in Figure 3.8 and consists of the mentioned tools, a converger, two additional scripts, and a single input and several output writers (eventually, only one output writer would be required, but additional ones are used for full data tracking). To establish the workflow, the additional scripts are required to handle the communication between the two tools, as both tools do not follow the CPACS format. The two required scripts for data handling between VTOL-AD and ConOBS, named `feedforward.py` and `feedback.py`, are part of the developed code and can be found in the digital appendix (see Appendix C). In order to open the interfaces, the following inputs and outputs have to be defined in the `feedforward.py` script as shown in Figure 3.9. The script reads the *aircraft_ output_ csv* file and prepares the ConOBS input format which is fed forward to the ConOBS tool in the *conobs_ input_ xlsx* file (see Table 3.3). Also, the *aircraft_ output_ csv* file is part of the outputs which is forwarded to the `feedback.py` script for further update of the aircraft data in the next step.

Consequently, the ConOBS tool is executed and provides the expected *conobs_ output_ xlsx* file as shown in Table 3.4. Thus, the `feedback.py` script has to be configured for the inputs and outputs depicted in Figure 3.10. As explained and expected, this script needs to read the *aircraft_ output_ csv* and the *conobs_ output_ xlsx* files in order to prepare the updated aircraft data which will be used for the next iteration. Subsequently, the updated aircraft as part of the new *aircraft_ input_ csv* file and the extracted *mtom* variable is provided to the converger so that the sizing loop can be run automatically until convergence

Figure 3.9: RCE Workflow Feedforward Script Settings

Figure 3.10: RCE Workflow Feedback Script Settings

of MTOM is achieved and the final converged aircraft data is saved as one of the output files.

Regarding the setup of the converger, the settings as depicted in Figure 3.11 have to be made. Also, the convergence criteria should be set based on absolute convergence only in order to minimize the convergence difference with respect to MTOM.

3.4 Limitations

Despite fulfilling the stated requirements in Section 3.1, few limitations with regard to the methods as well as the software architecture exist and will be explained in the following.

Since the VTOL-AD tool has been developed specifically for the conceptual design mostly with regard to initial sizing and performance computations, the design approach is limited

Figure 3.11: RCE Workflow Converger Settings

by its nature within this early design phase. Generally, the tool is currently restricted to the design of eVTOL aircraft configurations with open rotors may cover most of the relevant design features, however limits the analysis of other configuration. An implementation of further design features for eVTOL aircraft or even conventional VTOL aircraft such as helicopters would be feasible within the tool. Some more specific points regarding the methodology are mentioned subsequently. Firstly, considering the use of empirical or semi-empirical equations should also be done with care due to the limited precision and applicability for the design of novel air vehicle architectures which generates a need for higher fidelity tools on the specific domains. Secondly, a more sophisticated aerodynamic parasite drag estimation is derived through a separate tool only which leads to manual iterations in the preparations of 3D models. Also, since geometric properties of onboard system components or cabin are not directly modeled within the VTOL-AD tool, the 3D model must be set up with some buffer. Thirdly, other domains of the conceptual design processes such as high-lift systems design, weight and balance analysis, and stability, control and handling qualities are not a part of the developed tool, yet. Also, cost analysis of the aircraft design concept is not a direct part of the methodology, but will be another building block coming through the entire SoS framework.

Considering the software architecture, the `Vehicle` data class does not hold any mission parameters which are only part of the `Mission` class itself. Thus, the mission parameters are currently missing in the CSV output file and must be traced manually to the aircraft input and output files. Some other limitations arise from the input and output approach using CSV files. Typically, the state-of-the-art approach on aircraft parameter schemes within and often even beyond the DLR is CPACS which provides a common parameter scheme not only for the aircraft design process but also the overall air transport system. Following this data scheme would allow easier RCE integration and also automatable 3D visualization of the designed air vehicle directly after the (initial) design and sizing process. Furthermore, optimization workflows could be carried out directly within RCE. Also, the tool itself is currently missing an optimization process for the overall aircraft design and is mostly focused on generating design sensitivities. Finally, the results plots are currently not directly generated through the tool itself which causes additional effort in post-processing.

As stated at the beginning of this section, none of the present limitations lead to failed requirements, but rather represent potentials for future work and continued development of the VTOL-AD tool. Specific ideas on future work will be provided in the concluding chapter of this thesis.

4 Design Studies

4.1 Validation Study

After the implementation of the VTOL-AD tool, a validation study is required to determine the tool's plausibility before further design studies can be carried out. Since the published specifications of existing industry concepts and prototypes are often incomplete and difficult to assess in terms of their feasibility as found in Section 2.2.3, conceptual eVTOL aircraft designs from other research publications shall be taken as a reference. Generally, the validation of novel aircraft configuration designs important even for higher-fidelity tools as shown in [66], where SUAVE and NDARC have been compared in the field of eVTOL aircraft design. Accordingly, NDARC is also chosen as a reference for design point comparison of two disparate fully battery-powered eVTOL aircraft configurations, namely multirotor and lift + cruise. Thus, the published NASA's concepts developed and well documented by Silva et al. [65] are taken as a reference. In the following validation study, this reference is referred to by the tool name and label NDARC, only.

In their work, Silva et al. [65] consider NASA's AAM mission that is essentially a longer range mission of 140 km in total which is divided over two legs. Furthermore, air vehicles for up to six passengers equal to a payload of 540 kg are designed, which makes the mission very challenging. Therefore, the authors consider advanced battery technology scenarios only and assume a battery cell specific energy of 650 W h/kg that is equal to 500 W h/kg at the pack level as modeled in the VTOL-AD tool. Furthermore, a maximum battery charge/discharge at 4C is allowed. Since the VTOL-AD mission definitions also considered NASA's mission profile in the setup, NASA's AAM mission requirements and profile can be directly input in VTOL-AD, for the most part.

As mentioned, both eVTOL aircraft concepts are very different from each other. On the one side, the multirotor configuration has four rotors, essentially a quadcopter, with large-diameter pitch-controlled rotors. On the other side, the lift + cruise configuration has eight pair- and spanwise-distributed, speed-controlled rotors, which are mounted on four booms connected to a high-wing. Propulsion is achieved by a tail-mounted pusher propeller. Eventually, to recreate the eVTOL aircraft, their geometry is determined from three view drawings together with published data. Here, also the geometry sizing methods presented in Section 3.2.2 helped to determine parameters of wing, empennage, and fuselage

geometry. In order to determine the equivalent flat-plate area for the performance computation, the provided drag area D/q can be directly taken for the multirotor configuration. Concerning the lift + cruise configuration, the equivalent flat-plate area is determined by matching the published performance specifications with regard to V_{br} and V_{be}. To model the powertrain in accordance with NDARC or both NASA concepts, the full electric variant 1, which includes a gearbox, is considered. Consequently, Table 4.1 provides a summary of the determined input parameters which are relevant for the validation study.

Table 4.1: Input Parameters for the Tool Validation Study

Parameter	Multirotor	Lift + cruise
Wing area, m^2	—	18
Wing span, m	—	14
Wing chord, m	—	1.28
Wing aspect ratio	—	10.9
Equivalent flat-plate area, m^2	1.2	0.9
Fuselage length, m	6	9
Fuselage wetted area, m^2	36	40
Horizontal tail area, m^2	—	2.25
Horizontal tail aspect ratio	—	4
Vertical tail area, m^2	—	1.6
Vertical tail aspect ratio	—	1.3
Number of rotors	4	8
Number of rotor blades	3	2
Rotor disk loading (max), N/m^2	250	750
Rotor solidity	0.09	0.075
Rotor lift coefficient (max)	0.35	1.6
Rotor diameter (max), m	8	3.05
Payload mass, kg	540	540
Battery specific energy, Wh/kg	500	500
Battery specific power, W/kg	2,000	2,000

For this validation study, the VTOL-AD standalone version is run. In the comparison and evaluation it was found that VTOL-AD underestimated the airframe masses compared to NDARC, and eventually the aircraft converged at lower MTOMs compared to NDARC. This is even without applying the proposed technology factors for composite masses of 0.8 as utilized by Kadhiresan & Duffy [60]. Eventually, since NDARC models the component masses by more refined semi-empirical methods, where also technology factors are used to account for crashworthiness, advanced materials, and further design considerations, it is taken as a reference. Thus, the VTOL-AD tool is extended by airframe component technology or adjustment factors, which are calibrated to NDARC. Consequently, all airframe component of the lift + cruise configuration, namely wing, empennage, fuselage, and landing gear, are assigned a factor of 1.4. In case of the multirotor, where only fuselage and landing gear are modeled, the fuselage factor is adjusted and set to 2.95. This large factor is expected to account for the structural integration of the rotor struts. The landing gear

factor of the multirotor is kept at 1.4 in order to maintain a similar mass fraction as for the lift + cruise configuration. The derived factors are implemented in the VTOL-AD tool and used throughout this work.

Finally, by the use of the aforementioned technology factors, the subsequently presented outputs are computed. Tables 4.2 and 4.3 provide a summary of the relevant output parameters as well as a direct comparison with NDARC. It should be noted that the percentage difference is calculated with respect to VTOL-AD.

Table 4.2: Multirotor Output Parameters for the Tool Validation Study

Parameter	VTOL-AD	NDARC	% difference
MTOM, kg	2,874	2,939	−2.3
Airframe mass, kg	751	744	0.8
Powertrain mass, kg	1,365	1,211	11.3
Battery mass, kg	979	924	5.6
Other systems mass, kg	217	243	−11.8
Disk loading, N/m^2	140	144	−2.5
Rotor diameter, m	8	8	0
Rotor tip speed, m/s	162	168	−3.8
Hover power, kW	366	345	5.8
Cruise power, kW	269	262	2.6

Table 4.3: Lift + Cruise Output Parameters for the Tool Validation Study

Parameter	VTOL-AD	NDARC	% difference
MTOM, kg	3,676	3,723	−1.3
Airframe mass, kg	1,168	1,168	0
Powertrain mass, kg	1,732	1,445	16.6
Battery mass, kg	953	998	−4.8
Other systems mass, kg	237	245	−3.5
Disk loading, N/m^2	617	627	−1.7
Rotor diameter, m	3.05	3.05	0
Rotor tip speed, m/s	173	178	−2.7
Hover power, kW	749	828	−10.5
Cruise power, kW	247	245	0.6

Regarding both aircraft, it can be seen that the airframe masses match each other after the introduction of the aforementioned technology factors. By this adjustment, the MTOMs converge at a very reasonable difference of less than 2.5%, both aircraft considered. The powertrain mass groups show a comparably larger difference of 11.3% and 16.6% for the multirotor and lift + cruise, respectively. This is despite the close match of battery mass, which is found to be around a reasonable 5% mark. Therefore, the modeling of all remaining powertrain components might be somewhat too rough in the VTOL-AD (and ConOBS) tool. Similar deviation applies to the other systems mass, yet, mostly in case of

the multirotor, where a fairly large difference of –11.8% is observed. However, due to the low mass fraction of these systems, the absolute difference of 23 kg in case of the multirotor is likely to be negligible. With regard to the rotor sizing, the disk loadings, rotor diameters, and rotor tip speeds match very well. Here, the rotor aerodynamics model typically converges at the maximum specific rotor diameter, thus no difference in terms of rotor diameter is found at all. Eventually, the flight performance is compared for both, hover and cruise. Despite the simple model used in the VTOL-AD tool that uses momentum theory and does not model each rotor separately as in NDARC, both, the multirotor's hover and cruise power match reasonably well with NDARC. A slightly higher difference of 5.8% is observed for the hover power compared to the difference of 2.6% for the cruise power. Regarding the lift + cruise aircraft, a difference of –10.5% is found for the hover flight, thus the VTOL-AD tool overestimates its vertical lift efficiency, but is still deemed to be sufficiently close considering the conceptual design stage. Since the cruise power matches very well at 0.6%, the earlier discussed difference in respect of battery mass might also be influenced by the hover power deviation.

It should be noted that the wing sizing was not run in this validation study in order to recompute the NASA concept aircraft regarding their aerodynamic and geometric properties. However, using the methods for the estimation of the equivalent flat-plate area proposed by Kadhiresan & Duffy [60], which are useful if very little information is available at the start of the design process, shows the potential inaccuracies. Accordingly, using the MTOMs of the NASA aircraft, the equivalent flat-plate drag area of the multirotor would be overestimated by a factor of approximately 6.3 and the lift + cruise underestimated by 25%. The multirotor configuration shows a substantially higher difference due to the comparably small dataset for this particular eVTOL aircraft configuration investigated by Kadhiresan & Duffy [60]. Thus, such empirical methods must always be used with care and higher-fidelity methods or tools are to be preferred for the estimation of the equivalent flat-plate drag area or aerodynamic characteristics, in general.

4.2 Multirotor Study

4.2.1 Urban Use Case Requirements and Assumptions

The first design study considers a typical UAM use case which is set in an urban environment. Correspondingly, the urban use case is a combination of the airport shuttle and intra-city use cases and CONOPS developed from workshop discussion in HorizonUAM and presented by Asmer et al. [41]. A schematic visualization of the use cases was depicted earlier in Figure 2.5.

Both use cases are characterized by relatively short-distance missions below 50 km at comparably low cruise speeds below 150 km/h. The mentioned cruise speed represents the

ground speed, which means that headwinds have to be considered for the sizing mission in addition. In case of high-frequented intra-city operations, the mission is laid out such that intermediate stops must be considered within the mission profile. Therein, stops at vertistops are assumed, which is the type of vertidrome with the least available infrastructure, thus no re-energizing is possible. Therefore, a multirotor configuration is chosen for this mission type due to its reduced complexity, lower number of airframe components, and especially high efficiency in vertical flight, which is more dominant regarding this use case. The seat requirements are specified by the number of Persons on Board (POB), which is, compared to the number of Passengers (PAX), unaffected by the assumption of autonomous or piloted control. In that context, note that autonomous flight is consistently chosen as a distinctive term, even if the highly automated or remote-piloted flight might technically be more applicable. Eventually, two or up to 4 POB are required, for the airport shuttle even together with no only their hand baggage, but also their luggage. Further details on both use cases can be found in the aforementioned publication by Asmer et al. [41].

Consequently, the aircraft requirements are derived from several sources involving the just explained HorizonUAM use cases as well as follow-up aircraft design meeting discussions, NASA's AAM mission requirements [102], and the Uber Elevate air vehicle and mission requirements [103]. Moreover, aviation regulations have to be considered, of course. The aforementioned regulations by EASA [36, 37] consider VTOL aircraft with an MTOM of 3,175 kg and also provide two types of certification categories which are Category Basic and Category Enhanced. The latter category is applicable for operations in urban environment and for commercial passenger air transport (either or both). Accordingly, aircraft certified under Category Enhanced must be able to continue safe flight and landing in all possible failure cases. Accordingly, the following list of TLARs can be derived:

The air vehicle ...

UR.01 must have VTOL capabilities for short hover times $\leq 30\,\text{s}$ per hover segment.

UR.02 must be able to continue safe flight and perform a safe vertical landing in any potential failure case.

UR.03 must not exceed an MTOM of 3,175 kg.

UR.04 must not exceed the dimensions of $15.24\,\text{m} \times 15.24\,\text{m} \times 6.09\,\text{m}$ in total length, width and height, respectively.

UR.05 must carry 4 POB and their hand baggage as well as luggage with a total payload mass of 360 kg to 440 kg.

UR.06 must achieve a total cruise distance of 50 km with two intermediate stops, where no re-energizing infrastructure is available.

UR.07 must achieve a cruise ground speed of 100 km/h to 150 km/h, while directly opposed to a headwind speed of 20 km/h.

UR.08 must be equipped for highly automated or remote-piloted control.

UR.09 shall be able to taxi on ground with the help of external devices.

UR.10 shall have an electric powertrain architecture.

UR.11 shall be compatible with state-of-the-art re-energizing infrastructure.

UR.12 should enable swift battery swapping times ≤ 5 min.

The mission profile definitions are set up with respect to the generic VTOL mission as described in Section 3.2.5. Accordingly, the values as summarized in Table 4.4 are set in the VTOL-AD mission inputs. It should be noted that segments $1-8$ are repeated thrice, so that a total cruise distance of 50 km is covered and the three legs (equal to two stops) are modeled as required. The altitudes as part of the mission profile are referred to Mean Sea Level (MSL) and consider ISA deviations. The deviation has been determined through the computation of density altitudes for a representative number of potential European cities where UAM might be deployable. Hence, the density altitudes have been computed from historic weather datasets similar to [102]. In a brief survey, the city of Madrid was found to be a very challenging location due to its comparably high elevation and atmospheric conditions in hot summers. Eventually, a density altitude of approximately 5,000 ft MSL is found to be sufficient by considering the 95th percentile, approximately. This finding seems to be reasonable as it also matches Uber's mission requirements published in [103]. For the transition segment, a horizontal acceleration needs to be assumed. Moreover, the aircraft has to accelerate to its climb speed V_{be} at $a = 0.2g$ as also used in [113]. The vertical climb speed in cruise climb represents a mean value between Uber's [103] and NASA's [102] mission requirement. The cruise altitude is also assumed by comparison of the two aforementioned references, thus a cruise height of 2,000 ft above ground level is deemed to be sufficient regarding obstacle clearance as well as vertical separation to other traffic and additional margins. Finally, the reserve segment consists of a 20-min loiter according to the regulations applicable to rotorcraft, notwithstanding the reserve speed requirement, which is reduced in comparison. Herein, loiter at V_{be} is assumed since there are no common reserve requirements for eVTOL aircraft and, actually, there are efforts within the domain to reduce the reserves for such short-distance missions even further. Therefore, 20-min loiter at V_{be} is set as a reasonable compromise.

Table 4.4: Urban Mission Profile Segment Definitions

No	Name	Horizontal speed, km/h	Vertical speed, ft/min	Altitude MSL, ft	Distance, km	Time, min	Power, kW
1	Taxi	—	—	5,000	—	0.5	P_{tx}
2	Vertical climb	—	100	5,000 to 5,050	—	t_{vd}	P_{vc}
3	Transition	0 to V_{be}	0	5,050	—	t_{tr}	P_{tr}
4	Cruise climb	V_{be}	700	5,050 to 7000	D_{cc}	t_{cc}	P_{cc}
5	Cruise	$V_{br} \geq 120$	0	7,000	$17 - D_{cc}$	t_{cr}	P_{cr}
6	Re-transition	V_{be} to 0	0	5,050	—	t_{tr}	P_{tr}
7	Vertical descent	—	−100	5,050 to 5,000	—	t_{vd}	P_{vd}
8	Taxi	—	—	5,000	—	0.5	P_{tx}
9	Loiter	V_{be}	0	7,000	—	20	P_{lo}

For the design, all available electric powertrain architectures, namely battery-electric, hydrogen fuel cell, and hybrid hydrogen fuel cell and battery, are considered, because it is expected that public acceptance of UAM with regard to emissions, i.e. greenhouse gases, pollutants, and noise, may only be achievable in this way. In this context, the standalone VTOL-AD tool is used for the sizing of battery-electric powertrains and the collaborative RCE workflow involving the ConOBS tool is utilized for the hydrogen-powered architectures. Moreover, two different technology scenarios, namely near-term and far-term time frame, will be addressed in the following design point analyses, where the state-of-the-art values derived by Bertram et al. [106, 107] and presented in Table 3.1 are doubled to account for a potential future scenario. Additionally, the cabin concepts developed in HorizonUAM are taken as inputs for the fuselage design. Herein, the cabin design approach focuses especially on the passenger perspective and experience involving surveys and workshops, whereon further information by Moerland-Masic et al. can be found in [114].

4.2.2 Multirotor Design

The conceptual design of the multirotor configuration has been discussed and streamlined within the regular HorizonUAM aircraft design meetings. Accordingly, this initial conceptual design considers a quadcopter configuration, where the rotors are mounted on four separate struts. Due to the desirable low disk loadings of this configuration, the rotor diameters are expected to be beyond a feasible size for the use of speed controlled rotors. Hence, three-bladed collective pitch-controlled rotors are assumed, also causing the need for a reduction ratio gearbox. The rotor disks are slightly tilted into the oncoming air stream so that high rotor angles of attack are avoided. Additionally, the rotors are displaced in the vertical direction in order to reduce blade-vortex interaction. In order to keep clearance between boarding or deboarding passengers as well as ground personnel, the rotor struts

are mounted in a high position of the fuselage. In the HorizonUAM project discussions, additional pusher propellers are deemed to be needed in order to achieve comparably high cruise speeds, where the pusher propellers could alleviate the rising parasite drag. However, this design decision is mostly be driven by the deployment for other use cases such as urban rescue, which has stricter cruise speed requirements. Therefore, the pusher propellers are omitted in this work, thus the required cruise speeds are tried to be reached without the propellers to reduce the complexity and mass caused by additional components. Aerodynamically faired skids are chosen as landing gear since no self-dependent taxi is required.

The fuselage is modeled based on the HorizonUAM cabin design inputs, where different layout variants are available. For this multirotor concept, the four-seater variant is of interest in order to comply with the use case requirements. Accordingly, two layouts options are available, where the one with a smaller frontal area and greater length is chosen in order to derive a streamlined teardrop shaped fuselage. The outer dimensions of this cabin option are 3,852 mm × 1,530 mm × 1,700 mm in length, width, and height, respectively. However, compared with existing eVTOL aircraft concepts, the cabin may be oversized, which is expected and somewhat intended by the chosen cabin design approach to develop a passenger-oriented cabin concept. Therefore, the collaborative aircraft design process foresees joint development of a feasible cabin size. Correspondingly, also a by 15% shrunk fuselage and cabin version is designed, which basically appears to be more in the range of other eVTOL aircraft and general aviation aircraft. The resulting outer dimensions of the proposed shrunk version are 3,274 mm × 1,300 mm × 1,445 mm in length, width, and height, respectively. It should be mentioned that in first approximation an estimate of the crashworthy fuselage structure was modeled by additional margins.

Next, the aircraft sizing process is described. For the rotor sizing, three-bladed rotors with comparably low solidity of $\sigma = 0.08$ are modeled. The rotor maximum mean lift coefficient is adjusted accordingly an set to $\overline{C_{lmean,max}} = 0.475$, which represents an intermediate value between the value derived during the validation from Silva et al. [65] and Brown & Harris [62]. Hence, the goal is to reach a fairly low disk loading at around $150 \, \text{N/m}^2$ with reasonably low rotor tip speeds in the range of 140 m/s to 150 m/s to design for reduced noise. The rotor sizing also has to comply with the required geometric design space constraints. From geometric analyses, a maximum rotor diameter of 7.3 m is found to be feasible. In the subsequent sizing process, the rotor diameter is varied in order to arrive at the desired disk loading and tip speed.

Due to the large uncertainties when using empirical methods for equivalent flat-plate drag estimation of the multirotor configuration, as shown in Section 4.1, the drag is estimated by a component drag build-up, which was explained in the design tool methodology (see Section 3.2.3). Therefore, the multirotor is preliminarily modeled in 3D using the software Open Vehicle Sketch Pad (OpenVSP), an open geometry modeling tool for conceptual aircraft design [115]. The developed 3D model can be found in Figure 4.1. Accordingly, the

equivalent flat-plate areas are estimated in OpenVSP by using the implemented methods from Torenbeek [116], where an interference factor $Q = 1.3$ is applied for the structural attachments such as rotor struts, motor nacelles, and skids. In addition, a 10% margin is added on the geometric drag in order to account for non-modeled parts as well as uncertainties. Eventually, the equivalent flat-plate drag area is determined in flow conditions comprising an air speed of 37.5 m/s and an altitude of 7,000 ft, which is supposed to represent the cruise flight accordingly.

Before providing the full dataset and performance specifications or MoP of the resulting multirotor concepts, a direct comparison of the nominal (large) and shrunk fuselage version is presented in Table 4.5. Here, both variants are sized for the urban use case, also regarding the required list of payload masses of 360 kg and 440 kg. Firstly, regarding the aerodynamic differences, the equivalent flat-plate area is found to be hardly affected by the change in fuselage size. This is due to the high percentage of parasite drag caused by the rotor struts and the adjacent motor nacelles. However, the impact of the larger fuselage is definitely traceable by regarding the converged MTOMs. This is due to the fuselage mass growth visible by comparing nominal (large) and shrunk fuselage variants. Eventually, this mass growth increases the power requirements, thus the battery mass and further component masses grow as per the aircraft design typical snowball effect, which is even more critical for VTOL and eVTOL aircraft, in particular. Regarding efficiency parameters such as lift-to-drag ratio and energy consumption per km, it can be seen that the heavier aircraft may have a slightly higher lift-to-drag ratio determined by WV/P, however, the energy consumption shows the bottom line results. Accordingly, the multirotor sized for the payload mass of 360 kg, the impact of the nominal (large) fuselage causes a fuselage mass growth of 27%, a battery mass growth of 11% an MTOM mass growth of 12%, which eventually results in an energy consumption increase of 11%. Even higher growth percentages can be found for the multirotor sized for the payload mass of 440 kg.

Table 4.5: Multirotor Comparison of Both Cabin or Fuselage Variants

Parameter	Nominal	Shrunk	Nominal	Shrunk
MTOM, kg	2,331	2,078	2,576	2,257
Payload mass, kg	360	360	440	440
Fuselage mass, kg	558	438	586	456
Battery mass, kg	843	757	929	808
Equivalent flat-plate area, m^2	1.82	1.79	1.82	1.79
Equivalent lift-to-drag ratio	5.3	5.2	5.4	5.3
Energy consumption, kWh/km	2.32	2.09	2.53	2.23

Comparing both shrunk versions with the two different payload masses shows slightly smaller increases concerning mass and energy consumption. However, the TLARs derived from the intra-city use case with the transport distance of 50 km and two intermediate stops do only specify a payload mass of 360 kg. Therefore, the airport shuttle use case

must be re-evaluated to see if sizing for the urban mission at a payload mass of 360 kg is sufficient to fulfill the combined set of TLARs. Following this approach, it is found that the multirotor sized for the urban mission at a payload mass of 360 kg is also capable of performing the airport shuttle mission, which has a shorter cruise range of 30 km without intermediate stops, but the higher payload mass of 440 kg.

Therefore, the fuselage sized by the nominal (large) cabin layout is only considered for comparison in the near-term time frame. Also, only the payload mass of 360 kg is considered in the near-term. This is justified by the weight sensitivity of VTOL aircraft, which must be handled carefully even in advanced technology scenarios in order to derive somewhat energy-efficient concepts (when compared within the domain of VTOL aircraft, of course). Also, the shrunk version should, according to this first assessment, provide plenty of cabin space for the underlying short-distance UAM missions. These design considerations are to be iterated together with the cabin design experts to trade-off aircraft weight and performance vs. passenger comfort and luggage stowage.

Eventually, Table 4.6 presents an excerpt of the most relevant sizing outputs, whereas the reader is directed to the supplementary information and comprehensive result datasets in Appendix C. Note that the results are presented per powertrain architecture, where the abbreviation FE 1 represents the battery-electric, FC the hydrogen fuel cell, and FC BAT the hybrid hydrogen fuel cell and battery powertrain architectures. Here, the sensitivities of the powertrain technology advancements are obvious and show similar trends, which are discussed with further details in the large sensitivity study by Bertram et al. [107].

Finally, the developed battery-electric multirotor concept for the far-term time frame is presented in Figure 4.1. Herein, the aforementioned aircraft design considerations and sizing computations can be found and represented by the three-view drawing of the configuration, which is representative for hover and cruise flight mode. It should be generally noted that this concept is still subject to further iterations within the HorizonUAM project together with the involved expert domains, thus it only represents a preliminary result as part of the project.

4.2.3 Urban Air Transport Fleet Assessment

This UAM transport case study considers a common UAM use case. In this case study, an urban air transport scenario is considered and set-up by a mostly point-to-point transport network as shown in Figure 4.2. This setup is taken from Shiva Prakasha et al. [40]. Accordingly, the urban air transport network is located in the city of Hamburg, which is also the reference city as part of the HorizonUAM project explained earlier (see Section 2.2.2). Here, the demands across the vertiport network are assumed from publicly available data on visitor and demand statistics of points of interest in the vicinity of the respective vertiports. A total demand of approximately 2,000 passengers has been assumed for 24-hr

Table 4.6: Multirotor Sizing Outputs and Performance Specifications

Parameter	FE 1	FC BAT	FE 1	FC	FC BAT
Time frame	Near	Near	Far	Far	Far
Battery specific energy, Wh/kg	250	250	500	500	500
Battery specific power, W/kg	625	625	2,000	2,000	2,000
Fuel cell specific power, W/kg	600	600	1,200	1,200	1,200
Disk loading, N/m^2	140	144	138	144	141
Number of rotors	4	4	4	4	4
Rotor diameter, m	6.8	6.4	5.9	6	5.7
Thrust weighted solidity	0.079	0.079	0.079	0.079	0.079
Hover tip speed, m/s	145	147	144	147	145
MTOM, kg	2,078	1,887	1,543	1,660	1,468
Payload, kg	360	360	440	440	440
Airframe, kg	540	514	462	480	450
Powertrain, kg	1,009	849	484	581	424
Battery, kg	758	175	299	—	66
Fuel cell, kg	—	434	—	362	172
Hydrogen, kg	—	8.5	—	15.5	7
Other systems, kg	169	164	157	159	154
Hover power, kW	238	219	175	192	168
Cruise power, kW	146	136	111	121	107
Best range speed at H_{cr}, m/s	37	36	34	35	34
Best endurance speed at H_{cr}, m/s	28	28	26	27	26
Usable mission energy, kWh	105	253	84	437	206
Figure of merit	0.7	0.7	0.7	0.7	0.7
Equivalent lift-to-drag ratio	5.2	4.9	4.7	4.7	4.5
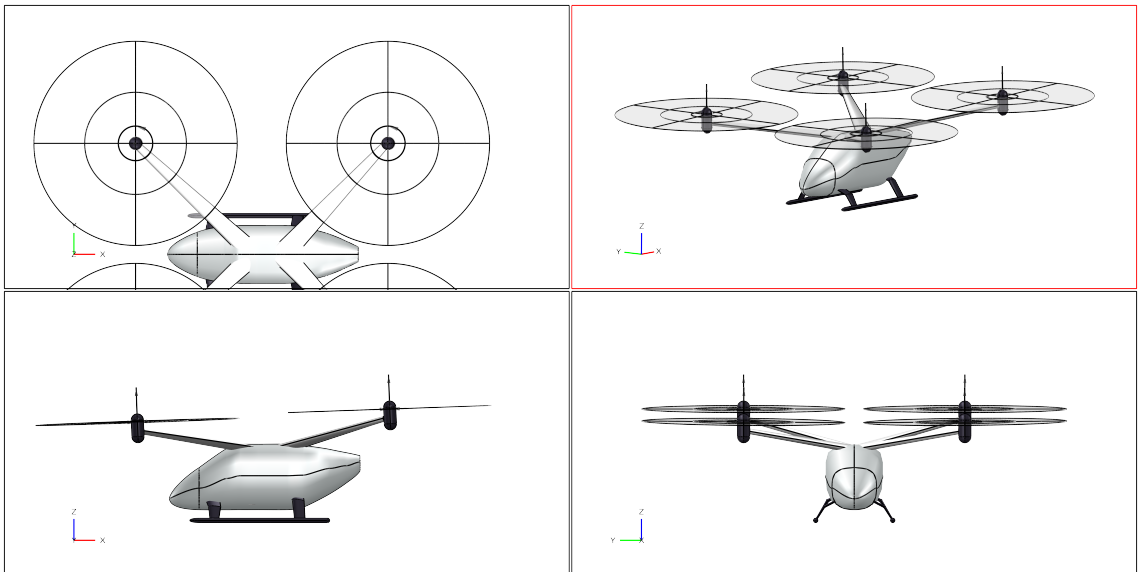
Figure 4.1: Three View Drawing of the Preliminary Battery-electric Multirotor Concept
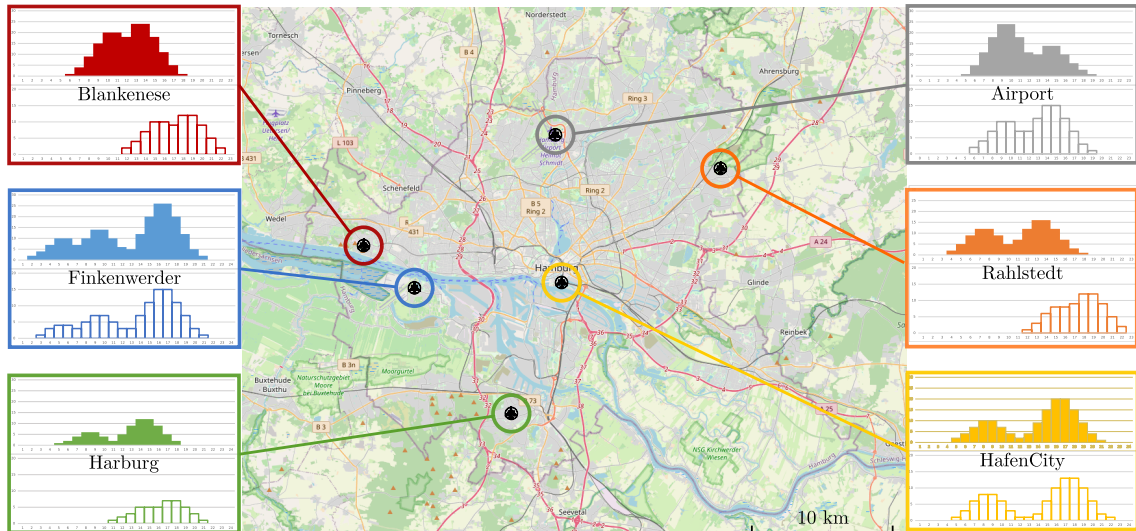
Figure 4.2: Case Study for the Urban Air Transport Fleet Assessment in the City of Hamburg (Outflow Demand in Solid Color and Inflow Demand With No Fill). Adapted from [40].

operations. As can be seen, the airport is also considered in the vertiport network which makes the case study relevant for both, airport shuttle and intra-city, UAM operations. The operations are still modeled by the same on-demand dispatching, where revenue and deadhead flights are modeled. Further information on the ABS and the involved algorithms regarding the UAM fleet dispatch and operations modeling can be found in [40]. The aircraft are dispatched considering a maximum passenger wait time of 15 min. Finally, it should be noted that this case study is purely academic and should only represent the notion of an urban UAM use case.

As already for the aircraft design, the simulation case study also considers two different time frames where technology improvements are assumed on subsystem and SoS aspects in addition. A summary of the case study parameters involved in the different time frames is provided in Table 4.7. Therein, different parameters are modeled for the fleet operations in many aspects. Regarding the piloting, all revenue flights are piloted flights, whereas remote-piloted deadhead flights are assumed for the near-term time frame. Eventually, fully autonomy or automation is assumed for the modeling of the far-term time frame. This has a direct impact on the aircraft's passenger capacity, of course. The cruise speed and passenger wait time are set with regard to previous explanations and match each other for the considered use case. In order to derive sensitivities with regard to required fleets, the fleet size is varied by increments of one additional aircraft per vertiport. Considering the re-energizing of the aircraft, which has a major impact on the turnaround time and thus also the dispatching, different options are available depending on the powertrain architecture and will be investigated in this case study.

The re-energizing is an important parameter of the UAM operations, thus further explanations are given in the following. Regarding the battery, either battery swapping, which is

Table 4.7: Urban Air Transport Case Study Parameters for Different Time Frames

Parameter	Near-term	Far-term
Autonomy	False, except for deadhead flights	True, for all flights
Cruise speed	120 km/h	
Fleet size	6, 12, 18, 24, 30, 36, 42, 48, 54, 60	
Passenger capacity	3	4
Passenger wait time	max. 15 min	
Re-energizing	Battery swap, 300 kW, 2C, hydrogen refill	Battery swap, 2C, 4C, hydrogen refill
Vertidrome capacity	100 (unlimited)	

the swift replacement of empty battery packs during a fixed 5 min turnaround, or battery charging are modeled. For the battery charging, different recharging options are examined, where either the charging station power or the C-rate of the battery are specified as input parameters. Here, the charging with 2C represents a more advanced technology level compared to the fixed charging station power and would allow for charging an empty battery within 30 min (note that the unit of C-rate is 1/h, thus the reciprocal gives the charging time). Hence, it would require even higher charging station powers regarding the near-term time frame. Such limitations are not expected in the far-term time frame, therefore a trade-off between charging rates of 2C and 4C is investigated. Moreover, for the hydrogen refilling, Datta [19] has provided a fueling rate of 1.67 kg/min, which is basically assumed from present terrestrial vehicle technology levels. This fueling rate is also acceptable for eVTOL aircraft, thus, as for the battery swapping, a fixed turnaround time of 5 min, which is equal to refilling a plenty amount of 8.33 kg hydrogen, is modeled in the ABS. Depending on the involved powertrain architecture, different re-energizing strategies apply, of course. The battery-electric and hydrogen fuel cell architectures are clearly allocated to their respective re-energizing, which are battery swapping or charging and hydrogen refilling, respectively. The turnaround times of the hybrid architecture comprising hydrogen fuel cell and battery is expected to be limited by the battery charging process. Hence, battery charging is applied in the modeling, whereas hydrogen refilling and battery swapping are also considered.

Eventually, the results will be presented and sensitivities regarding the required fleet size will be discussed. Before, the involved MoEs are explained as reproduced from Shiva Prakasha et al. [40], below:

- **Revenue passengers** = Total number of passengers transported

- **Wait time** = Elapsed time from demand creation in the simulation until take-off

- **Average wait time** = Average wait time of all revenue passengers

- **Success percentage** = Percentage of revenue passengers waiting less than the target wait time

- **Deadhead ratio** = Ratio of deadhead flights (non-passenger carrying flights)

- **Load factor** = Average load factor of all revenue and deadhead flights (computed excluding the pilot)

- **Fleet energy** = Total energy used by the UAM network or UAM SoS fleet

- **Energy per km** = Energy used by the network divided by the total distance travelled within the network

- **Energy per PAX-km** = Energy used by the aircraft per kilometer accounting for the load factor

The first SoS assessment considers the near-term time frame, where both multirotor architectures, namely the fuel cell battery and full electric powertrain architectures, are assessed as a homogeneous air taxi fleet for the urban operations scenario. The re-energizing is assumed to be set at hydrogen refilling (if applicable) and battery swapping for both multirotors. Thus, it may represent a technology best-case scenario. Figure 4.3 shows a trade-off study, where autonomy might be already feasible in the near-term time frame. Consequently, the different impacts on the UAM SoS are analyzed. Firstly, regarding the general trends that occur for both, autonomous and piloted operations. With regard to the number of revenue passengers, it can be seen that a certain fleet size is needed in both cases so that all passengers raising transport requests can also be catered. Initially, comparably high deadhead ratios of around 0.35 are found, which gradually decrease with increasing fleet size. Eventually, the deadhead ratio converges at approximately 0.2. At the same time the deadhead ratio converges, the success percentage starts to rise, hence, emergent behavior can be observed. This means that as soon as a certain fleet size is deployed in the urban UAM SoS, positive emergence is found, which is depicted by the fairly strong increase of the success percentage which reaches about 70%. At the same fleet size, the average wait time converges, too, and lies around a reasonable 10 min mark. Thus, from this MoEs it can be determined that a fleet size of around 30 four-seater multirotors is need to cater the assumed demand of 2,000 passengers. Therein, the autonomous aircraft might require a slightly smaller fleet size, which can be seen by the higher success ratio at a fleet size of 30 aircraft. Regarding the load factor, it is clearly visible that four seats solely available for passengers in the scenario where autonomy is enabled decrease the load factor, of course. But still, the energy efficiency is impacted and should be discussed. Initially, when regarding the fleet energy and comparing the fuel cell battery and the full electric powertrain architectures, the clear difference between their powertrain efficiency becomes clear. Despite their similar aerodynamic performance, which is provided in Table 4.6, the fuel cell battery powertrain architecture requires about 40% more energy compared to the more efficient battery-electric multirotor. The reason why the fuel cell battery powertrain
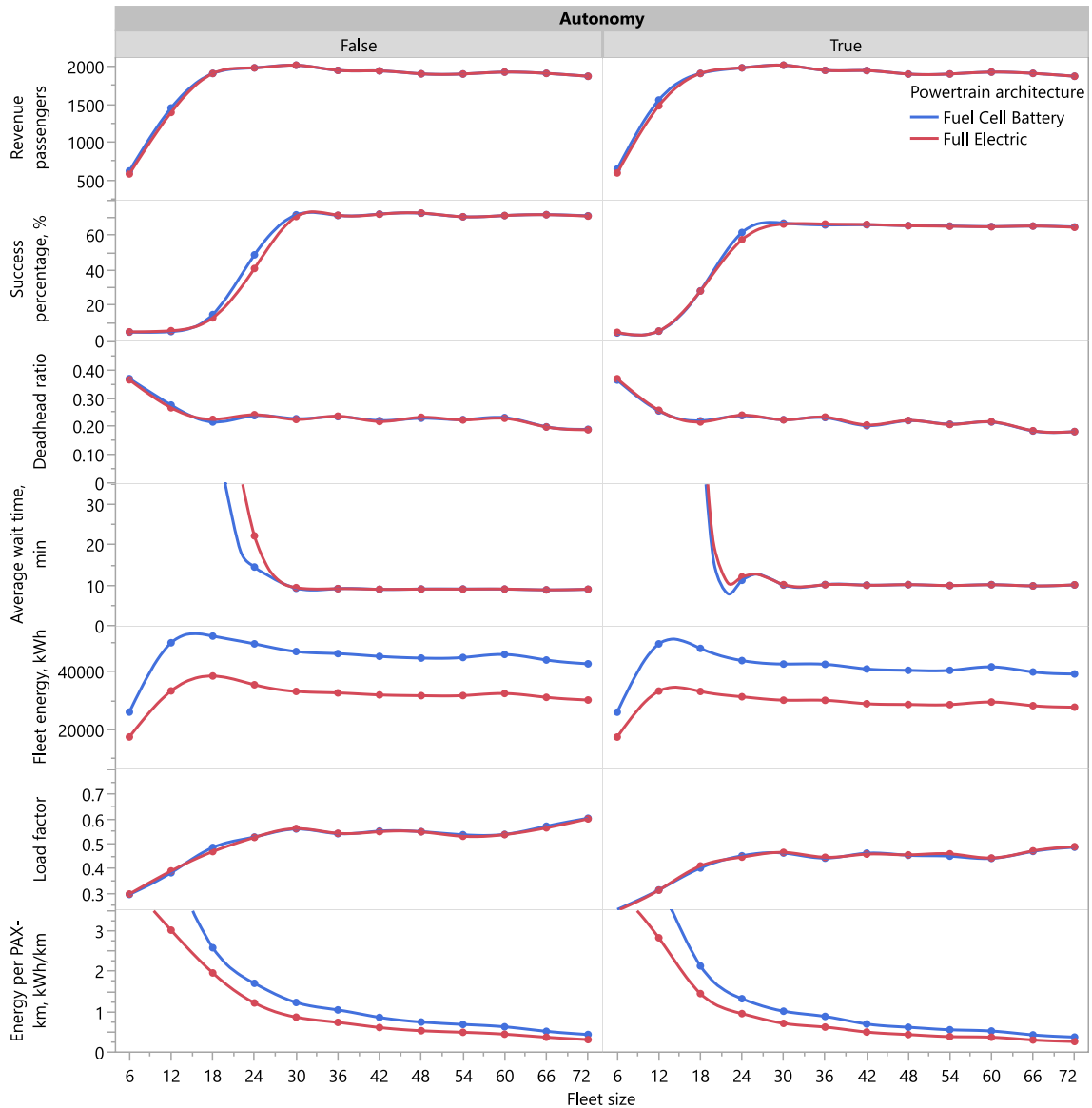
Figure 4.3: Impact of Autonomy on the Urban SoS in the Near-term Time Frame

architecture is still having a similar aerodynamic efficiency is due to the high specific energy of hydrogen, of course. However, thinking of the primary energy use, which also considers the hydrogen production, considerably more energy must be produced for this multirotor architecture and should be considered by holistic SoS approaches. Eventually, the energy per PAX-km is found to be continuously decreasing over the entire fleet size sweep. This is due to the gradually climbing load factor, which keeps on increasing even beyond a fleet size of 60 aircraft. Note that also the deadhead ratio decreases, respectively. However, UAM operators may not be willing to deploy such large fleet sizes, since the success percentage cannot be increased further. Thus, this represents a point of diminishing return, where capital investment and direct operating cost of the fleet might have to be traded against energy efficiency.

Increasing the complexity, Figure 4.4 shows the impact of different re-energizing strategies where the baseline near-term time frame without fully autonomous operations is presented. The results show similar trends as before, yet, this time different re-energizing strategies ranging from available charging station power of 300 kW over charging at 2C to the quickest and probably most complex strategy of hydrogen refilling and battery swapping at maximum 5 min. In these results, it appears that both multirotor architectures perform fairly similar even under the consideration of different re-energizing strategies. Not even the comparably low charging station power of 300 kW seems to affect the battery-electric fleet much compared to charging at higher C-rates or even when battery swapping is enabled. Thus, these efforts do not seem to be necessary for four-seater multirotor fleets, which rises the question if a heterogeneous fleet including two-seater multirotors in addition could provide benefits over the single solution presented in this case study. For smaller capacity air taxis, these re-energizing strategies might be of higher importance. Eventually, a fleet size of around 30 multirotor air vehicles is deemed to be sufficient in order to cater the assumed demand of 2,000 revenue passengers. At this fleet size, the full electric multirotor fleet consumes approximately 0.876 kWh/PAX-km (at a load factor of 0.55).
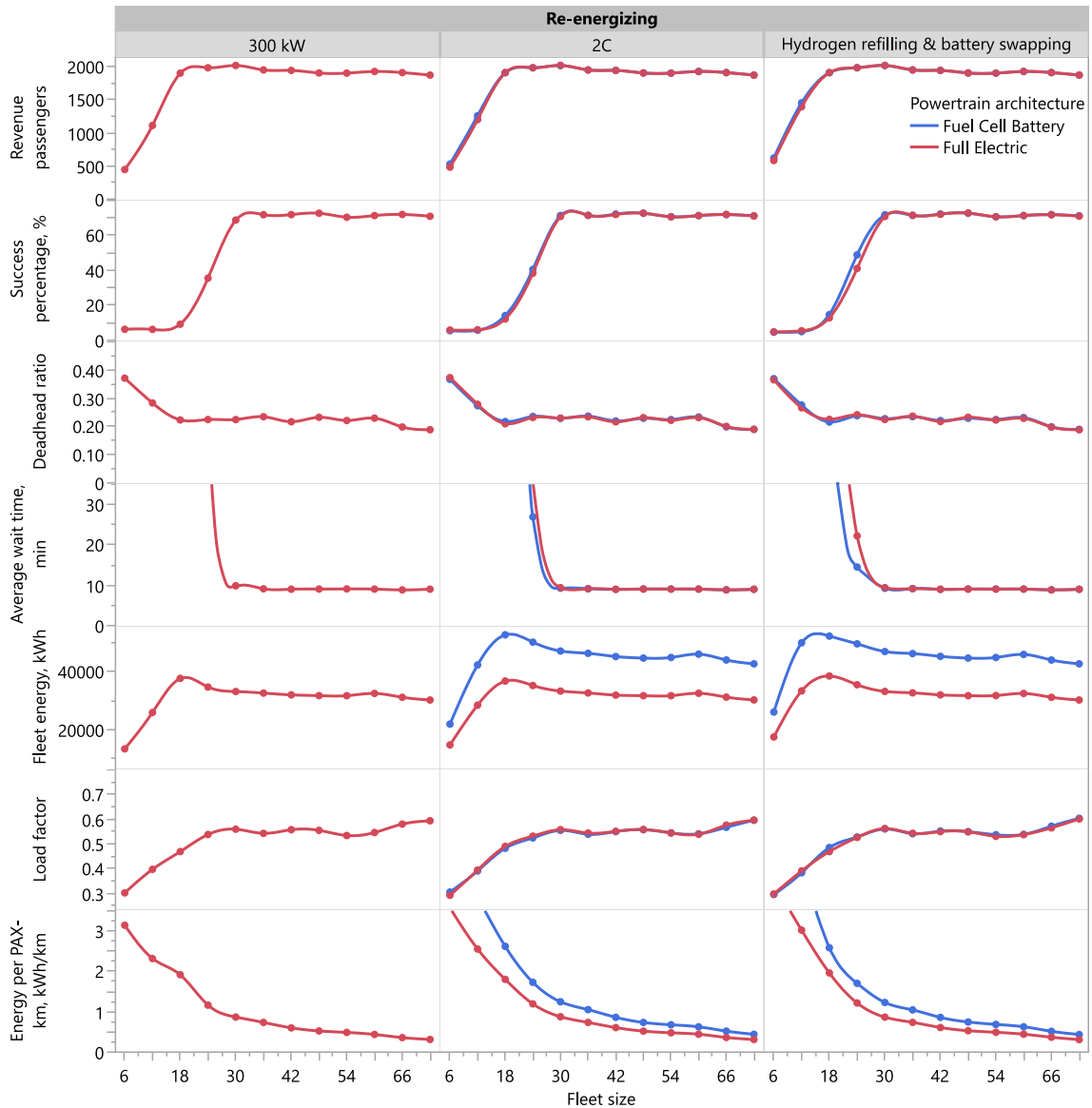
Figure 4.4: Impact of Different Re-energizing Strategies on the Urban SoS in the Near-term Time Frame

As before, the fuel cell battery powertrain architecture requires about 40% more energy. Thus, a comparison with terrestrial battery electric vehicles (assuming 180 W h/km at single occupancy) shows that the full electric multirotor requires around 4.8 times more energy, while even accounting for the load factor. This stresses again that decisions have to be taken in the aircraft design process to reduce the weight of the VTOL aircraft as much as possible. The short-distance UAM missions have high requirements for hover efficiency, the MTOM should be reduced by all means to improve the energy efficiency of urban operations.

Eventually, the far-term time frame is assessed. Here, different re-energizing strategies are compared again. In this time frame, also the pure hydrogen fuel cell multirotor is also modeled as a fleet. Before discussing the results and especially energy consumption, it should be

noted again that the payload mass has been increased from 360 kg to 440 kg in this design point. Consequently, the multirotor air vehicles are now capable of extended-range airport shuttle missions, which does not affect the simulation case study, however. Eventually, Figure 4.5 shows that smaller fleet sizes may be feasible for the far-term time frame, where advanced aircraft technologies considering the subsystem (i.e. control, navigation, and powertrain) and the operational levels (i.e. automated flight or remote-piloting). Hence, positive emergence can seemingly be observed at fleet sizes of around 24 multirotor air vehicles of any architecture. Apart from that, most trends stay similar as described before. Yet, it is worth looking at the newly introduced hydrogen fuel cell multirotor depicted in blue. As the fuel cell's efficiency is significantly lower compared to the full electric powertrain, for example, the total fleet energy required by the fuel cell powertrain architecture is vastly higher. Regarding the swift re-energizing strategy of hydrogen refilling and battery swapping, the multirotor powered by the hydrogen fuel cell requires about 2.2 times more energy when compared with the full electric multirotor. This brings up again the notion that one should think above all about primary energy production and implications to other life cycle stages. Thus, only evaluating the subsystem or aircraft level MoPs (e.g. powertrain efficiency, aerodynamic efficiency, and MTOM) may not be enough to obtain a holistic picture. This is where the SoS approach can sensitize aircraft designers to consider impacts on areas outside their field of work. Finally, the energy consumption in the far-term time frame is to be revisited an compared to the near-term. Here, feasible fleet sizes of around 24 aircraft would require around 0.453 kWh/PAX-km in case of full electric powertrain architectures. This is almost half of the energy consumption found for the near-term time frame, but still more than 2.5 times the energy consumption of a single-occupied terrestrial battery electric vehicle. However, going beyond the minimum required fleet size of 24 aircraft, a fleet of 36 full electric multirotor air vehicles yields the potential to reduce the energy consumption to around 0.312 kWh/PAX-km if the re-energizing strategy of charging at 4C is applied. In the end, it will have to be considered if urban air taxi operations are sensible regarding the high energy consumption due to the short-distance missions, where vertical flight phases mostly dominate. Even if energy is mostly generated through renewable energy production methods in the far-term time frame, energy may still be a more or less limited resource, which eventually demands efficient use.

Figure 4.5: Impact of Different Re-energizing Strategies on the Urban SoS in the Far-term
Time Frame

4.3 Tiltrotor Study

4.3.1 Suburban Use Case Requirements and Assumptions

For the second design study, a suburban use case with longer distances compared to the urban use case is considered and defined. Correspondingly, the suburban use case regarded in this work is a combination of the suburban and mega-city use cases and CONOPS developed from HorizonUAM workshop discussion, which were presented by Asmer et al. [41].

Both use cases are characterized by longer-distance missions of up to 100 km, where one intermediate stop at a vertistop without re-energizing infrastructure is required for the megacity use case. The proposed cruise speed is defined as a ground speed of 150 km/h. However, according to the emerging industry, higher cruise speeds may be desired for the longer-distance UAM missions (see Uber [103], for example). Consequently, cruise speed beyond the previously mentioned 150 km/h are to be considered. Therefore, a winged configuration is chosen for this mission type due to the need for higher cruise speeds and aerodynamic cruise efficiency compared to the previous use case and the designed multirotor configuration. For this design study, a tiltrotor configuration is preferred over a lift + cruise configuration, because the tiltrotor is able to utilize all its propulsors during vertical and forward flight, thus no unnecessary masses with regard to stopped rotors must be carried. The complexity of the tiltrotor is higher, yet, it may still be more feasible compared to a tiltwing configuration, where the heavier wing must be tilted compared to tilting the rotors, only (potentially, these other configurations could also be investigated in the future). Regarding the payload capacity, 4 POB and their hand baggage are set as requirements in the two underlying HorizonUAM use cases. Further details on both use cases can be found in the aforementioned publication by Asmer et al. [41].

Again, a list of TLARs is compiled, whereas the requirements for the derived suburban use case mostly consist of the same requirements similar to the urban use case. However, for overview and completeness, the list is updated according to the previous explanations and presented below:

The air vehicle . . .

SU.01 must have VTOL capabilities for short hover times ≤ 30 s per hover segment.

SU.02 must be able to continue safe flight and perform a safe vertical landing in any potential failure case.

SU.03 must not exceed an MTOM of 3,175 kg.

SU.04 must not exceed the dimensions of 15.24 m × 15.24 m × 6.09 m in total length, width and height, respectively.

SU.05 must carry 4 POB and their hand baggage with a total payload mass of 360 kg.

SU.06 must achieve a total cruise distance of 100 km with one intermediate stop, where no re-energizing infrastructure is available.

SU.07 must achieve a cruise ground speed of ≥ 150 km/h, while directly opposed to a headwind speed of 20 km/h.

SU.08 must be equipped for highly automated or remote-piloted control.

SU.09 shall be able to taxi on ground with the help of external devices.

SU.10 shall have an electric powertrain architecture.

SU.11 shall be compatible with state-of-the-art re-energizing infrastructure.

SU.12 should enable swift battery swapping times $\leq 5\,\text{min}$.

Table 4.8: Suburban Mission Profile Segment Definitions

No	Name	Horizontal speed, km/h	Vertical speed, ft/min	Altitude MSL, ft	Distance, km	Time, min	Power, kW
1	Taxi	—	—	5,000	—	0.5	P_{tx}
2	Vertical climb	—	100	5,000 to 5,050	—	t_{vd}	P_{vc}
3	Transition	0 to V_{be}	0	5,050	—	t_{tr}	P_{tr}
4	Cruise climb	V_{be}	700	5,050 to 7000	D_{cc}	t_{cc}	P_{cc}
5	Cruise	$V_{br} \geq 170$	0	7,000	50–D_{cc}	t_{cr}	P_{cr}
6	Re-transition	V_{be} to 0	0	5,050	—	t_{tr}	P_{tr}
7	Vertical descent	—	–100	5,050 to 5,000	—	t_{vd}	P_{vd}
8	Taxi	—	—	5,000	—	0.5	P_{tx}
9	Loiter	V_{be}	0	7,000	—	20	P_{lo}

4.3.2 Tiltrotor Design

For the winged aircraft design, the tiltrotor configuration is chosen due to the previously mentioned drivers. The principal configuration design is inspired by the Joby Aviation S4 (see Figure 2.8) and is intended to represent a modular family design, thus the shrunk fuselage variant developed for the multirotor configuration is taken as a starting point for the development. Similar to the multirotor, the boarding and deboarding of passengers drives the layout of the structural attachments. Therefore, the wing is foreseen to be mounted in a high-wing configuration at a slight anhedral angle. Also, a high-lift system is eventually needed for the wing to allow slow flight speeds and low stall speeds for transition. Further, the eVTOL aircraft configuration is intended to have six tilting, collective pitch-controlled proprotors integrated into pod-shaped nacelles, where four proprotors are span-wise distributed along the wing leading edge and two proprotors are mounted at the tail. By this approach, a comparably low disk loading is achievable, while also reaching hover stability by longitudinally and laterally distributed thrust and ensuring sufficient ground clearance of the proprotors over all tilt angles. The proprotor integration at the wingtips may also provide aerodynamic benefits compared to propellers integrated at the inboard part of the wing as has been found by wind tunnel testing [117]. In this case, a tractor configuration is chosen to allow geometric spacing in the transition and tilting phase of the proprotors. Yet, further considerations regarding the eVTOL aircraft configuration could also investigate a wingtip-mounted propeller in a pusher configuration which bears further potentials as shown by follow-up wind tunnel testing on propeller-wing interactions

[118]. Eventually, wing structural design aspects must also be considered and should be traded-off against the discussed benefits purely arising from the aerodynamic performance. Compared to the multirotor fuselage, here, an extended tail cone or arm must be developed in order to mount the tail at the required tail arm length. Eventually, different tail layouts such as conventional, T-Tail, and V-tail, are considered in the following steps. Moreover, a conventional fixed tricycle landing gear with wheel fairings is assumed to be reasonable as the mission distances are short in comparison to CTOL general aviation aircraft and the additional mass of retractable landing gear system may lead to undesirable mass growth. However, trade-offs on this aspect can be carried out together with further configuration options in the future. Regarding the powertrain architecture, the same architectures are considered as for the multirotor concept, also involving the gearbox.

In contrast to the sizing procedure demonstrated for the multirotor configuration, here, the design starts from scratch without a fully modeled aircraft geometry to begin with. Therefore, the empircal methods for the estimation of the equivalent flat-plate drag are utilized which appeared to be fairly usable for winged configurations (see Section 4.1). Therefore, the wing sizing parameters have to be input for the wing sizing, in addition. For this purpose, Figure 4.6 shows an exemplary matching chart for a tiltrotor configuration. As can be seen, the power loading is sized due to the vertical flight requirements, whereas the sizing constraint for the maximum wing loading is determined by the combination of stall speed and maximum lift coefficient. Also, to reach efficient cruise flight characteristics at high best range speeds as well as a structurally-sound wing design, a high wing loading is to be chosen while keeping a reasonable aspect ratio. Eventually, the wing sizing parameters are given: The intended high-lift system is expected to achieve $C_{L,max} = 2$. Finger et al. [63] have used an assumption on the stall speed for their VTOL design which is based off its intended cruise speed, i.e. $0.5V_{cr} = 33.5\,\text{m/s}$. However, for this design study, a higher wing loading is desired as explained before, and due to the lack of regulations on this matter in the case of eVTOL aircraft, a slightly higher stall speed $V_s = 36\,\text{m/s}$ is chosen, which is deemed to be reasonable for the transition in combination with the high-lift system. Finally, the wing is sized at $WL = 1{,}587\,\text{N/m}^2$ and an aspect ratio $AR = 10$ is selected to trade-off wing mass growth and cruise efficiency (see Appendix C).

Next, the aircraft rotor sizing process is described. Here, the representative five-bladed proprotor with a higher solidity of $\sigma = 0.2$ compared with the multirotor is modeled. Hence, the goal is to reach a comparably low loading in a range of $560\,\text{N/m}^2$ to $580\,\text{N/m}^2$ to increase vertical flight efficiency, and to achieve a reasonably low rotor tip speeds around the $150\,\text{m/s}$ mark, enabling reduced noise design. The rotor maximum mean lift coefficient is adjusted accordingly and set to $\overline{C_{lmean,max}} = 0.7$. Again, the proprotor sizing also has to comply with the required geometric design space constraints. From geometric analyses, a maximum rotor diameter of $3.2\,\text{m}$ is found to be feasible. In the subsequent sizing process, the rotor diameter is varied in order to arrive at the desired disk loading and tip speed. Eventually, the ratio of total wing-mounted rotor diameter and wing span has to
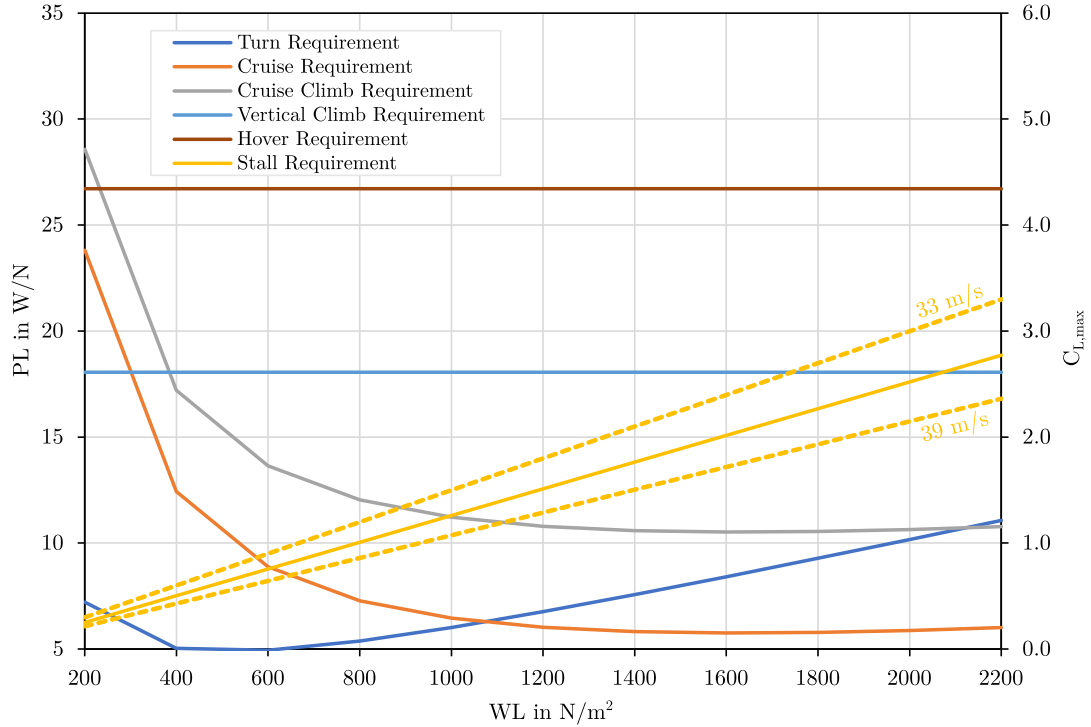
Figure 4.6: Exemplary Matching Chart for the Tiltrotor Sizing

be checked, also accounting for the fuselage diameter and additional margins, in order to arrive at a feasible design point.

However, the sizing of an eVTOL tiltrotor aircraft appears to be challenging in the near-term time frame for the derived set of requirements, while trying to size the aircraft with any of the powertrain architectures foreseen in this study. Therefore, alleviation must be granted in order to size the aircraft. Consequently, the first alleviation considers the intermediate stop within the mission, which requires high power demands during vertical flight, and was omitted. Still, none of the aircraft architectures converges due to limited specific power of the involved powertrain components. This was also found by Silva et al. [65] in case of the battery-electric powertrains for their AAM aircraft concepts. In the underlying work, especially the battery and also the fuel cell impose restrictions in the near-term time frame. Therefore, as a second alleviation, the battery-electric architecture is allowed a higher maximum C-rate of 4C, equal to a battery specific power of $1\,\mathrm{kW/kg}$. It should be noted that this alleviation might reduce the battery lifetime and may only be feasible with advanced battery technologies. Still, the vertical flight phases with its associated high power demands have a comparably small portion, so that this alleviation may be justified by the mission profile considerations.

Regarding the far-term time frame, all powertrain architectures except the hydrogen fuel cell powered architecture converge at the previously explained design point. This is likely due to the limitation in terms of specific power from the fuel cell, where higher specific

powers of up to 4C are granted for the battery-electric powertrain architecture. Also, for the far-term time frame, the aircraft design output at the specified design point is taken as an input for the 3D modeling in OpenVSP, as shown in Figure 4.7, in order to re-evaluate the empirically determined equivalent flat-plate area. Again, the implemented methods from Torenbeek [116] are used, where an interference factor $Q = 1.3$ is applied for the motor nacelles and landing gear struts. In addition, a 10% margin is added on the geometric drag in order to account for non-modeled parts as well as uncertainties. Eventually, the equivalent flat-plate area is determined in flow conditions comprising an air speed of 60 m/s and an altitude of 7,000 ft, which is supposed to represent the cruise flight accordingly. Eventually, the far-term tiltrotor concepts are re-computed with the newly determined equivalent flat-plate area.

Eventually, Table 4.9 presents an excerpt of the most relevant sizing outputs, whereas the reader is directed to the supplementary information and comprehensive result datasets in Appendix C. Again, note that the tiltrotor for the near-term time frame is size with the two granted alleviations, namely omitted intermediate stop and higher battery discharge of 4C.

As mentioned for the conceptual configuration and layout considerations, the selection of a tail layout still needs to be discussed. While the VTOL-AD tool computes a conventional tail geometry, the computed outputs are also directly usable for the design of a T-tail. However, both design options seem to be unfavorable. Firstly, the proprotors are to be integrated at the tail also, which makes a conventional tail undesirable, because it would place the tail-mounted proprotors directly into the slipstream of the wing-mounted proprotors during forward flight. Therefore, an elevated position is to be favored in order to reduce such interactions, which may inflict noise due to potential blade-vortex interaction. Additionally, the horizontal spacing between wing and tail is of importance to allow an obstacle-free tilting path for the tail-mounted proprotors. Eventually, the V-tail is chosen over the T-tail as it is expected to be structurally-beneficial due to reduced mass, also considering the reduced control system mass. Beyond, stability and control of the V-tail and its ruddervators can be additionally supported by meaningful use of DEP, thus using the tail-mounted proprotors for active yaw control by varying proprotor thrust. To model the V-tail, the computed tail geometry is simply converted by methods used in [119]. However, from the 3D modeling it was found that the actual area is slightly bigger compared to the required tail area due to the elevated proprotor position. Thus, this may bear potential configuration changes in future work.

Finally, the developed battery-electric tiltrotor concept for the far-term time frame is presented in Figure 4.7. Herein, the aforementioned aircraft design considerations and sizing computations can be found and represented by the three-view drawing of the configuration in cruise flight mode. In hover, the rotors would be tilted by 90°, of course. It should be generally noted that this concept is still subject to further iterations within the

Table 4.9: Tiltrotor Sizing Outputs and Performance Specifications

| Parameter	FE 1	FE 1	FC BAT
Time frame	Near	Far	Far
Battery specific energy, Wh/kg	250	500	500
Battery specific power, W/kg	1,000	2,000	2,000
Fuel cell specific power, W/kg	600	1,200	1,200
Disk loading, N/m^2	569	568	577
Number of proprotors	6	6	6
Rotor diameter, m	3.2	2.75	2.9
Thrust weighted solidity	0.117	0.117	0.117
Hover tip speed, m/s	152	152	153
Wing loading, N/m^2	1,587	1,582	1,589
Wing area, m^2	17.3	12.8	14.4
Wing aspect ratio	10	10	10
MTOM, kg	2,803	2,065	2,334
Payload, kg	360	360	360
Airframe, kg	912	740	793
Powertrain, kg	1,345	797	1,006
Battery, kg	758	365	290
Fuel cell, kg	—	—	214
Hydrogen, kg	—	—	9.6
Other systems, kg	186	168	175
Hover power, kW	564	415	473
Cruise power, kW	149	121	134
Best range speed at H_{cr}, m/s	62	56	58
Best endurance speed at H_{cr}, m/s	47	43	44
Usable mission energy, kWh	104	107	383
Figure of merit	0.8	0.8	0.8
Equivalent lift-to-drag ratio	11.5	9.4	9.9
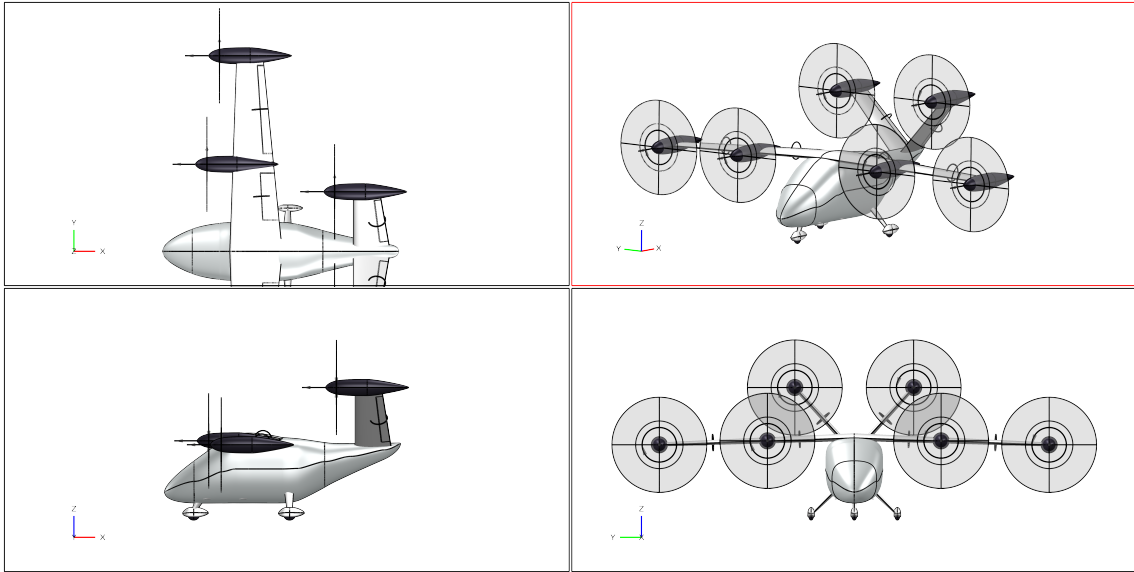
Figure 4.7: Three View Drawing of the Preliminary Battery-electric Tiltrotor Concept

HorizonUAM project together with the involved expert domains, thus it only represents a preliminary result as part of the project.

4.3.3 Suburban Air Transport Fleet Assessment

This further UAM transport case study considers a vastly different use case compared to the urban air transport case study. In this case study, a suburban air transport scenario is considered and set-up by a more or less hub-and-spoke transport network as shown in Figure 4.8. The setup is inspired by a report on the commuter traffic in the Hamburg Metropolitan Region [120]. Accordingly, Hamburg forms the central part and represents the most frequented vertihub with peak inflow demands in the morning and peak outflow demands in the evening. Only small outflow demand from Hamburg to the suburban or remote veriports is modeled. Considering the remote vertiports, those are located in cities or administrative districts in the Hamburg Metropolitan Region where potential commuters might travel to Hamburg from. These vertiports are located at fairly well-connected central locations that could allow a bigger catchment area for demand generation and also enable inter-modal transport, e.g. by car and train. A total demand of approximately 4,000 passengers has been assumed for 24-hr operations and represents less than 1% of the daily commuters in the Hamburg Metropolitan Region according to [120]. The operations are still modeled by the same on-demand dispatching as explained before, whereas the maximum passenger wait time has been doubled to 30 min so that deadhead flights are able to reach passengers in time for all the possible transport requests. Accordingly, also the MoE considering the wait time based success percentage changes by the extended target wait time. As mentioned before, further information on the ABS can be found in
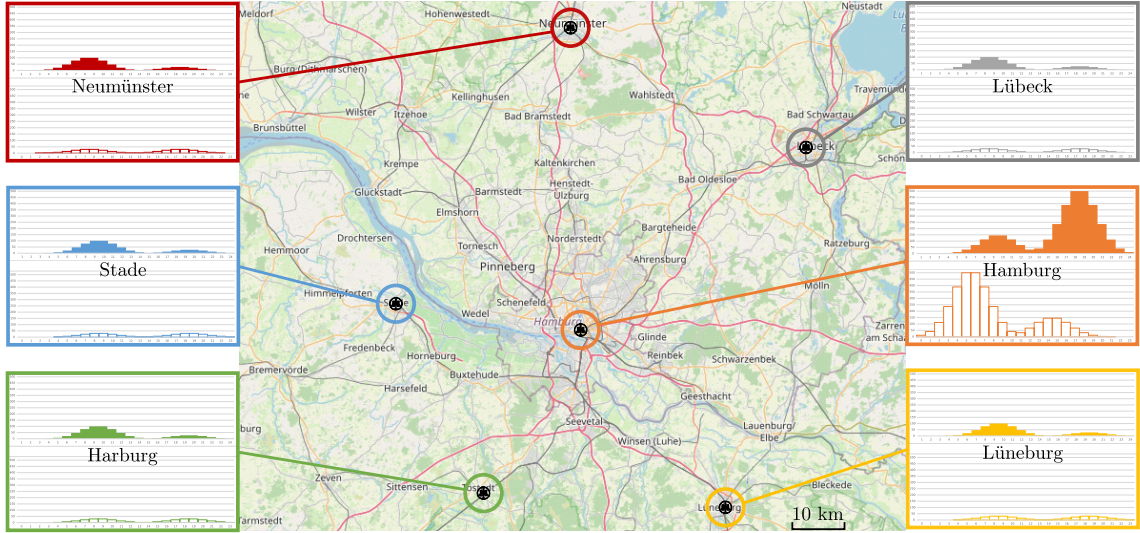
Figure 4.8: Case Study for the Suburban Air Transport Fleet Assessment in the Hamburg Metropolitan Region (Outflow Demand in Solid Color and Inflow Demand With No Fill)

Table 4.10: Suburban Air Transport Case Study Parameters for Different Time Frames

Parameter	Near-term	Far-term
Autonomy	False, except for deadhead flights	True, for all flights
Cruise speed	210 km/h	
Fleet size	6, 12, 18, 24, 30, 36, 42, 48, 54, 60, 66	
Passenger capacity	3	4
Passenger wait time	max. 30 min	
Re-energizing	Battery swap, 300 kW, 2C, hydrogen refill	Battery swap, 2C, 4C, hydrogen refill
Vertidrome capacity	100 (unlimited)	

[40]. Finally, it should be noted that this case study is purely academic and should only represent the notion of a suburban UAM use case.

As before, this case study considers two different time frames where technology improvements are also assumed on the further subsystem and SoS aspects. A summary of the case study parameters involved in the different time frames is provided in Table 4.10. Basically, most parameters remain unchanged compared to the previous explanations of the urban air transport case study (see Section 4.2.3). Here, the cruise speed and the passenger wait time are adjusted and matched as explained before.

For the evaluation of the suburban case study results, the same MoEs as for the urban SoS results are considered (see Section 4.2.3). Starting with the near-term time frame, the first SoS results consider the impact of re-energizing for the battery-electric tiltrotor on the

MoE parameters. Here, the re-energizing is performed by 300 kW available at the charging station, charging at a constant C-rate of 2C, and battery swapping within 5 min. The results are depicted in Figure 4.9 and also show a trade-off scenario in which autonomy might already be fully feasible for the near-term time frame. Very different plots with regard to the revenue passengers and the success percentage are presented here. It can be clearly seen from both MoEs that the suburban use case is vastly different and demands for even higher fleet sizes than expected. Especially for the baseline near-term time frame, where no autonomy is enabled, the success percentage is very poor. It also becomes visible that the different re-energizing strategies might be alleviating these issues, however, no sufficient fleet size can be found at this parameter sweep. Thus, most discussions will follow on the assumed autonomous scenario depicted on the right of Figure 4.9. In this case, all 4,000 revenue passengers can be transported at a fleet size of around 36 tiltrotor aircraft. However, the associated success percentage and average wait time are outside the sensible range. The eventually required fleet size may not even be in the range of 60 aircraft, even if autonomous operations are enabled. Also, for this use case it is found that the deadhead ratio behaves differently compared to the urban use case, where a stable deadhead ratio was reached as soon as positive emergence is found. Here, the deadhead ratio does not converge or stay constant more or less, but rather increase again after a local minimum at a comparably small fleet size. This shows that for this use case probably adapted dispatch algorithms are needed with which possibly also scheduled operations might have to be mixed in order to avoid deadhead flights and reduce the wait times as much as possible. Due to the centralized demand at certain peak hours, higher load factors compared with the urban use case can be found here. Finally, picking a fleet size of 72 tiltrotor aircraft that make use of battery swapping, a success percentage of approximately 80% can be found. Also, the resulting energy per PAX-km is found to be at around 0.314 kWh/km which is a significant improvement compared to the short-range urban missions involving the multirotor concept. This is due to the focus of this case study on longer-distance commute, of course. A comparison with the aforementioned single-occupied terrestrial battery-electric vehicle shows that suburban operations might be around 1.7 times less energy efficient in the near-term time frame.
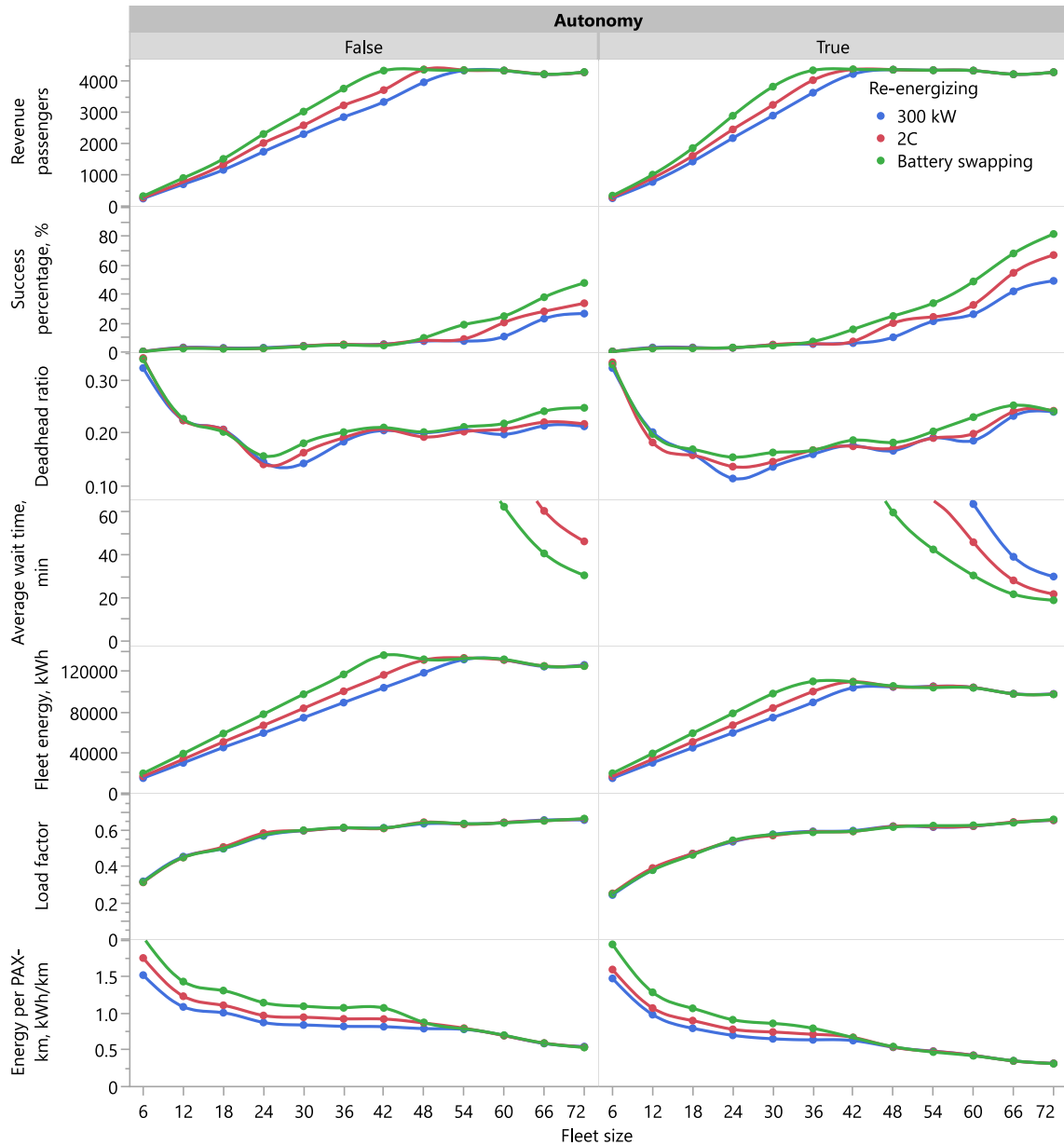
Figure 4.9: Impact of Different Re-energizing Strategies and Autonomy on the Suburban SoS in the Near-term Time Frame

Finally, in the far-term time frame, one additional powertrain architecture is converging, namely the hybrid hydrogen fuel cell battery architecture. Consequently, the differences between the two tiltrotor aircraft are shown in Figure 4.10. Here, also different re-energizing strategies are considered, which are charging at 4C or swapping the batteries and for the hybrid powertrain also refilling of hydrogen, of course. Since the aircraft are also operated fully autonomously, the observed trends are similar to the previous results discussed in detail. Also, only the highest fleet sizes start to become successful by consideration of the success percentage and average wait time MoEs. It is found that the fuel cell battery architecture seems to have a slight advantage in comparison. However, again the energy consumption is higher in case of the aforementioned architectures due to the same reasons

as discussed previously. Having a closer look on the energy per PAX-km, it shows that for a fleet size of 66 aircraft around 0.2 kWh/PAX-km are consumed in case of the full electric tiltrotor, whereas the fuel cell battery electric powertrain architecture has an around 36% higher energy consumption in comparison. Thus, using this full electric fleet would actually allow reaching reasonable energy consumption levels, which are close to terrestrial battery electric vehicles at a single occupancy. Eventually, other researchers and potential operators would have to determine the feasibility of this suburban use case, when cost is also accounted for. Eventually, it can also be concluded that UAM might not be a new alternative to public transport or other means of mass transportation due to the large fleet size required to cater a minor portion of the overall (commuter) market.
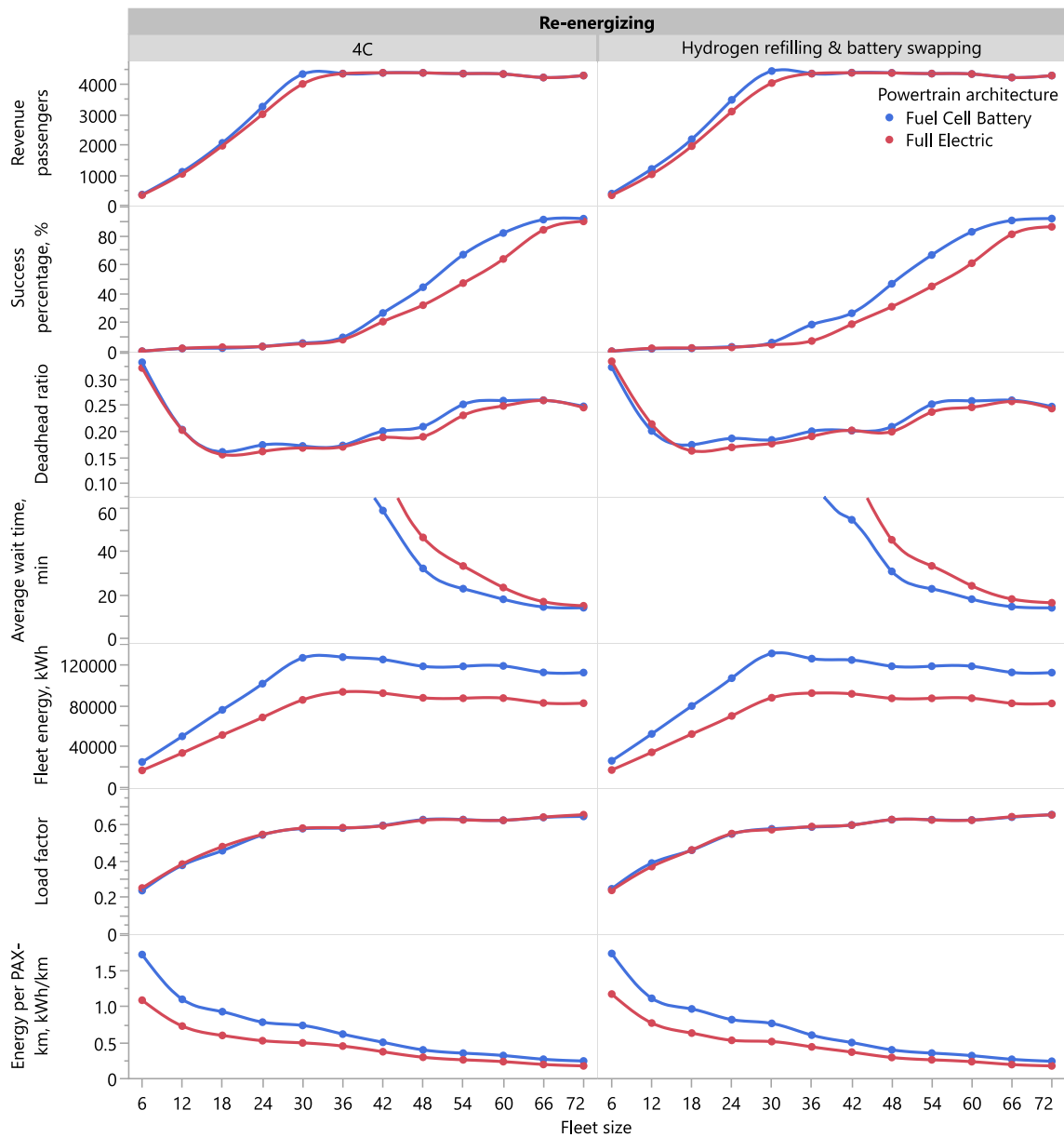

Figure 4.10: Impact of Different Powertrain Architectures and Re-energizing Strategies on the Suburban SoS in the Far-term Time Frame

4.4 Aerial Firefighting Study

Even if it is not a major part of this thesis, another ABS for SoS aircraft design and assessment should be mentioned since it has been developed more or less simultaneously and also contains contributions by this author. Technical details on the implementation as well as the proof of concept for this SoS simulation use case can be found in publications by Shiva Prakasha et al. [121, 122]. The main ideas and findings from the cited research papers as well as the connection with this thesis will be explained in the following paragraphs.

Accordingly, the motivation for this use case is as follows: due to the increasing threats of wildfires across the globe, modern aerial firefighting concepts are needed to provide an effective means of firefighting which can protect people, wildlife and forestland using advanced technologies compared to today's fleets. Due to global warming not only do the wildfire seasons get longer, but they also become more and more threatening, especially in cases where wildland-urban interfaces are affected endangering human lives and properties. In addition, wildfires also cause carbon dioxide emissions which further drive global warming leading to a viscous circle in the drying out of nature and further increase in risk of as well as danger from wildfires. Aviation could help to mitigate the risks and tackle the threats of wildfires, as aerial firefighting is mostly a very effective measure if designed properly and deployed quickly. Eventually, the referred research papers envision the development of new air vehicles that could potentially be derived from the extensive research and development in the field of AAM. Thus, different eVTOL aircraft configurations are conceptually designed and assessed in the wildfire fighting use case.

Because of the complex interaction between the suppression air vehicles, the fire, the environment, and the operational tactics, impacts on the MoPs and MoEs must be analyzed by a SoS simulation approach. Therefore, the SoS simulation framework for aerial firefighting allows operating fleets of suppression air vehicles in different wildfire scenarios. Similar as in the SoS simulation framework for UAM, the aircraft agents do also account for their performance characteristics and follow an aerial firefighting CONOPS including low altitude suppression drops as well as scooping from water sources. Of course, the agents have to return to their base in order to re-energize as soon as their mission energy depletes. Cost aspects of the aerial firefighting fleet operations are also considered by a dedicated cost model for eVTOL aircraft.

Thereby, the SoS simulation framework allows drawing different conclusions with regard to design and operational parameters. The proof of concept studies [121, 122] have shown that higher cruise speeds, payloads, and design ranges would be beneficial to maintain a high firefighting effectiveness. However, trade-offs with regard to operating cost and fleet size are needed and can be qualitatively derived from the sensitivity studies. In this context, different trade-offs can be performed not only with regard to the aircraft, but also the fleet design. Eventually, the operational environment also has major impacts on the firefighting effectiveness. Here, the scenario settings which include the distances between

operational base, wildfire location and water sources, as well as the response time between fire outbreak and aircraft deployment, must be given special attention in the design and assessment of such advanced aerial firefighting fleets.

As the SoS simulation studies within this framework have been mostly conducted using the previous eVTOL aircraft design and modeling tool, the newly developed VTOL-AD tool would allow for further investigation thanks to the refined models. Also, the connection of the VTOL-AD tool and the ABS is directly possible through the common use of JSON input files as described earlier in Section 3.3.3. Besides the design and assessment of eVTOL aircraft from the field of AAM, other aircraft types could also be modeled by extending the tool, which will be further elaborated in the final chapter of this thesis.

Generally, this use case provides a prospective opportunity to continue the exploration and investigation of aircraft design in simulation-driven SoS applications and further provide useful aviation concepts or even products to the society. Accordingly, AAM aircraft may provide advanced and useful capabilities that could be added to the existing fleet of aerial firefighting vehicles as also envisioned by NASA [123]. Furthermore, the recently kicked-off DLR Design Challenge 2022, a student design challenge for education and training, has also picked up this theme, and asks aeronautical and aerospace engineering students to design advanced air vehicle and fleet concepts for this futuristic idea [124].

5 Conclusions

In the context of advanced digital methods and approaches in aeronautical research and development, the goal of this thesis was the tool development for the conceptual design of VTOL aircraft. The tool had to be developed for the application in an SoS simulation framework, which is primarily focused on the simulation-driven design and assessment of the emerging aviation use case of UAM air taxi transport operations. Thus, the contextual background of this thesis, namely VTOL aircraft, UAM and SoS, had to be established in the beginning. The main objective was to code a robust and integrated tool as a part of the overall framework, where certain interfaces with other tools and simulations had to be matched. Furthermore, a tool demonstration by the design and assessment of two disparate eVTOL aircraft, i.e. multirotor and tiltrotor, had to be presented in separate exemplary design studies.

From the background and literature review conducted as part of this thesis, it was found that the technology advancements in the fields of VTOL aircraft, UAVs, and (more) electric aircraft allow new design solutions, e.g. by DEP. Those advancements may not only potentially enable the deployment of advanced and (locally) emission free aircraft, but may also yield the opportunity of providing novel aviation use cases such as UAM and RAM to the society. However, similar visions have already existed in the past and clearly faced limitations due to the challenges in individual domains as well as the highly complex interplay of several involved systems. To overcome and provide methodologies for such research and engineering problems, the principles of holistic SoS approaches are introduced, where non-analytical methods such as ABS are used to investigate the interactions of constituent systems and to find desired or non-desired emergent behaviors in the early SoS (aircraft) design process. This approach is also recognized within the HorizonUAM project and the DLR-internal development of a holistic UAM SoS simulation framework, in the context of which this thesis has been prepared. Considering the design tool development, industry and research eVTOL aircraft designs and corresponding methods as well as tools have been reviewed prior to the design tool development.

Consequently, the developed VTOL-AD design tool has been laid out and explained by the selective choice of conceptual eVTOL aircraft design methods from the preceding literature review. Subsequently, the software architecture implementation in Python 3 is highlighted. The VTOL-AD tool does not only overcome the faced limitations with earlier used eVTOL design tools, where most aircraft characteristics had to be assumed, and

mission segments were only roughly defined, but also successfully adapts and manages all required interfaces. Herein, the VTOL-AD design tool has been integrated into the current state of development of the UAM SoS simulation framework, where connections with onboard systems design and the ABS of air transport fleet operations have been firmly established. Accordingly, the VTOL-AD tool is capable of performing initial sizing as well as performance evaluations of different eVTOL aircraft configurations involving winged and wingless open rotor aircraft, e.g. multirotor and tiltrotor. Thus, the VTOL-AD tool provides an important contribution to the overall UAM SoS simulation framework, the collaborative conceptual aircraft design workflow together with rotorcraft, onboard systems, and cabin design experts, and is readily usable for further studies in this field.

While all the formulated requirements on the tool methodology development have been successfully fulfilled by this work and the tool has been validated by design point analyses of higher-fidelity eVTOL aircraft concepts from the literature, there are different opportunities that could be considered for continued and future development. Some mentioned limitations consider the methodology of the VTOL-AD tool, where higher-level semi-empirical methods can be implemented, e.g. in the aerodynamics and airframe models. Since the airframe mass estimation represents a major challenge for the design and assessment of such unconventional air vehicles, physics-based methods might be preferred over historic semi-empirical methods from other air vehicle classes and can be implemented in addition to the current models. Also, the geometry and aerodynamics modeling should be directly connected within the VTOL-AD tool in order to enable more sophisticated aerodynamics modeling as well as geometry sizing and to reduce the number of interfaces to separate tools. Thanks to the readily available interfaces to subsystem and SoS design and assessment, the VTOL-AD tool could also be set up more broadly and consider different air vehicle classes in the context of SoS simulation-driven aircraft design. After the sizing process implemented in the underlying tool, further higher- and mixed-fidelity tools could be included in the design process to further refine the approach.

Considering the software architecture, all the stated development requirements have been successfully fulfilled by this thesis. The designs are developed by user inputs and sensitivity analyses. However, optimization algorithms might need to be implemented in order to automatically derive design point optimized aircraft designs. This may also be feasible through a concurrent future work potential, where the ad-hoc data-format VTOL-AD tool should be transferred to a CPACS based tool. Therefore, complex RCE workflows could be set-up more easily and also involve optimization and DoE. Also, the interface to the ABS and the corresponding DoE set-up may be further simplified and harmonized in the future, where performance methods and atmosphere models could also partly be implemented inside the ABS, if computational performance allows. This digital thread between the aircraft design and simulation environment will become even more crucial when automatic feedback from simulation to design shall be implemented. However, since the basis has

been successfully set through this thesis, further development can build on and extend the current implementation.

Beyond the tool methodology implementation, software architecture development, and tool validation, further demonstration studies have been conducted in the field of UAM aircraft design and simulation-driven assessment by exemplary scenario case study. Herein, not only two disparate eVTOL aircraft configurations, i.e. multirotor and tiltrotor, but also two fundamentally different UAM use cases, i.e. intra-city and suburban transport, and time frames, i.e. near-term and far-term, have been considered. Different subsystem designs range from the powertrain architecture, i.e. battery-electric or hydrogen fuel cell, to the charging infrastructure available at the vertidromes. With regard to the eVTOL aircraft design, expected difficulties have been identified when it comes to high mission requirements such as payload or range. In this context, the importance of energy-efficient design is stressed and demonstrated by the consideration of two different size cabin layouts. In the near term, the hydrogen fuel cell as well as hybrid hydrogen fuel cell and battery powertrain architectures were deemed to be too inefficient and heavy for most of the design points, thus mostly battery-electric eVTOL aircraft have been sized. However, all three powertrain architectures became feasible in the far-term scenario, whereas the hydrogen-powered concepts could be able to carry more energy while sized at fairly similar MTOMs compared to battery-electric powertrain architectures. Beyond the subsystem and system MoPs, also MoEs will be summarized and discussed in the following paragraph on SoS results. Generally, the design of eVTOL aircraft and onboard systems has only been performed on an initial conceptual level and these domains impose even more complex challenges in the preliminary and detailed design process which were not addressed in this work. Eventually, the two preliminary eVTOL aircraft design concepts form the start of a UAM aircraft family. Both concepts, multirotor and tiltrotor, are pictured together in Figure 5.1. Future work on the aircraft concepts should involve further architecture or configuration trade-offs regarding certification, safety and security under different failure conditions or misuse cases, enhanced aerodynamics and performance, low noise design and assessment, weight and balance, passenger comfort and accessibility, and maintenance, repair and overhaul aspects, namely reliability, availability, maintainability and serviceability.

The SoS findings are currently limited due to the framework's current state of development concerning the demand, cost, trajectory, and vertiport modeling. Also, the underlying demonstrations may have only revealed the tip of the iceberg of further, more comprehensive SoS investigation. The UAM case studies mainly intended to represent the robust tool and framework connection, which was the major focus of this thesis. Yet, interesting insights and trends have been found, which demonstrate the need for holistic SoS design and assessment considering the interplay of multiple constituent systems and the resulting multi-level impacts on the subsystem, systems and SoS level. By varying different UAM aircraft fleet sizes in an on-demand operations simulation, the ABS allows identifying an-

Figure 5.1: Compilation of the Developed eVTOL Aircraft Family Concept Consisting of Multirotor and Tiltrotor Configurations (Background Image Source: DLR)

ticipated, but also unforeseeable emergent behaviors, which analytical methods would not be able to determine. By trying to achieve certain MoEs, e.g. success rate measured by wait time, deadhead ratio measured by empty flights, etc., it was shown that intra-city and suburban operations may require different strategies due to their disparate nature. Here, the intra-city has more short-distance point-to-point connections and distributed demands, whereas the suburban represents a longer-distance hub-centric network with low off-peak and high peak demands, which lead to comparably high fleet sizes to reach high success rate. Therefore, scheduled operations might be preferable for the suburban use case. Beyond the network operations, the influence of charging powers and the corresponding turnaround times is of importance for all the UAM use cases. Accordingly, downtimes and turnaround times shall be reduced as much as possible, either by battery fast-charging, or even better, battery swapping or hydrogen refilling. In this context, the hybrid hydrogen fuel cell battery powertrain architecture may on the one side allow for better performance and flight operational flexibilities, but on the other side impose operational constraints due to its increased complexity and need for two different re-energizing infrastructure types at the vertidromes. Similar applies to the battery swapping strategy, which may result in a high logistical burden. Moreover, the efficient use of energy is of importance, not only for the near-term since green primary energy is still very limited, but prospectively also for the far-term. Thus, energy efficiency must be kept high and the overall energy production and primary energy effort must be considered by SoS driven LCA, for example. Generally, it may be more advisable to intensify the work on further subsystem technology improvements in order to achieve more efficient, thus justifiable energy consumption metrics, which may also be needed for operational scaling. Moreover, longer-distance op-

erations using aerodynamically-efficient winged eVTOL aircraft configurations paired with high load factors thanks to smart dispatching are to be preferred in order to reduce the energy consumption metrics further. Regarding the suitability for mass use, it appears to be unlikely regarding transported passengers vs. required fleet sizes determined by the underlying models and simulations. Eventually, the operational benefit of autonomous, automated or remote-piloted flight has been demonstrated by the SoS simulation, where the additional seat available for passengers yielded improved SoS capabilities. Thus, research and development should work closely together with regulators and potential users in order to reach this vision while adhering to high safety standards. For future work considering the current framework development stage, the impacts of design uncertainties on the overall SoS effectiveness could be already investigated. In order to determine those uncertainty effects, large DoE studies should be carried out, where aircraft design parameter sweeps are input to the ABS. Thus, uncertainties can not only be traced from the system to the SoS level, but can also be quantified. The large datasets may also be used for deriving feedback on SoS driven UAM aircraft design, which may eventually be achievable by automated feedback loops.

While the VTOL-AD tool on its own may not yield findings beyond the state-of-the-art, it represents an indispensable building block within the overall UAM SoS simulation framework. Thus, knowledge beyond state-of-the-art can be achieved through its integration, where several research questions can be investigated in future work. Among others, addressing further SoS related aircraft design impacts, e.g. caused by vertidrome and air traffic management, will be important for the eVTOL aircraft design considering geometric constraints and performance. In this context, not only the overall aircraft size and design performance, but also its operational flexibility when it comes to different changing cruise speeds or delay procedures due to airspace management limitations or inclement weather. Therein, also the prospective passenger demand is a highly uncertain, yet, highly influential factor that drives the overall SoS and eVTOL aircraft design. Thus, the aircraft family should be extended by additional aircraft configurations as well as sizes that could accommodate only two or up to six POB. In this context, the cost of UAM operations must be assessed where also significant capital and operating costs are directly linked to the aircraft design. Accordingly, the costs will of course also determine the ticket prices and thus also have an impact on passenger demand. Since the overall seat utilization plays an important role for the general fleet dispatch and operations, a heterogeneous fleet mix may provide advantages over a purely homogeneous fleet, which might be too inflexible when it comes to serving varying demands and missions. Due to varying mission performances and corresponding loads on the powertrain components, especially the battery, not only their reliabilities and maintenance intervals, but also the implications on the reduced aircraft performance and correspondingly limited fleet dispatch should be considered for future work. Also, to provide more sophisticated answers on the sustainability of UAM, further LCA studies should be carried out with more refined insights on the aircraft's production

and operations phases, which can also be extended to hydrogen-powered eVTOL aircraft, where the entire life cycle and energy grid is considered.

Eventually, to successfully achieve the vision of UAM, all systems and their respective stakeholders, e.g. air vehicle designers, manufacturers and operators, air navigation service providers, infrastructure developers, transport network planners, and last but not least aviation authorities and further regulators, have to follow intensive cooperation and consultation in the process of the development of this prospective aviation use case. However, the potential users and communities also have to be closely involved in this process so that passenger and public acceptance of this urban air transport service can be established in the future. This is as per the set-up of the HorizonUAM project and the associated UAM SoS simulation framework, which will provide further answers on the potentials and limitations of UAM and the involved architectural design decisions in the remaining project runtime.

Despite the air taxi passenger transport and aerial firefighting use cases addressed in this thesis, other exemplary aviation use cases for future work which do not only involve VTOL aircraft but also necessitate an SoS simulation design and assessment approach could include sustainable ecotourism transport (e.g. utilizing efficient zero-emission propulsion systems), ground plus air cargo transportation and logistics (e.g. last mile delivery), disaster relief evacuation and logistics missions (e.g. wildfires, floods, earthquakes, etc.), coast guard missions (e.g. maritime air patrol, search and rescue, etc.), urban and suburban rescue missions (e.g. emergency doctor or medicine goods transport, etc.), and law enforcement missions (e.g. air patrol, search and rescue, observation, etc.).

Finally, the list of use cases within public services would potentially increase the acceptance of other commercial UAM applications such as air taxi passenger transport and parcel delivery, and yield a further boost to the development and deployment of eVTOL aircraft. Accordingly, to round off this thesis, the statement from Sikorsky quoted in the preface can be taken up, since it is possible that in the (near) future not only helicopters but also eVTOL aircraft can be used for social and public services, thus also help to save lives.

Bibliography

[1] National Science and Technology Foundation. *Igor I. Sikorsky – National Medal of Science Engineering 1967.* URL: https://nationalmedals.org/laureate/igor-i-sikorsky/ (visited on 06/06/2022).

[2] IPCC. "Global Warming of $1.5\,°C$. An IPCC Special Report on the impacts of global warming of $1.5\,°C$ above pre-industrial levels and related global greenhouse gas emission pathways, in the context of strengthening the global response to the threat of climate change, sustainable development, and efforts to eradicate poverty". In: ed. by V. Masson-Delmotte, P. Zhai, H.-O. Pörtner, D. Roberts, J. Skea, P.R. Shukla, A. Pirani, W. Moufouma-Okia, C. Péan, R. Pidcock, S. Connors, J.B.R. Matthews, Y. Chen, X. Zhou, M.I. Gomis, E. Lonnoy, T. Maycock, M. Tignor, and T. Waterfield. 2020.

[3] D. S. Lee, D. W. Fahey, A. Skowron, M. R. Allen, U. Burkhardt, Q. Chen, S. J. Doherty, S. Freeman, P. M. Forster, J. Fuglestvedt, A. Gettelman, R. R. de León, L. L. Lim, M. T. Lund, R. J. Millar, B. Owen, J. E. Penner, G. Pitari, M. J. Prather, R. Sausen, and L. J. Wilcox. "The contribution of global aviation to anthropogenic climate forcing for 2000 to 2018". In: *Atmospheric Environment* 244 (2021), p. 117834. DOI: 10.1016/j.atmosenv.2020.117834.

[4] European Commission. *The European Green Deal.* COM(2019) 640 final. Brussels, 2019.

[5] Deutsches Zentrum für Luft- und Raumfahrt e. V. (DLR). *Auf dem Weg zu einer emissionsfreien Luftfahrt – Luftfahrtstrategie des DLR zum European Green Deal.* 2021.

[6] P. Ratei. "Conceptual Aircraft Design and Comparison of Different eVTOL Aircraft for Urban Air Mobility". Project. HAW Hamburg, 2021. URL: https://elib.dlr.de/148037/.

[7] J. G. Leishman. *Principles of Helicopter Aerodynamics.* Cambridge: Cambridge University Press, 2006.

[8] S. B. Anderson. *Historical Overview of V/STOL Aircraft Technology.* NASA-TM-81280. National Aeronautics and Space Administration (NASA), 1981.

[9]   National Museum of The United States Air Force. *Sikorsky R-4B Hoverfly*. URL: https://www.nationalmuseum.af.mil/Visit/Museum-Exhibits/ Fact-Sheets/Display/Article/195868/sikorsky-r-4b-hoverfly/ (visited on 06/06/2022).

[10]   M. J. Hirschberg. "V/STOL: The First Half-Century". In: *Vertiflight* (Mar. 1997).

[11]   M. J. Hirschberg. "Commentary: Electric VTOL Wheel of Fortune". In: *Vertiflight* (Mar. 2017).

[12]   Leonardo. *Next Generation Civil Tiltrotor (NGCTR)*. URL: https://www.leon ardo.com/en/business/next-generation-civil-tiltrotor-ngctr (visited on 06/06/2022).

[13]   Clean Aviation. *The only way is up: NextGenCTR takes shape*. URL: https:// www.clean-aviation.eu/the-only-way-is-up-nextgenctr-takes- shape (visited on 06/06/2022).

[14]   GE Aviation. *Leonardo Next-Generation Civil Tiltrotor Demonstrator Powered by GE*. 2019. URL: https://blog.geaviation.com/technology/leonardo- next-generation-civil-tiltrotor-demonstrator-powered-by-ge/ (visited on 06/06/2022).

[15]   Harbour Air. *Harbour Air, magniX and H55 Partner for The World's First Certified All Electric Commercial Airplane*. 2021. URL: https://www.harbourair. com/harbour-air-magnix-and-h55-partner-for-the-worlds- first-certified-all-electric-commercial-airplane/ (visited on 06/06/2022).

[16]   Pipistrel. *Velis Electro – The First and Still the Only Type-Certified Electric Aircraft in the World*. URL: https://www.pipistrel-aircraft.com/aircraft/ electric-flight/velis-electro-easa-tc/ (visited on 06/06/2022).

[17]   V. Viswanathan, A. H. Epstein, Y.-M. Chiang, E. Takeuchi, M. Bradley, J. Lang- ford, and M. Winter. "The challenges and opportunities of battery-powered flight". In: *Nature* 601.7894 (2022), pp. 519–525. DOI: 10.1038/s41586-021-04139-1.

[18]   M. Hepperle. "Electric Flight - Potential and Limitations". In: *Energy Efficient Technologies and Concepts of Operation*. 2012. URL: https://elib.dlr.de/ 78726/.

[19]   A. Datta. *PEM Fuel Cell Model for Conceptual Design of Hydrogen eVTOL Air- craft*. NASA/CR—20210000284. National Aeronautics and Space Administration (NASA), Jan. 2021.

[20]   H. D. Kim, A. T. Perry, and P. J. Ansell. "A Review of Distributed Electric Propul- sion Concepts for Air Vehicle Technology". In: *2018 AIAA/IEEE Electric Aircraft Technologies Symposium*. 2018. DOI: 10.2514/6.2018-4998. eprint: https: //arc.aiaa.org/doi/pdf/10.2514/6.2018-4998. URL: https://arc. aiaa.org/doi/abs/10.2514/6.2018-4998.

[21]   The Vertical Flight Society. *The Vertical Flight Society*. URL: https://vtol.org (visited on 06/06/2022).

[22]   D. F. Finger, C. Braun, and C. Bil. "A Review of Configuration Design for Distributed Propulsion Transitioning VTOL Aircraft". In: *Asia-Pacific International Symposium on Aerospace Technology*. Seoul, Korea, 2017.

[23]   K. P. Valavanis. *Advances in Unmanned Aerial Vehicles – State of the Art and the Road to Autonomy*. Dordrecht, The Netherlands: Springer, 2007.

[24]   United Nations, Department of Economic and Social Affairs, Population Division. *World Urbanization Prospects: The 2018 Revision*. ST/ESA/SER.A/420. United Nations (UN), 2019.

[25]   Inrix. *INRIX 2021 Global Traffic Scorecard*. URL: https://inrix.com/scorecard/ (visited on 06/06/2022).

[26]   P. D. Vascik. "Systems Analysis of Urban Air Mobility Operational Scaling". PhD thesis. Massachusetts Institute of Technology, Feb. 2020.

[27]   M. D. Moore. "Aviation Frontiers – On Demand Aircraft". In: *10th AIAA Aviation Technology, Integration, and Operations (ATIO) Conference*. 2010. DOI: 10.2514/6.2010-9343.

[28]   M. D. Moore and K. H. Goodrich. "High Speed Mobility through On-Demand Aviation". In: *2013 Aviation Technology, Integration, and Operations Conference*. 2013. DOI: 10.2514/6.2013-4373.

[29]   K. R. Antcliff, M. D. Moore, and K. H. Goodrich. "Silicon Valley as an Early Adopter for On-Demand Civil VTOL Operations". In: *16th AIAA Aviation Technology, Integration, and Operations Conference*. 2016. DOI: 10.2514/6.2016-3466.

[30]   Blade. *Fly the future, today*. URL: https://www.blade.com (visited on 06/06/2022).

[31]   Acubed. *Voom – Transformed the urban commute by making helicopter taxis affordable and accessible*. URL: https://acubed.airbus.com/projects/voom/ (visited on 06/06/2022).

[32]   C. Monnet. *Closing This Chapter: Our Learnings On Transforming How People Move*. 2020. URL: https://acubed.airbus.com/blog/voom/closing-this-chapter-our-learnings-on-transforming-how-people-move/ (visited on 06/06/2022).

[33]   J. Holden and N. Goel. "Fast-Forwarding to a Future of On-Demand Urban Air Transportation". Uber Elevate. Oct. 2016.

[34]   M. Hader, S. Baur, S. Kopera, T. Schönberg, and J.-P. Hasenberg. "Urban Air Mobility – USD 90 billion of potential: How to capture a share of the passenger drone market". Roland Berger. Nov. 2020.

[35] R. Rothfeld, M. Fu, M. Balać, and C. Antoniou. "Potential Urban Air Mobility Travel Time Savings: An Exploratory Analysis of Munich, Paris, and San Francisco". In: *Sustainability* 13.4 (2021). DOI: 10.3390/su13042217.

[36] European Union Aviation Safety Agency (EASA). *Special Condition – Vertical Take-Off and Landing (VTOL) Aircraft*. SC-VTOL-01. EASA, July 2019.

[37] European Union Aviation Safety Agency (EASA). *Second Publication of Proposed Means of Compliance with the Special Condition VTOL*. MOC-2 SC-VTOL. EASA, June 2021.

[38] Airbus. *Airbus lays the foundations for future urban air mobility in Germany with the Air Mobility Initiative Airbus lays the foundations for future urban air mobility in Germany with the Air Mobility Initiative*. May 2022. URL: https://www.airbus.com/en/newsroom/press-releases/2022-05-airbus-lays-the-foundations-for-future-urban-air-mobility-in (visited on 06/06/2022).

[39] B. I. Schuchardt, D. Becker, R.-G. Becker, A. End, T. Gerz, F. Meller, I. C. Metz, M. Niklaß, H. Pak, S. Schier-Morgenthal, K. Schweiger, P. Shiva Prakasha, J. D. Sülberg, M. Swaid, C. Torens, and C. Zhu. "Urban Air Mobility Research at the DLR German Aerospace Center – Getting the HorizonUAM Project Started". In: *AIAA Aviation 2021 Forum*. 2021. DOI: 10.2514/6.2021-3197.

[40] P. Shiva Prakasha, N. Naeem, P. Ratei, and B. Nagel. "Aircraft architecture and fleet assessment framework for urban air mobility using a system of systems approach". In: *Aerospace Science and Technology* 125 (2022). SI: DICUAM 2021, p. 107072. DOI: 10.1016/j.ast.2021.107072.

[41] L. Asmer, H. Pak, P. Shiva Prakasha, B. I. Schuchardt, P. Weiand, F. Meller, C. Torens, D. Becker, C. Zhu, K. Schweiger, A. Volkert, and R. Jaksche. "Urban Air Mobility Use Cases, Missions and Technology Scenarios for the HorizonUAM Project". In: *AIAA Aviation 2021 Forum*. 2021. DOI: 10.2514/6.2021-3198.

[42] K. Schweiger, F. Knabe, and B. Korn. "An exemplary definition of a vertidrome's airside concept of operations". In: *Aerospace Science and Technology* 125 (2022). SI: DICUAM 2021, p. 107144. DOI: https://doi.org/10.1016/j.ast.2021.107144.

[43] N. Ahrenhold, O. Pohling, and S. Schier-Morgenthal. "Impact of Air Taxis on Air Traffic in the Vicinity of Airports". In: *Infrastructures* 6.10 (2021). DOI: 10.3390/infrastructures6100140.

[44] F. Naser, N. Peinecke, and B. I. Schuchardt. "Air Taxis vs. Taxicabs: A Simulation Study on the Efficiency of UAM". In: *AIAA Aviation 2021 Forum*. DOI: 10.2514/6.2021-3202.

[45] C. Torens, A. Volkert, D. Becker, D. Gerbeth, L. Schalk, O. Garcia Crespillo, C. Zhu, T. Stelkens-Kobsch, T. Gehrke, I. C. Metz, and J. Dauer. "HorizonUAM: Safety and Security Considerations for Urban Air Mobility". In: *AIAA Aviation 2021 Forum*. DOI: 10.2514/6.2021-3199.

[46] Electric VTOL News. *eVTOL Aircraft Directory*. URL: https://evtol.news/aircraft (visited on 06/06/2022).

[47] The Vertical Flight Society. *Vertical Flight Society Electric VTOL Directory Hits 600 Concepts*. URL: https://vtol.org/news/press-release-vfs-electric-vtol-directory-hits-600-concepts (visited on 06/06/2022).

[48] SMG Consulting. *Advanced Air Mobility Reality Index*. 2022. URL: https://aamrealityindex.com/aam-reality-index (visited on 06/06/2022).

[49] Airbus. *CityAirbus NextGen – Safe, sustainable and integrated urban air mobility*. 2022. URL: https://www.airbus.com/en/innovation/zero-emission/urban-air-mobility/cityairbus-nextgen (visited on 06/06/2022).

[50] S. Sripad and V. Viswanathan. "The promise of energy-efficient battery-powered urban aircraft". In: *Proceedings of the National Academy of Sciences* 118.45 (2021), e2111164118. DOI: 10.1073/pnas.2111164118.

[51] P. Nathen. *Architectural performance assessment of an electric vertical take-off and landing (e-VTOL) aircraft based on a ducted vectored thrust concept*. Lilium, Apr. 2021.

[52] R. A. McDonald and B. J. German. "eVTOL Stored Energy Overview". In: *Uber Elevate Summit*. 2017, pp. 14–20.

[53] M. A. Clarke and J. J. Alonso. "Evaluating the Performance and Acoustic Footprint of Aircraft for Regional and Urban Air Mobility". In: *AIAA Aviation 2021 Forum*. 2021. DOI: 10.2514/6.2021-3205.

[54] M. A. Clarke and J. J. Alonso. "Forecasting the Operational Lifetime of Electric Aircraft Through Battery Degradation Modeling". In: *AIAA SciTech 2022 Forum*. 2022. DOI: 10.2514/6.2022-1996.

[55] W. Johnson and C. Silva. "NASA concept vehicles and the engineering of advanced air mobility aircraft". In: *The Aeronautical Journal* 126.1295 (2022), pp. 59–91. DOI: 10.1017/aer.2021.92.

[56] N. André and M. Hajek. "Robust Environmental Life Cycle Assessment of Electric VTOL Concepts for Urban Air Mobility". In: *AIAA Aviation 2019 Forum*. 2019. DOI: 10.2514/6.2019-3473.

[57] G. Palaia, K. Abu Salem, V. Cipolla, V. Binante, and D. Zanetti. "A Conceptual Design Methodology for e-VTOL Aircraft for Urban Air Mobility". In: *Applied Sciences* 11.22 (2021). DOI: 10.3390/app112210815.

[58]   A. M. Stoll, E. V. Stilson, J. Bevirt, and P. P. Pei. "Conceptual Design of the Joby S2 Electric VTOL PAV". In: *14th AIAA Aviation Technology, Integration, and Operations Conference.* 2014. DOI: 10.2514/6.2014-2407.

[59]   J. A. Cole, L. Rajauski, A. Loughran, A. Karpowicz, and S. Salinger. "Configuration Study of Electric Helicopters for Urban Air Mobility". In: *Aerospace* 8.2 (2021). DOI: 10.3390/aerospace8020054.

[60]   A. R. Kadhiresan and M. J. Duffy. "Conceptual Design and Mission Analysis for eVTOL Urban Air Mobility Flight Vehicle Configurations". In: *AIAA Aviation 2019 Forum.* 2019. DOI: 10.2514/6.2019-2873.

[61]   A. Brown and W. L. Harris. "A Vehicle Design and Optimization Model for On-Demand Aviation". In: *2018 AIAA/ASCE/AHS/ASC Structures, Structural Dynamics, and Materials Conference.* DOI: 10.2514/6.2018-0105.

[62]   A. Brown and W. L. Harris. "Vehicle Design and Optimization Model for Urban Air Mobility". In: *Journal of Aircraft* 57.6 (2020), pp. 1003–1013. DOI: 10.2514/1.C035756.

[63]   D. F. Finger, F. Götten, C. Braun, and C. Bil. "Initial Sizing for a Family of Hybrid-Electric VTOL General Aviation Aircraft". In: *Deutsche Gesellschaft für Luft- und Raumfahrt – Lilienthal-Oberth e. V.* Bonn, Germany, 2018. DOI: 10.25967/480102.

[64]   W. Johnson, C. Silva, and E. Solis. "Concept Vehicles for VTOL Air Taxi Operations". In: *AHS Technical Conference on Aeromechanics Design for Transformative Vertical Flight.* San Francisco, California, 2018.

[65]   C. Silva, W. R. Johnson, E. Solis, M. D. Patterson, and K. R. Antcliff. "VTOL Urban Air Mobility Concept Vehicles for Technology Development". In: *2018 Aviation Technology, Integration, and Operations Conference.* 2018. DOI: 10.2514/6.2018-3847.

[66]   J. M. Vegh, E. Botero, M. A. Clarke, J. Smart, and J. J. Alonso. "Current Capabilities and Challenges of NDARC and SUAVE for eVTOL Aircraft Design and Analysis". In: *AIAA Propulsion and Energy 2019 Forum.* 2019. DOI: 10.2514/6.2019-4505.

[67]   M. A. Clarke, J. Smart, E. Botero, W. Maier, and J. J. Alonso. "Strategies for Posing a Well-Defined Problem for Urban Air Mobility Vehicles". In: *AIAA SciTech 2019 Forum.* 2019. DOI: 10.2514/6.2019-0818.

[68]   INCOSE. *INCOSE Systems Engineering Handbook: A Guide for System Life Cycle Processes and Activities.* Ed. by D. D. Walden, G. J. Roedler, K. J. Forsberg, R. D. Hamelin, and T. M. Shortell. 4th ed. Wiley, 2015.

[69]   A. Gorod, B. Sauser, and J. Boardman. "System-of-Systems Engineering Management: A Review of Modern History and a Path Forward". In: *IEEE Systems Journal* 2.4 (2008), pp. 484–499. DOI: 10.1109/JSYST.2008.2007163.

[70]   R. M. Jaradat, C. B. Keating, and J. M. Bradley. "A histogram analysis for system of systems". In: *International Journal of System of Systems Engineering* 5.3 (2014), pp. 193–227. DOI: 10.1504/IJSSE.2014.065750.

[71]   M. Jamshidi and A. P. Sage, eds. *System of Systems Engineering: Innovations for the 21st Century*. Hoboken, New Jersey: Wiley, 2014.

[72]   J. Dahmann. "The state of systems of systems engineering knowledge sources". In: *2015 10th System of Systems Engineering Conference (SoSE)*. 2015, pp. 475–479. DOI: 10.1109/SYSOSE.2015.7151979.

[73]   L. B. Rainey and A. Tolk, eds. *Modeling and Simulation Support for System of Systems Engineering Applications*. Wiley, 2014. DOI: https://doi.org/10.1002/9781118501757.

[74]   Department of Defense, Office of the Deputy Under Secretary of Defense for Aquisition and Technology. *Systems Engineering Guide for Systems of Systems*. 1.0. Washington, DC, Aug. 2008.

[75]   M. Jamshidi. "System of systems engineering - New challenges for the 21st century". In: *IEEE Aerospace and Electronic Systems Magazine* 23.5 (2008), pp. 4–19. DOI: 10.1109/MAES.2008.4523909.

[76]   ISO/IEC/IEEE 21839:2019. *Systems and software engineering – System of systems (SoS) considerations in life cycle stages of a system*. International Standard. International Organization for Standardization (ISO), International Electrotechnical Commission (IEC), Institute of Electrical and Electronics Engineers (IEEE), 2019.

[77]   ISO/IEC/IEEE 15288:2015. *Systems and software engineering – System life cycle processes*. International Standard. International Organization for Standardization (ISO), International Electrotechnical Commission (IEC), Institute of Electrical and Electronics Engineers (IEEE), 2015.

[78]   M. W. Maier. "Architecting Principles for Systems-of-Systems". In: *INCOSE International Symposium* 6.1 (1996), pp. 565–573. DOI: 10.1002/j.2334-5837.1996.tb02054.x.

[79]   M. W. Maier. "Architecting principles for systems-of-systems". In: *Systems Engineering* 1.4 (1998), pp. 267–284. DOI: 10.1002/(SICI)1520-6858(1998)1:4%3C267::AID-SYS3%3E3.0.CO;2-D.

[80]   J. Boardman and B. Sauser. "System of Systems - the meaning of of". In: *2006 IEEE/SMC International Conference on System of Systems Engineering*. 2006, pp. 118–123. DOI: 10.1109/SYSOSE.2006.1652284.

[81]   W. A. Owens. "The Emerging U.S. System-of-Systems". In: *Dominant Battlespace Knowledge*. Ed. by M. C. Libicki and S. E. Johnson. Washington, DC: National Defense University Press, Oct. 1995.

[82] J. S. Dahmann and K. J. Baldwin. "Understanding the Current State of US Defense Systems of Systems and the Implications for Systems Engineering". In: *2008 2nd Annual IEEE Systems Conference*. 2008, pp. 1–7. DOI: `10.1109/SYSTEMS.2008.4518994`.

[83] Airbus. *Future Combat Air System (FCAS) – Shaping the future of air power*. URL: `https://www.airbus.com/en/products-services/defence/multi-domain-superiority/future-combat-air-system-fcas` (visited on 06/06/2022).

[84] P. T. Biltgen. "A Methodology for Capability-Based Technology Evaluation for Systems-of-Systems". PhD thesis. Georgia Institute of Technology, May 2007.

[85] IEEE 1220-2005. *IEEE Standard for Application and Management of the Systems Engineering Process*. Standard. Institute of Electrical and Electronics Engineers (IEEE), 2005.

[86] D. DeLaurentis. "Understanding Transportation as a System-of-Systems Design Problem". In: *43rd AIAA Aerospace Sciences Meeting and Exhibit*. 2005. DOI: `10.2514/6.2005-123`.

[87] E. Bonabeau. "Agent-based modeling: Methods and techniques for simulating human systems". In: *Proceedings of the National Academy of Sciences* 99.3 (2002), pp. 7280–7287. DOI: `10.1073/pnas.082080899`.

[88] P. Ranque, D. Freeman, K. Kernstine, D. Lim, E. Garcia, and D. Mavris. "Stochastic Agent-Based Analysis of UAV Mission Effectiveness". In: *11th AIAA Aviation Technology, Integration, and Operations (ATIO) Conference*. 2011. DOI: `10.2514/6.2011-6956`.

[89] A. Papageorgiou, J. Ölvander, K. Amadori, and C. Jouannet. "Multidisciplinary and Multifidelity Framework for Evaluating System-of-Systems Capabilities of Unmanned Aircraft". In: *Journal of Aircraft* 57.2 (2020), pp. 317–332. DOI: `10.2514/1.C035640`.

[90] I. Staack, K. Amadori, and C. Jouannet. "A Holistic Engineering Approach for Aeronautical Product Development". In: *31st Congress of the International Council of the Aeronautical Sciences*. International Council of the Aeronautical Sciences (ICAS). 2018. URL: `https://www.icas.org/ICAS_ARCHIVE/ICAS2018/data/papers/ICAS2018_0724_paper.pdf`.

[91] H. Liu, Y. Tian, Y. Gao, J. Bai, and J. Zheng. "System of systems oriented flight vehicle conceptual design: Perspectives and progresses". In: *Chinese Journal of Aeronautics* 28.3 (2015), pp. 617–635. DOI: `10.1016/j.cja.2015.04.017`.

[92] M. Niklaß, N. Dzikus, M. Swaid, J. Berling, B. Lührs, A. Lau, I. Terekhov, and V. Gollnick. "A Collaborative Approach for an Integrated Modeling of Urban Air Transportation Systems". In: *Aerospace* 7.5 (2020). DOI: `10.3390/aerospace7050050`.

[93] P. Shiva Prakasha, P. Ratei, N. Naeem, B. Nagel, and O. Bertram. "System of Systems Simulation driven Urban Air Mobility Vehicle Design". In: *AIAA Aviation 2021 Forum*. 2021. DOI: 10.2514/6.2021-3200.

[94] S. Kilkis, P. Shiva Prakasha, N. Naeem, and B. Nagel. "A Python Modelling and Simulation Toolkit for Rapid Development of System of Systems Inverse Design (SoSID) Case Studies". In: *AIAA Aviation 2021 Forum*. 2021. DOI: 10.2514/6.2021-3000.

[95] P. Shiva Prakasha, V. Papantoni, B. Nagel, U. Brand, T. Vogt, N. Naeem, P. Ratei, and S. Villacis. "Urban Air Mobility Vehicle and Fleet-level Life-Cycle Assessment Using a System-of-Systems Approach". In: *AIAA Aviation 2021 Forum*. 2021. DOI: 10.2514/6.2021-2457.

[96] R. Rothfeld, M. Balać, K. O. Ploetner, and C. Antoniou. "Agent-based Simulation of Urban Air Mobility". In: *2018 Modeling and Simulation Technologies Conference*. DOI: 10.2514/6.2018-3891.

[97] L. W. Kohlman, M. D. Patterson, and B. E. Raabe. *Urban Air Mobility Network and Vehicle Type—Modeling and Assessment*. NASA/TM–2019–220072. National Aeronautics and Space Administration (NASA), 2019.

[98] D. S. Santos, B. R. N. Oliveira, R. Kazman, and E. Y. Nakagawa. "Evaluation of Systems-of-Systems Software Architectures: State of the Art and Future Perspectives". In: *ACM Computing Surveys* (Feb. 2022). Just Accepted. DOI: 10.1145/3519020.

[99] D. P. Raymer. *Aircraft Design: A Conceptual Approach*. 6th ed. AIAA Eduation Series. Reston, Virginia: American Institute of Aeronautics and Astronautics, 2018.

[100] L. M. Nicolai and G. E. Carichner. *Fundamentals of Aircraft and Airship Design, Volume 1 – Aircraft Design*. Reston, Virginia: American Institute of Aeronautics and Astronautics, 2010.

[101] S. Gudmundsson. *General Aviation Aircraft Design – Applied Methods and Procedures*. Boston: Butterworth-Heinemann, 2014. DOI: 10.1016/B978-0-12-397308-5.00001-5.

[102] M. D. Patterson, K. R. Antcliff, and L. W. Kohlman. "A Proposed Approach to Studying Urban Air Mobility Missions Including an Initial Exploration of Mission Requirements". In: *AHS International 74th Annual Forum & Technology Display*. 2018.

[103] Uber. *UberAir Vehicle Requirements and Missions*. URL: https://s3.amazonaws.com/uber-static/elevate/Summary+Mission+and+Requirements.pdf (visited on 06/06/2022).

[104] J. Roskam. *Airplane Design Part V: Component Weight Estimation*. Lawrence, Kansas: DARcorportation, 1999.

[105] R. W. Prouty. *Helicopter Performance, Stability, and Control.* Malabar, Florida: Krieger, 2002.

[106] O. Bertram, F. Jäger, V. Voth, and J. Rosenberg. "Impact of Different Powertrain Architectures on UAM Vehicle Concepts". In: *Deutscher Luft- und Raumfahrtkongress 2021.* 2021. URL: https://elib.dlr.de/143785/.

[107] O. Bertram, F. Jäger, V. Voth, and J. Rosenberg. "UAM Vehicle Design with Emphasis on Electric Powertrain Architectures". In: *AIAA SciTech 2022 Forum.* 2022. DOI: 10.2514/6.2022-1995.

[108] R. de Vries, M. Brown, and R. Vos. "Preliminary Sizing Method for Hybrid-Electric Distributed-Propulsion Aircraft". In: *Journal of Aircraft* 56.6 (2019), pp. 2172–2188. DOI: 10.2514/1.C035388.

[109] G. Van Rossum and F. L. Drake. *Python 3 Reference Manual.* Scotts Valley, CA: CreateSpace, 2009.

[110] E. Burnell, N. B. Damen, and W. Hoburg. "GPkit: A Human-Centered Approach to Convex Optimization in Engineering Design". In: *Proceedings of the 2020 CHI Conference on Human Factors in Computing Systems.* 2020. DOI: 10.1145/3313831.3376412.

[111] B. Boden, J. Flink, N. Först, R. Mischke, K. Schaffert, A. Weinert, A. Wohlan, and A. Schreiber. "RCE: An Integration Environment for Engineering and Science". In: *SoftwareX* 15 (2021), p. 100759. DOI: 10.1016/j.softx.2021.100759.

[112] M. Alder, E. Moerland, J. Jepsen, and B. Nagel. "Recent Advances in Establishing a Common Language for Aircraft Design with CPACS". In: *Aerospace Europe Conference 2020.* 2020.

[113] A. Bacchini and E. Cestino. "Electric VTOL Configurations Comparison". In: *Aerospace* 6.3 (2019). DOI: 10.3390/aerospace6030026.

[114] I. Moerland-Masic, F. Reimer, T.-M. Bock, and L. Kamens. "A user centric Cabin Design using the Design Thinking approach". In: *HorizonUAM Symposium 2021.* Sept. 2021. URL: https://elib.dlr.de/144883/.

[115] R. A. McDonald and J. R. Gloudemans. "Open Vehicle Sketch Pad: An Open Source Parametric Geometry and Analysis Tool for Conceptual Aircraft Design". In: *AIAA SciTech 2022 Forum.* 2022. DOI: 10.2514/6.2022-0004.

[116] E. Torenbeek. *Synthesis of subsonic airplane design.* Delft, The Netherlands: Delft University Press, 1982.

[117] T. Sinnige, N. van Arnhem, T. C. A. Stokkermans, G. Eitelberg, and L. L. M. Veldhuis. "Wingtip-Mounted Propellers: Aerodynamic Analysis of Interaction Effects and Comparison with Conventional Layout". In: *Journal of Aircraft* 56.1 (2019), pp. 295–312. DOI: 10.2514/1.C034978.

[118]   T. Sinnige, R. Nederlof, and N. van Arnhem. "Aerodynamic Performance of Wingtip-Mounted Propellers in Tractor and Pusher Configuration". In: *AIAA Aviation 2021 Forum*. 2021. DOI: 10.2514/6.2021-2511.

[119]   N. Battaini. "Design and dynamic modeling of a VTOL UAV". PhD thesis. Politecnico di Milano, May 2020.

[120]   L. Holtermann, A. Otto, and S. Schulze. *Pendeln in Hamburg*. HWWI Policy Paper 83. Hamburgisches WeltWirtschaftsinstitut (HWWI), 2013.

[121]   P. Shiva Prakasha, B. Nagel, S. Kilkis, N. Naeem, and P. Ratei. "System of Systems Simulation Driven Wildfire Fighting Aircraft Design". In: *AIAA Aviation 2021 Forum*. 2021. DOI: 10.2514/6.2021-2455.

[122]   P. Shiva Prakasha, N. Naeem, P. Ratei, N. Cigal, and B. Nagel. "Exploration of Aerial Firefighting Fleet Effectiveness and Cost by System of Systems Simulations". In: *32nd Congress of the International Council of Aeronautical Sciences*. International Council of Aeronautical Sciences (ICAS), 2021. URL: https://www.icas.org/ICAS_ARCHIVE/ICAS2020/data/papers/ICAS2020_0997_paper.pdf.

[123]   J. T. Doo, M. A. Tsairides, M. D. Pavel, M. Smith, A. Didey, E. Bennet, C. Hange, M. Bromfield, N. P. Diller, and J. Mooberry. *NASA Electric Vertical Takeoff and Landing (eVTOL) Aircraft Technology for Public Services – A White Paper*. 20205000636. National Aeronautics and Space Administration (NASA), Aug. 2021.

[124]   German Aerospace Center (DLR). *DLR Design Challenge 2022 – seeking ideas to fight forest fires from the air*. Mar. 2022. URL: https://www.dlr.de/content/en/articles/news/2022/01/20220311_dlr-seeking-ideas-to-fight-forest-fires-from-the-air.html (visited on 06/06/2022).

A Task

The official task for this master thesis can be found on the two subsequent pages. It contains all relevant information on the agreed thesis title, topic, background, and deliverables. Note that the signatures are only present on the original document submitted to the examination office for thesis registration. Please see the two following pages.

Hochschule für Angewandte Wissenschaften Hamburg
Hamburg University of Applied Sciences

FACULTY OF ENGINEERING AND COMPUTER SCIENCE
DEPARTMENT OF AUTOMOTIVE AND AERONAUTICAL ENGINEERING
Prof. Dr.-Ing. Martin Wagner

Task for a Master Thesis

Student: Patrick Ratei (2294725)

Topic: Development of a Vertical Take-Off and Landing Aircraft Design Tool
                 for the Application in a System of Systems Simulation Framework

Cooperation: German Aerospace Center (DLR), Institute of System Architectures in
                 Aeronautics, c/o ZAL TechCenter, Hein-Saß-Weg 22, 21129 Hamburg
                 Supervisor: Prajwal Shiva Prakasha, E-Mail: prajwal.prakasha@dlr.de

Background

Urban Air Mobility (UAM) is a future vision of urban air transport systems in big cities
for different services including on-demand passenger transport promising affordable
as well as comfortable journeys, and especially travel time savings compared to
congested road transport.
The project "HorizonUAM – Urban Air Mobility Research at the German Aerospace
Center (DLR)" addresses several research questions and provides first results with
regards to efficiency, safety, feasibility, sustainability, and affordability of this future
passenger transport system. UAM research at DLR does not only focus on vehicles
but also considers the associated infrastructure, the operations, as well as the public
acceptance of future urban air transport services. For this purpose, the required
competences of several DLR institutes are brought together in HorizonUAM.[1]
Regarding the conceptual design of future UAM vehicles, the Institute of System
Architectures in Aeronautics eventually aims for a System of Systems (SoS) driven
vehicle design approach. Therefore, an initial vehicle configuration must be designed
and sized. Subsequently, additional vehicles must be developed and combined to a
vehicle family. Finally, the overall framework for SoS driven vehicle design must be
finalized by March 2023.

---

[1] HorizonUAM – Urban Air Mobility Research at the German Aerospace Center (DLR), retrieved
01 December 2021 from https://www.dlr.de/fl/desktopdefault.aspx/tabid-1149/1737_read-69326/.

118

Task

The task of this thesis is related to the field of conceptual aircraft design for different vertical take-off and landing vehicle configurations, whereas the main objective is the development of a design tool for initial sizing and conceptual design. For this purpose, a literature study must be conducted, and a suitable design approach must be developed.

In summary, the task can be divided into the following subtasks:

- Outlining the design space of different UAM vehicle configurations
- Researching conceptual design methods and methodologies for different UAM vehicle configurations
- Developing a tool for initial vehicle sizing and performance computations in Python (considering the integration into the SoS simulation framework)
- Demonstrating the design tool by the development of a UAM vehicle concept
- Identifying future work potentials of the developed design tool

The thesis must be written in English in accordance with standards for academic and scientific writing.

A non-disclosure agreement is not required.

Hamburg, 6. May 2022

Prof. Dr.-Ing. Martin Wagner	Prajwal Shiva Prakasha, M. Sc.	Patrick Ratei
1st Examiner	2nd Examiner	Student

B Tool Inputs and Outputs

The VTOL-AD tool inputs and outputs are fully documented in Table B.1. The tabular summary follows the input and output CSV file structure and lists the tool variables defined in the tool together with the symbols used in this work. Also, the sequence and data types of the variables are given and abbreviated by "S Type" and "D Type", respectively. It should be noted that the presented default values with their associated units are set with regard to the winged eVTOL aircraft configuration. Also, if a value is given as zero, it represents an output parameter that is computed by the VTOL-AD tool. In that context it is important to mention that the tool is set-up for the sizing of an eVTOL aircraft. If an existing aircraft should be analyzed, the respective boolean variable `run_sizing` has to be triggered and the geometric variables regarding wing, empennage, fuselage, and equivalent flat-plate drag have to be input in addition. As noted in the tool methodology and limitations in Section 3.4, the mission input variables are currently not part of the input and output CSV file and must be stored and traced separately. For full information and details on the input and output CSV files, the reader is directed to the digital appendix (see Appendix C).

Table B.1: Tool Inputs and Outputs

Parameter Name	Symbol	S Type	D Type	Value	Unit
run_sizing	—	None	bool	True	—
run_sosid	—	None	bool	True	—
study	—	None	str	default	—
conobs	—	None	str	Study 0	—
config	—	None	str	tiltrotor	—
is_winged	—	None	bool	True	—
is_autonomous	—	None	bool	False	—
footprint	—	None	float64	15	m
wing_max_aspect_ratio	AR_{max}	None	float64	15	—
wing_aspect_ratio	AR	None	float64	10	—
wing_area	S	None	float64	0	m^2
wing_span	b	None	float64	0	m
wing_chord	c	None	float64	0	m
wing_loading	WL	None	float64	0	N/m^2
stall_speed	V_s	None	float64	36	m/s
max_lift_coefficient	$C_{L,max}$	None	float64	2	—
flat_plate_drag_area	f	None	float64	0	m^2
ultimate_load_factor	N_{ult}	None	float64	5.7	—
fuselage_cockpit_length	L_1	None	float64	1.7	m
fuselage_cabin_length	L_2	None	float64	2.2	m
fuselage_empennage_length	L_3	None	float64	3.1	m

Table B.1 Tool Inputs and Outputs – Continued From Previous Page

Parameter Name	Symbol	S Type	D Type	Value	Unit
fuselage_length	L_F	None	float64	6.8	m
fuselage_max_diameter	$2R_1$	None	float64	1.75	m
fuselage_empennage_radius	R_2	None	float64	0.25	m
fuselage_wetted_area	$S_{wet,F}$	None	float64	0	m^2
horizontal_stabilizer_aspect_ratio	AR_H	None	float64	2	—
horizontal_stabilizer_area	S_H	None	float64	0	m^2
horizontal_stabilizer_chord	—	None	float64	0	m
horizontal_stabilizer_span	—	None	float64	0	m
vertical_stabilizer_aspect_ratio	AR_V	None	float64	2	—
vertical_stabilizer_area	S_V	None	float64	0	m^2
vertical_stabilizer_chord	—	None	float64	0	m
vertical_stabilizer_span	—	None	float64	0	m
tail_arm	L_T	None	float64	0	m
number_of_wheels	N_{wheels}	None	int32	2	—
persons_on_board	POB	None	int32	4	—
wing_technology_factor	—	None	float64	1.4	—
empennage_technology_factor	—	None	float64	1.4	—
fuselage_technology_factor	—	None	float64	1.4	—
landing_gear_technology_factor	—	None	float64	1.4	—
maximum_takeoff_mass	m_{mto}	None	float64	2000	kg
payload_mass	m_{pl}	None	int32	400	kg
airframe_mass	m_{af}	None	float64	0	kg
wing_mass	m_w	None	float64	0	kg
empennage_mass	m_{emp}	None	float64	0	kg
fuselage_mass	m_{fus}	None	float64	0	kg
landing_gear_mass	m_{lg}	None	float64	0	kg
onboard_systems_mass	m_{obs}	None	float64	0	kg
powertrain_mass	—	None	float64	0	kg
rotor_mass	—	None	float64	0	kg
gearbox_mass	—	None	float64	0	kg
motor_mass	—	None	float64	0	kg
power_management_mass	—	None	float64	0	kg
gasturbine_mass	—	None	float64	0	kg
fuel_cell_mass	—	None	float64	0	kg
battery_mass	m_{bat}	None	float64	0	kg
hydrogen_mass	m_{hyd}	None	float64	0	kg
kerosene_mass	m_{krs}	None	float64	0	kg
other_systems_mass	m_{os}	None	float64	0	kg
empty_mass_fraction	f_e	None	float64	0	—
zero_fuel_mass_fraction	f_{zf}	None	float64	0	—
payload_mass_fraction	f_{pl}	None	float64	0	—
airframe_mass_fraction	f_{af}	None	float64	0	—
onboard_systems_mass_fraction	f_{obs}	None	float64	0	—
energy_mass_fraction	f_{egy}	None	float64	0	—
battery_mass_fraction	f_{bat}	None	float64	0	—
hydrogen_mass_fraction	f_{hyd}	None	float64	0	—
kerosene_mass_fraction	f_{ker}	None	float64	0	—
max_disk_loading	DL_{max}	None	float64	750	N/m^2
n_rotors	N	None	int32	6	—
n_rotors_wing	—	None	int32	4	—
rotor_is_speed_controlled	—	None	bool	False	—
rotor_n_blades	N_b	None	int32	5	—
rotor_solidity	σ	None	float64	0.2	—
rotor_relative_thickness	—	None	float64	0.12	—
rotor_induced_power_factor	κ	None	float64	1.15	—

Table B.1 Tool Inputs and Outputs – Continued From Previous Page

Parameter Name	Symbol	S Type	D Type	Value	Unit
rotor_parasite_drag	$C_{d,0}$	None	float64	0.01	—
rotor_max_tip_mach_number	—	None	float64	0.7	—
rotor_max_cl_mean	$\overline{C_{l_{max}}}$	None	float64	0.7	—
rotor_max_diameter	D_{max}	None	float64	3	—
thrust_coefficient	C_T	None	float64	0	—
disk_loading	DL	None	float64	0	N/m^2
disk_area	A	None	float64	0	m^2
rotor_diameter	D	None	float64	0	m
rotor_figure_of_merit	FOM	None	float64	0	—
rotor_tip_speed	V_t	None	float64	0	m/s
rotor_cl_mean	$\overline{C_l}$	None	float64	0	m/s
battery_specific_energy	SE_{bat}	None	float64	250	Wh/kg
battery_specific_power	SP_{bat}	None	float64	625	W/kg
fuel_cell_specific_power	—	None	float64	0	kW/kg
powertrain_architecture	—	None	str	FullElectric1	—
powertrain_efficiency	η_{tot}	None	float64	0.912	—
powertrain_reliability	—	None	float64	0.857	—
powertrain_supplied_power_ratio	—	None	float64	1	—
propeller_efficiency	—	None	float64	0.8	—
max_available_power	—	None	float64	0	kW
hover_power	P_{ho}	None	float64	0	kW
taxi_power	P_{tx}	None	float64	0	kW
vertical_climb_power	P_{vc}	None	float64	0	kW
transition_power	P_{tr}	None	float64	0	kW
cruise_climb_power	P_{cc}	None	float64	0	kW
cruise_power	P_{cr}	None	float64	0	kW
loiter_power	P_{lo}	None	float64	0	kW
retransition_power	P_{tr}	None	float64	0	kW
vertical_descent_power	P_{vd}	None	float64	0	kW
taxi_time	t_{tx}	None	float64	0	hr
vertical_climb_time	t_{vc}	None	float64	0	hr
transition_time	t_{tr}	None	float64	0	hr
cruise_climb_time	t_{cc}	None	float64	0	hr
cruise_time	t_{cr}	None	float64	0	hr
loiter_time	t_{lo}	None	float64	0	hr
vertical_climb_time	t_{vc}	None	float64	0	hr
retransition_time	t_{tr}	None	float64	0	hr
vertical_descent_time	t_{vd}	None	float64	0	hr
best_range_speed	V_{br}	None	float64	0	m/s
best_endurance_speed	V_{be}	None	float64	0	m/s
total_energy	—	None	float64	0	kJ
useable_energy	—	None	float64	0	kJ
reserve_energy	—	None	float64	0	kJ
lift_to_drag_ratio	L/D	None	float64	0	—
energy_per_km	—	None	float64	0	kWh/km
energy_per_pax_km	—	None	float64	0	kWh/km
charging_station_power	—	None	float64	0	kW
charging_c_rate	—	None	float64	0	1/hr
charging_power	—	None	float64	0	kW
charging_time	—	None	float64	0	hr
performance_aerodrome_altitude	H_{ad}	None	float64	0	m
performance_vertical_climb_altitude	—	None	float64	15.24	m
performance_cruise_altitude	H_{cr}	None	float64	457.2	m
performance_aerodrome_density	—	None	float64	1.225	kg/m^3
performance_cruise_density	—	None	float64	1.172	kg/m^3

Table B.1 Tool Inputs and Outputs – Continued From Previous Page

Parameter Name	Symbol	S Type	D Type	Value	Unit
performance_best_range_speed	V_{br}	None	float64	0	m/s
performance_best_endurance_speed	V_{be}	None	float64	0	m/s
performance_max_mission_speed	—	None	float64	0	m/s
performance_cruise_speed	V_{cr}	None	float64	0	m/s
performance_reserve_energy	—	None	float64	0	kJ
performance_mission_range	—	None	float64	0	km
performance_ferry_range	—	None	float64	0	km
performance_transition_time	t_{tr}	None	float64	0	s
performance_taxi_power	P_{tx}	Tuple	float64	()	kW
performance_hover_power	P_{ho}	Tuple	float64	()	kW
performance_vertical_climb_power	P_{vc}	Tuple	float64	()	kW
performance_transition_power	P_{tr}	Tuple	float64	()	kW
performance_cruise_climb_power	P_{cc}	Tuple	float64	()	kW
performance_cruise_power	P_{cr}	Tuple	float64	()	kW
performance_taxi_battery_power	—	Tuple	float64	()	kW
performance_hover_battery_power	—	Tuple	float64	()	kW
performance_vertical_climb_battery_power	—	Tuple	float64	()	kW
performance_transition_battery_power	—	Tuple	float64	()	kW
performance_cruise_climb_battery_power	—	Tuple	float64	()	kW
performance_cruise_battery_power	—	Tuple	float64	()	kW

C Digital Appendix

The digital appendix can be found on the enclosed compact disk. For a better overview, the folder structure of the digital appendix is shown below with main folders in bold and files in italics.

```
Digital Appendix
└─ 1_Tool
   ├─ data
   │  ├─ Default
   │  │  ├─ multirotor_input.csv
   │  │  └─ tiltrotor_input.csv
   │  ├─ RCE
   │  │  ├─ aircraft_input.csv
   │  │  ├─ aircraft_output.csv
   │  │  └─ aircraft_output.json
   │  ├─ aircraft_input.csv
   │  ├─ aircraft_output.csv
   │  └─ aircraft_output.json
   ├─ docs
   │  ├─ conobs_input_template.xlsx
   │  └─ conobs_output_template.xlsx
   ├─ scripts
   │  ├─ ConOBStoVTOLAD.py
   │  └─ VTOLADtoConOBS.py
   ├─ src
   │  ├─ atmosphere
   │  │  ├─ sdtatmo.py
   │  │  └─ stdatmo_table.txt
   │  ├─ rotor
   │  │  ├─ rotor_analysis.py
   │  │  └─ rotor_model.py
   │  ├─ aerodynamics.py
   │  ├─ csv_reader.py
   │  ├─ geometry.py
   │  ├─ json_reader.py
   │  ├─ mission.py
   │  ├─ performance.py
   │  ├─ units.py
   │  ├─ vehicle.py
   │  └─ weights.py
   └─ main.py
```

Digital Appendix – Continued From Previous Page

- **2_Results**
  - *multirotor.csv*
  - *tiltrotor.csv*
- **3_Documentation**
  - *Report_Master_Thesis_Ratei.pdf*
  - *Poster_Master_Thesis_Ratei.pdf*
  - *Poster_Master_Thesis_Ratei.pptx*
  - *Abstract_Master_Thesis_Ratei.pdf*
  - *Abstract_Master_Thesis_Ratei.docx*

Erklärung zur selbstständigen Bearbeitung einer Abschlussarbeit

Gemäß der Allgemeinen Prüfungs- und Studienordnung ist zusammen mit der Abschlussarbeit eine schriftliche Erklärung abzugeben, in der der Studierende bestätigt, dass die Abschlussarbeit „— bei einer Gruppenarbeit die entsprechend gekennzeichneten Teile der Arbeit [(§ 18 Abs. 1 APSO-TI-BM bzw. § 21 Abs. 1 APSO-INGI)] — ohne fremde Hilfe selbständig verfasst und nur die angegebenen Quellen und Hilfsmittel benutzt wurden. Wörtlich oder dem Sinn nach aus anderen Werken entnommene Stellen sind unter Angabe der Quellen kenntlich zu machen.“

Quelle: § 16 Abs. 5 APSO-TI-BM bzw. § 15 Abs. 6 APSO-INGI

Dieses Blatt, mit der folgenden Erklärung, ist nach Fertigstellung der Abschlussarbeit durch den Studierenden auszufüllen und jeweils mit Originalunterschrift als letztes Blatt in das Prüfungsexemplar der Abschlussarbeit einzubinden.

Eine unrichtig abgegebene Erklärung kann -auch nachträglich- zur Ungültigkeit des Studienabschlusses führen.

Erklärung zur selbstständigen Bearbeitung der Arbeit

Hiermit versichere ich,

Name: _____

Vorname: _____

dass ich die vorliegende Masterarbeit mit dem Thema:

Development of a Vertical Take-Off and Landing Aircraft Design Tool for the Application in a System of Systems Simulation Framework

ohne fremde Hilfe selbständig verfasst und nur die angegebenen Quellen und Hilfsmittel benutzt habe. Wörtlich oder dem Sinn nach aus anderen Werken entnommene Stellen sind unter Angabe der Quellen kenntlich gemacht.

_____   _____   _____
        Ort   Datum   Unterschrift im Original